Melting and fining of arsenic-containing silicate glass batches

MELTING AND FINING OF ARSENIC-CONTAINING SILICATE GLASS BATCHES

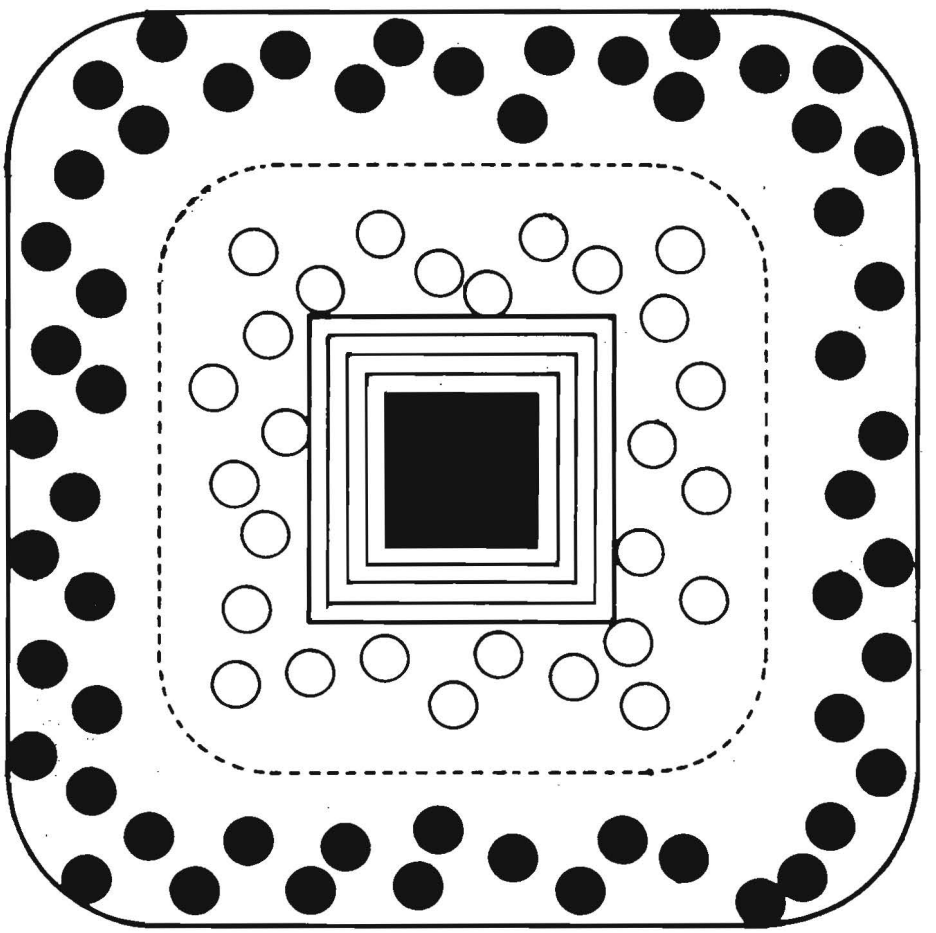

HENDRIK VERWEIJ

MELTING AND FINING OF ARSENIC-CONTAINING SILICATE GLASS BATCHES

PROEFSCHRIFT

TER VERKRIJGING VAN DE GRAAD VAN DOCTOR
IN DE TECHNISCHE WETENSCHAPPEN
AAN DE TECHNISCHE HOGESCHOOL EINDHOVEN,
OP GEZAG VAN DE RECTOR MAGNIFICUS,
PROF. IR. J. ERKELENS,
VOOR EEN COMMISSIE AANGEWEZEN
DOOR HET COLLEGE VAN DEKANEN
IN HET OPENBAAR TE VERDEDIGEN
OP DINSDAG 21 OKTOBER 1980 TE 16.00 UUR

DOOR

HENDRIK VERWEIJ

GEBOREN TE 'S-GRAVENHAGE

DIT PROEFSCHRIFT IS GOEDGEKEURD DOOR DE PROMOTOREN

Prof. Ir. A.L. Stuijts

en

Prof. Dr. Ir. H. de Waal

Voor mijn ouders,
Voor Irene

DANKBETUIGING EN VERANTWOORDING

Het onderzoek, in dit proefschrift beschreven, is uitgevoerd in de periode van medio 1975 tot medio 1980 in de groep "Glas" van het Philips' Natuurkundig Laboratorium te Eindhoven. Ik ben veel medewerkers van dit laboratorium mijn dank verschuldigd voor hun bijdragen aan dit onderzoek.

In het bijzonder wil ik noemen: dr. F. Meijer, dr. ir. R.G. Gossink, dr. ir. W.L. Konijnendijk en drs. K.C. van Erk voor diskussies en het kritisch doorlezen van mijn manuscripten en A.J. Hendriks voor assistentie bij het opzetten van de automatisering van de Raman spectrometer.

Mijn co-auteurs Ing. H. van den Boom en R.E. Breemer hebben in de beginfase van het onderzoek vele Raman metingen verricht en mij ingewijd in de geheimen van de laser Ramanspectroscopie.

Door drs. J. Hornstra ben ik geconfronteerd met röntgen éénkristaldiffractiemetingen en het oplossen van kristalstructuren hieruit.

De technische vaardigheden en de inventiviteit van J.G. van Lierop bij het bereiden van een aantal vaak zeer moeilijke preparaten zijn van groot nut geweest voor het onderzoek.

De N.V. Philips' Gloeilampenfabrieken ben ik zeer erkentelijk voor de ondersteuning bij het tot stand komen van dit proefschrift.

CONTENTS

INTRODUCTION

This thesis contains a collection of papers and manuscripts concerning the mechanisms of melting and fining reactions in a model silicate glass-forming mixture containing As_2O_3. Fining is the process of disappearance of gasbubbles from glass melts. As_2O_3 is a fining agent. Fining agents are added to glass-forming mixtures to reduce the time needed for glass melts to become bubble free. The aim of the investigations, presented in this thesis, was to clarify the complete reaction mechanism of As_2O_3 fining.
In this introduction a short description of silicate glass melting and fining will be given together with a literature review and a resumé of the papers and manuscripts included in this thesis.

I. Silicate glasses, melting and fining

The glass that is generally used for windowpanes, kitchenware or bottles is described in the glass technology as soda-lime-silica glass. It is prepared for more than 3000 years by melting appropriate mixtures of sand (SiO_2), soda (Na_2CO_3) and lime ($CaCO_3$) to a viscous liquid which can be cooled without crystallization to a transparent solid material, "glass".
Soda-lime-silica glasses usually show a good corrosion resistance and are shaped relatively easily at temperatures above 800°C for instance by blowing or pressing. The basic composition of the glass-forming mixture is:

15 mol% Na_2CO_3 – 10 mol% $CaCO_3$ – 75 mol% SiO_2.

In a practical glass, part of the sodium is replaced by lithium or potassium and part of the calcium is replaced by other alkaline earth metal ions. Some aluminium oxide is added to decrease the tendency towards crystallization of the glass melt and to increase the corrosion resistance.
For decorative or technical purposes glass may be colored by the introduction of transition metal ions.
Sometimes extra iron oxides are added to improve the heat absorption of the glass melt.
By changing the glass composition important properties such as refractive index, thermal expansion, viscosity and electrical conductivity can be varied over wide ranges.
An important class of glasses, based on the soda-lime-silica formula compromises glasses which are used for the production of television screens. The main difference with normal soda-lime-silica glasses is that in these glasses calcium is replaced for a large part by barium. The presence of barium in the glass largely increases the absorption of UV- and X-rays.

The viscosity of silicate glasses shows a remarkable dependence on the temperature. An example is given in fig. 1 for NBS 710 glass. Blowing of this glass can be performed at temperatures from 700 to 820°C, corresponding to $\log(\eta)$ = 6-8. Pressing of the glass may be done at 900°C where $\log(\eta)$ is about 5.

The "glass transition point" of NBS 710 glass is found at 544°C. This point is usually taken as the temperature where $\log(\eta)$ = 13.6. Here the characteristic times for deformation processes become of the order of one minute. The glass transition point indicates the transition of the glass from a "solid" to a "liquid" or vice versa.
The viscosity of NBS 710 glass, which is a soda-lime-silica glass, decreases by more than ten decades, going from the glass transition temperature, at 544°C, to the melting temperature, at 1400°C, where $\log(\eta)\approx 2$. The large viscosity-temperature range of practical silicate glasses gives the possibility of a large number of fast forming techniques, but is also the cause of serious glass-melting problems.
This can be seen when the simplified overall melting reaction of soda-lime-silica glass batches is considered:

$$15\ Na_2CO_3 + 10\ CaCO_3 + 75\ SiO_2 \xrightarrow{1400^\circ C}$$
$$15\ Na_2O.10\ CaO.75\ SiO_2\ \text{(viscous glass melt)} + 25\ CO_2\uparrow$$

The carbonates originally present in the batch decompose and large quantities of CO_2 gas will develope. This results in a large quantity of bubbles in the glass melt. Besides CO_2 these bubbles may also contain other gases such as N_2, O_2, H_2O, CO and SO_2 from furnace atmosphere or from other decomposing batch components.
Gas bubbles may disappear from a glass melt either by *dissolution* or by *rising* to the surface of the melt. In practice both processes are important. The dissolution speed of the various gases depends on the chemical nature

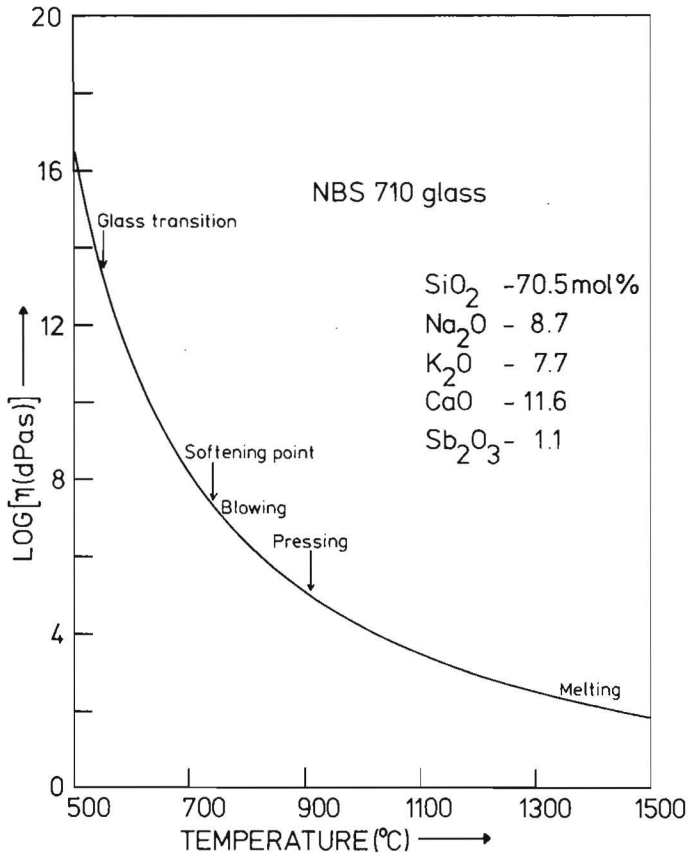

Fig. 1 Viscosity-temperature curve of NBS 710 glass.

of the glass melt but especially on the presence of redox couples. The gases N_2 and CO_2 generally have a very low dissolution speed so that they have to disappear by rising to the surface of the melt.

At practical melting temperatures, for silicate glasses 1400-1600°C, the viscosity of the glass is still about 100 d Pas. This relatively high viscosity results in a sluggish homogenization of the melt and a very slow disappearance of bubbles by rising to the surface of the melt. According to Stokes' law the rising velocity is:

$$V = \frac{D^2 g \Delta\rho}{18\eta}.$$

D = bubble diameter
g = acceleration due to gravity
$\Delta\rho$ = glass-gas density difference
η = viscosity

The average rising speed for non-dissolving gas bubbles in a silicate glass melt at melting temperature is given in the table below for various bubble diameters.

diameter (μm)	rising speed
10	1.6 years/m
100	5.8 days/m
1000	1.4 hours/m
10000	0.83 minutes/m

Bubbles of 10μm diameter or less are generally unstable due to their relatively high surface energy. They dissolve rapidly in the melt if they are accidently formed. Bubbles with diameters of 1 mm and more rise to the surface of the melt within reasonable times. Bubbles with diameters around 400μm constitute a serious problem, especially where the demands for optical quality are high.
Several methods have been proposed to minimize the time needed for glass melts to become bubble free ([1-3]); in other words to optimize the "fining" or "refining" process:

- Control of glass streams by means of special furnace constructions and heating methods and by means of gas streams.
- Application of ultra sound or low pressure.
- Boosting: application of local high temperatures by means of electrode heating.
- Selection of special raw materials.
- Addition of fluoride to speed up the batch reactions.
- Application of "fining agents".

The application of fining agents is the oldest and most common of these methods. Fining agents are added to glass-forming batches in quantities of 0.1 - 1 weight%. They may result in reduction of the bubble-free time by as much as a factor of ten. The most important fining agents are:

- Sulphates in combination with carbon; mainly used in the flat glass and container glass production.
- As_2O_3 and Sb_2O_3 in combination with nitrates; used for the production of optical glasses and television screen glasses.

The aim of the investigations, presented in this thesis, was to clarify the complete reaction mechanism of As_2O_3 fining.
A literature review of studies on the function of As_2O_3 during melting and fining of silicate glass-forming batches is given in section 2 of this introduction. A description of the experimental methods, used for the investigations, is given in section 3.
A survey of the papers and manuscripts is given in section 4.

II. Literature on melting and fining of As_2O_3-containing silicate glass batches

The total glass melting process can be divided into a batch reaction process and a fining process.
The batch reaction process contains the primary chemical reactions of the raw materials with the formation of crystalline and liquid silicates and the dissolution of sand into the silicates initially formed. The fining process can be regarded to some extent as a separate process of bubble dissolution or growth and rising to the surface of the melt ([1-3]).
As was already pointed out by Cable ([4]) a strong relation between the batch reactions and the fining process will always exist. This relation has not received much attention in the literature. Batch reactions in glass-forming batches have mainly been studied in the Na_2CO_3-$CaCO_3$-SiO_2 systems using X-ray diffraction or thermal analysis techniques ([1-4]). No direct studies of the reaction mechanisms for As_2O_3 during the batch reactions have been published. Cable ([5]) studied mixtures of molar composition $3Na_2CO_3$ – $1As_2O_3$, heated at various temperatures. He concluded that Na_3AsO_4 (As^{5+}) is formed at 700°C and some As at lower temperatures.
A detailed proposal for the low temperature reactions of arsenic in soda-lime-silica batches was given by Eichorn ([6]) who also studied mixtures of Na_2CO_3 and As_2O_3:

$$5\ As_2O_3 + 5\ Na_2CO_3 \xrightarrow{180\text{-}350^\circ C} 10\ NaAsO_2 + CO_2\uparrow\ *)$$

$$10\ NaAsO_2 + 4\ Na_2CO_3 \xrightarrow{300\text{-}500^\circ C} 6\ Na_3AsO_4 + 4\ CO_2\uparrow + 4\ As\ *)$$

$$4\ As + 3\ O_2 \longrightarrow 2\ As_2O_3$$

The oxygen in the last reaction may be obtained from the furnace atmosphere or from decomposed nitrates, which are always added in combination with arsenic.
Reactions as mentioned above do not consider the interaction with the silicate reactions which occur at higher temperatures.

The most general view from the literature on the function of As_2O_3 in the fining process of silicate glass melts is at follows:

*) The formation of $NaAsO_2$ and As was also found in preliminary experiments by the present author.

- After the initial batch reaction process a silicate melt is formed with many bubbles. Arsenic is present in this melt partly as As^{3+} and partly as As^{5+}.
- When the temperature in the melt increases the lower valency state of arsenic is thermodynamically favored which causes an oxygen release. This can be given schematically as:

$$As_2O_5 \xrightarrow{+\Delta T} As_2O_3 + O_2\uparrow.$$

- The oxygen which is released by this reaction inflates the bubbles in the melt so that they can rise to the surface of the melt with a sufficient speed.

When this hypothesis is true there must be an change of the As^{3+}/As^{5+} ratio as a function of the melting temperature of glasses. To the knowledge of the author there are no systematic studies of the effect of temperature on this As^{3+}/As^{5+} ratio in the literature. This is probably related to the many problems encountered with wet-chemical As^{3+}/As^{5+} analyses of silicate glasses ([7]).

Indirect studies of the function of As_2O_3 in the fining part of the glass melting process are given in refs. 5, 8-16. Cable et al ([5,8-11]) performed analyses of bubble content, bubble size distribution and number of bubbles as a function of melting temperature and time. They used a soda-lime-silica batch with and without small additions of As_2O_3 and/or $NaNO_3$ as fining agents.
It was found that when As_2O_3 was used as a fining agent the O_2/CO_2 ratio in the bubbles increased with the melting time. From this a bubble growth mechanism by oxygen in-diffusion was concluded.
The optimum concentration of fining agents was shown to correspond with a maximum in the concentration of oxygen in the bubbles formed. A bubble growth mechanism by oxygen in-diffusion was also concluded by Nemec ([12]), who used direct observation of large bubbles at melting temperatures, and Mulfinger ([13]) and Van Erk et al ([14]), who studied bubble content as a function of melting time in various glasses. It was suggested in ref. 14 that small oxygen bubbles which did not disappear by rising to the surface of the melt are resorbed upon cooling.

Oxygen resorption upon cooling has been experimentally confirmed by investigations of Greene et al ([9,13]), who studied the dissolution of oxygen bubbles in well-refined soda-lime-silica glass melts.
An As_2O_3 fining mechanism for small bubbles of bubble inflation by O_2 in-diffusion, followed by O_2 resorption upon cooling cannot work, however. Bubbles, which are found at the end of a normal melting process, always contain N_2 and/or CO_2.
When during melting a badly soluble N_2/CO_2 bubble is formed it may be inflated by O_2 in-diffusion upon temperature increase. If this inflated bubble does not rise to the surface of the melt and O_2 is resorbed again upon cooling a N_2/CO_2 bubble still remains. The disappearance of insoluble bubbles from a glass melt is an irreversible process; a thermally induced shift in As^{3+}/As^{5+} ratio, causing oxygen release or resorption is a reversible process. A simplification that has always been made in previous studies on fining mechanisms is that the fining part of the melting process is regarded separately from the initial batch reactions.
It is shown in the investigations of this thesis that this is an oversimplification. Important irreversible shifts in the As^{3+}/As^{5+} ratio are found to occur just in the initial batch reactions before the formation of the product glass melt.

III. Experimental work

The experimental work consisted in essence of the measurement and interpretation of laser Raman spectra taken from glass-forming batches which had reacted for different times under various conditions. A simple model system was chosen of composition:

30 mol% K_2CO_3 – 70 mol% SiO_2 with and without
0.5 or 1 mol% As_2O_3.

The system offered the following advantages:

- The composition is the simplest possible for silicate batches, reducing the number of intermediate compounds in the reactions.
- Raman spectra of potassium silicate glasses are relatively well resolved compared to sodium (and lithium) silicate glasses.
- The system shows similar melting and fining characteristics as the practical systems.
- 30 K_2O.70 SiO_2 glass shows no phase separation effects ([17]) which may result in special effects as regards the fining process.
- The glass composition corresponds to disilicate ($K_2Si_2O_5$) which is also the case for practical soda-lime-silica based systems.
- Arsenic compounds give relatively intense and well resolved Raman peaks, compared to antimony compounds.

In laser Raman spectroscopy (LRS) samples are irradiated with an intense laser beam and the inelastic components of the scattered light are analysed using a high performance spectrometer system. A Raman spectrometer system consists of a double monochromator and a Peltier-cooled photomultiplier tube together with a photon counting or direct current amplication system.
In many cases the spectra of the scattered light show peaks at frequencies ν higher and lower than the frequency ν_0 of the primary light source. The energy differences $h\nu_v = |h(\nu - \nu_0)|$ correspond to energy differences between quantum levels in the irradiated systems.
The spontaneous Raman effect, considered here, is shown schematically in fig. 2. Normally the "Stokes" spectrum is measured as it is more intense as the "Anti-Stokes" spectrum. In the investigations presented in this thesis the vibrational Raman effect is measured in which the energy levels, involved in the Raman process, are caused by vibrational modes of molecular bonds.

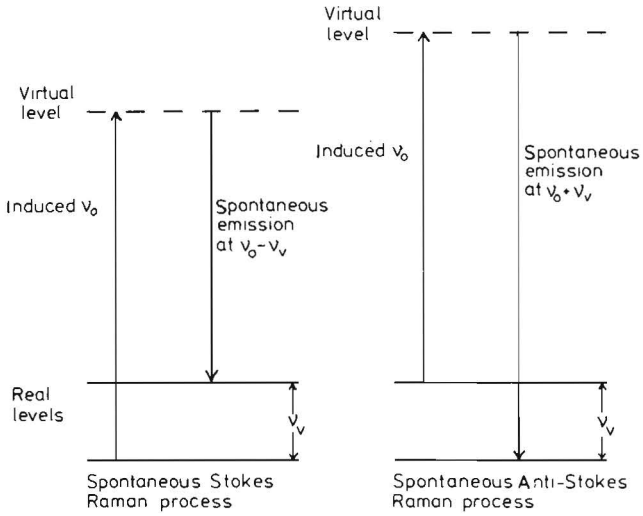

Fig. 2 The Stokes and Anti-Stokes spontaneous Raman processes, schematic.

The use of LRS as an analytical technique for identification and quantitative determination of vitreous and crystalline phases in glass-forming mixtures offered the following advantages:

- The method is non-destructive.
- There are no surface effects.
- Quantitative determination of both crystalline and vitreous phases.
- No absorption effects for the systems investigated.
- Identification of unknown phases by group frequencies.
- Raman spectra of glasses with networks which are based on XO_4 tetrahedra or XO_3 pyramids are well resolved and characteristic. This makes LRS particular useful for identification of these glasses in multi-phase solid state mixtures.

For identification purposes a number of glasses and crystalline compounds were prepared and their Raman spectra were taken and interpreted in terms of network structure. The following systems have been investigated:

- $K_2O - SiO_2 - CO_2$ glasses,
- $K_2O - As_2O_5$ glasses and the compounds γ-$KAsO_3$, $K_5As_3O_{10}$, $K_4As_2O_7$ and α-K_3AsO_4,
- $K_2O - As_2O_3$ glasses and the compounds K_3AsO_3, $KAsO_2$ and KAs_3O_5.

An attempt was made to obtain an accurate non-destructive determination of shifts in As^{3+}/As^{5+} ratios in potassium silicate glasses as a function of melting temperature and composition. For this purpose high accuracy Raman glass spectra were recorded under full computer control after which the intensity ratio of characteristic As^{3+} and As^{5+} peaks was determined.

IV. Summary of the papers and manuscripts in this thesis

In this section an outline is given of the results and discussions of the papers and manuscripts in this thesis. They are listed in chronological order in the reference list as refs. 18-24. Ref. 20 gives the basic ideas of the author on As_2O_3 fining. It contains a Raman study of the batch reactions in a 30 K_2CO_3 – 70 SiO_2 – 1 As_2O_3 batch together with a proposal for the fining mechanism of As_2O_3.

An older study of batch reactions in the same system, but without As_2O_3, is given in ref. 19.

A study of the fining part of the melting process is given in ref. 24, where arsenate and arsenite structures, occuring in potassium silicate glass melts, are identified by their Raman spectra. The intensities of arsenate and arsenite Raman peaks are used in ref. 24 to study the effect of temperature and glass composition on the As^{3+}/As^{5+} ratio.

For identification purposes Raman studies were performed of arsenates (ref. 21) and arsenites (ref. 23) in the vitreous and crystalline state.

In ref. 18 a study of the Raman spectra of carbonate ions, dissolved in potassium silicate glasses, is reported. It appeared that in glasses with batch composition x K_2CO_3 (100-x) SiO_2 large amounts of CO_2 remained dissolved for compositions with $x > 40$, especially at low melting temperatures. The peaks in the Raman spectra of the glasses, caused by dissolved CO_2, could be very well ascribed to CO_3^{2-} with D_{3h} symmetry. The results of ref. 18 were used in the batch reaction studies of refs. 19 and 20.

In ref. 19 the chemical reactions in a model glass-forming system with batch composition 30 K_2CO_3 – 70 SiO_2 were followed.

Batch mixtures were fired for various times and temperatures and the Raman spectra of the quenched powdered reaction products were taken. Crystalline potassium disilicate ($K_2Si_2O_5$) was identified in the mixtures in addition to carbonate rich silicate glass in the initial stage of the reaction, while disilicate glass was found when the reaction approached completion. The glasses found in the mixtures after quenching to room temperature correspond to liquid phases at the reaction temperatures.

From the Raman spectra a reaction process was derived which was divided into three stages:

1. SiO_2 grains in the batch are attacked by K_2CO_3 with the formation of a crystalline $K_2Si_2O_5$ layer directly around them and a potassium-rich liquid layer containing metasilicate chains and carbonate ions.
2. When all the K_2CO_3 has been used in the reactions of stage 1, the potassium concentration in the liquid phase decreases by diffusion of potassium into the SiO_2 grains (the cores of which are still present) and more crystalline $K_2Si_2O_5$ is formed.
   The carbonate solubility decreases rapidly with the decrease of the potassium concentration in the liquid phase and CO_2 has therefore to escape (cf. refs. 18, 25).
3. After completion of the diffusion process small SiO_2 cores are still present, surrounded by crystalline $K_2Si_2O_5$ and a liquid phase with about the same composition. When the reaction temperature remains below the melting

temperature of $K_2Si_2O_5$ (1015°C), the liquid phase will convert slowly into crystalline $K_2Si_2O_5$. A mixture of SiO_2 and mainly $K_2Si_2O_5$ will be the result.
However, at temperatures above 1015°C the $K_2Si_2O_5$ phase will melt completely, and the remaining SiO_2 will dissolve.

Apparently CO_2 does not escape directly with the reaction of K_2CO_3 and SiO_2 but instead a carbonate-containing liquid is formed which releases CO_2 slowly with the formation of the silicate melt.

In ref. 21 a Raman study of glasses and crystalline compounds in the K_3AsO_4 – $KAsO_3$ system is given. The results of this study were used for identification purposes in refs. 20 and 24.
The compounds α-K_3AsO_4, $K_4As_2O_7$, $K_5As_3O_{10}$ and γ-$KAsO_3$ were prepared by solid state reaction of $KHAsO_4$ and K_2CO_3.
Glasses of composition x $K_2O.As_2O_5$ with x = 1-2, were prepared by fast quenching of melts.
The structures of the compounds γ-$KAsO_3$, $K_4As_2O_7$ and α-K_3AsO_4 were deduced from analogy with sodium arsenates, the structures of which were known from the literature.
The compounds γ-$KAsO_3$, $K_4As_2O_7$ and α-K_3AsO_4 were concluded to consist of $As_nO_{3n+1}^{-n-2}$ chains of AsO_4 tetrahedra.
The structure of the compound $K_5As_3O_{10}$ was determined, as described in ref. 22, by X-ray single crystal diffraction and was found to consist of strongly bent $As_3O_{10}^{5-}$ chains.
The network structure of the x $K_2O.As_2O_5$ glasses was derived by comparison of their Raman spectra with the powder spectra of the crystalline compounds and proved to resemble closely the structure of the arsenate ions in the crystalline compounds. It was concluded that $As_nO_{3n+1}^{-n-2}$ chains were present in the glasses with $n = \infty$ for x = 1 to n = 2 for x = 2.

In ref. 23 the preparation and Raman spectra of compounds and glasses in the system K_2O – As_2O_3 are described. The spectral data from this study were used again for identification purposes in refs. 20 and 24.
The crystalline compounds K_3AsO_3, $KAsO_2$ and KAs_3O_5 were identified in fired mixtures of KOH and As_2O_3 by inspection of the Raman spectra of these mixtures. The structure of the compound K_3AsO_3 was concluded from stoichiometry to contain AsO_3^{3-} pyramids.
The structure of the compound $KAsO_2$ was deduced from analogy with the compound $NaAsO_2$, whose structure is known to contain chains of AsO_3 pyramids. A hypothesis for the structure of KAs_3O_5 was given, proposing a network of chains of As_3O_3 rings connected via a bridging oxygen atom.
Potassium arsenite glasses with molar composition $K_2O.xAs_2O_3$ with x = 1,2 and 3, were prepared in sealed quartz tubes and their Raman spectra were taken. By comparison of these Raman spectra with those of the crystalline compounds, a network structure of interconnected As_2O_3 rings was concluded for the glasses with x = 2 and 3 and a structure of simple chains of AsO_3 pyramids for the glass with x = 1.

In ref. 24 a Raman study is reported of arsenate and arsenite structures in potassium silicate glasses. In this study an analysis is made of the As^{3+}/As^{5+} ratio in 30 K_2O.70 SiO_2 glasses as a function of temperature to study the reactions of arsenic in the fining region of the glass melting process. The glasses had a batch composition: x K_2CO_3-(100-x)SiO_2-0.5 As_2O_3 with x = 10, 20, 30, 35, 40 and 50. The melting temperatures were 1400°C for x = 20, 35, 40 and 50; 1600°C for x = 10 and 1300, 1400, 1500 and 1600°C for x = 30. The melting atmosphere was oxygen.
The contributions to the Raman spectra of the glasses, which were caused by the As_2O_3 additions were obtained by preparing difference spectra of glasses with the same x with and without As_2O_3 additions, using computer controlled data acquisition.

It was found that for $35 < x < 50$ arsenic is mainly present in the pentavalent state as AsO_4^{3-} ions, while for $x < 35$ pentavalent arsenic was found in $As_2O_7^{4-}$ or $As_3O_{10}^{5-}$ ions and trivalent arsenic as $As_nO_{2n+1}^{-n-2}$ chains which n increasing at decreasing x.
From the intensities of the Raman peaks caused by the arsenite and arsenate structures it was found that, besides the strong increase of the As^{3+}/As^{5+} ratio going from x = 50 to x = 30, there is a weaker increase going from x = 30 to 10.
For the glasses with x = 30 no significant temperature effect was found on the As^{3+}/As^{5+} ratio. So, using this result, the "classical" hypothesis for arsenic fining, which assumes a temperature induced O_2 development, cannot be true for 30 K_2O.70 SiO_2 glass.
It is interesting to remark at this point that preliminary results of a study of the 15 Na_2CO_3-10 $BaCO_3$-75 SiO_2-0.5 As_2O_3 system indicate that liquid-liquid phase separation phenomena above 1400°C may give a chemically induced O_2 development, which can be interpreted as a temperature effect.

In ref. 20 a study is reported of the batch reactions in a glass-forming mixture of molar composition 30 K_2CO_3-70SiO_2-1 As_2O_3 using the same techniques as in ref. 19.
It was found that the chemical reactions in this mixture follow the same path as in the mixture without arsenic as far as the silicates and carbonates are concerned. The reaction path of the arsenic compounds could be followed very well and turned out to be connected with the formation of silicate during the reactions.
In accordance with the division for the 30 K_2CO_3-70 SiO_2 mixture (ref. 19) three reaction stages were again distinguished:

1. SiO_2 grains are attacked by K_2CO_3 with the formation of $K_2Si_2O_5$ and a potassium-rich liquid containing carbonate. As_2O_3 forms crystalline K_3AsO_4, possibly by the mechanism of Eichorn (cf. ref. 6 and section 2). This K_3AsO_4 dissolves in the liquid phase, forming AsO_4^{3-} tetrahedra.
2. The potassium concentration in the liquid phase decreases gradually by out-diffusion, accompanied by the release of CO_2.

During this process the dissolved AsO_4^{3-} ions become instable because of the lower cation concentration and condense according:

$$2\,K_3AsO_4 + 2\,SiO_2 \longrightarrow K_4As_2O_7 + K_2Si_2O_5$$

The lower potassium concentration also favors the trivalent state of arsenic and part of the $As_2O_7^{4-}$ ions react in its turn according to:

$$n\,K_4As_2O_7 + (2n-4)SiO_2 \longrightarrow 2\,K_{n+2}As_nO_{2n+1} + (n-2)\,K_2Si_2O_5 + nO_2\uparrow$$

In this reaction $As_nO_{2n+1}^{n-2}$ chains are formed which is accompanied by the formation of oxygen.

3. The remaining SiO_2 cores dissolve in the silicate melt. During this process more arsenite and O_2 is formed as the potassium concentration in the melt lowers further (cf. ref. 24).

From the observed reaction path of arsenic during the melting reactions a mechanism for the fining action of arsenic in silicate glass batches is formulated which is based on the oxygen release, triggered by the chemical reactions during the melting process.

In the first stages of the melting reactions a foamy mixture of various phases is formed, with bubbles or pores containing CO_2 form the carbonates in the batch and N_2 from the furnace atmosphere or from decomposed nitrates. The initially formed liquid phase is rich in alkali and/or alkaline earth ions and contains carbonate and AsO_4^{3-} ions. As the reaction proceeds the cation concentration in the liquid phase decreases so that the solubility of the carbonate decreases drastically and CO_2 gas is liberated.

When after the bulk release of CO_2 gas the final (disilicate) composition is reached in the liquid phase, the AsO_4^{3-} ions react to more condensed arsenates and arsenites. This causes an increasing release of O_2 from the liquid phase which sweeps CO_2 and N_2 in open pores away and which inflates closed bubbles in the melt. The sweep effect is particularly effective as O_2 is formed near the surface of dissolving SiO_2 grains where the cation concentration is lowest.

Finally in the raw silicate melt only O_2 bubbles remain which disappear very easily by dissolution.

This mechanism is different from the "classical" hypothesis of temperature induced oxygen release. It does not reject the classical hypothesis of temperature triggered O_2 release, but it forms at least a very important contribution to the process of As_2O_3 fining.

V. Final remarks

In the authors' opinion a fairly consistent picture has now been obtained of the behavior of arsenic in glass melting reactions and of its function in the fining process. It was found that it is very well possible to follow chemical processes, which occur during glass-formation, by the use of laser Raman spectroscopy as an analytical technique.

When the method of LRS is applied to study practical large scale processes it will be possible to obtain optimal temperature – time curves for the melting process and it will also be possible to obtain an optimal choice of raw materials and batch preparation. In conclusion the following topics are interesting for future studies:

- The behavior of Sb_2O_3 during glass-melting. Preliminary studies have indicated that "antimony peaks" in Raman glass spectra can be obtained from computer-processed difference spectra.
- The function of nitrate additions.
- Non-destructive CO_2 analyses in practical glasses from their Raman spectra. Previous attempts to do this have failed but the recently available computer-controlled data acquisitation opens new perspectives.
- Quantitative Raman studies of batch reaction and fining kinetics in practical glass-forming systems to support furnace design an process control.
- Further accurate As^{3+}/As^{5+} (and Sb^{3+}/Sb^{5+}) analyses in various glass systems using computer processed Raman data, chemical analysis or ESCA. Continued work in this field would be particularly useful for studies of the effect of temperature, atmospheric conditions and phase-separation phenomena on the As^{3+}/As^{5+} ratio in various glass systems.

References

[1] G. Rindone, "Fining: I", Glass Ind., **38** [9] 489-93, 516, 526, 528 (1957).

[2] Glass Making (Melting and Fining): Bibliographic Review of the Union Scientifique Continentale du Verre, Charleroi, Belgium, 1973.

[3] J. Stanek, "New Aspects in Melting of Glass", J. Non-Cryst. Solids, **26** [1-3] 158-178 (1977).

[4] M. Cable, "Glass Making, The Melting Process", Glastekn. Tidskr., **24** [6] 147-152 (1969).

[5] M. Cable, "Study of Refining III", Glass Technol., **2** [4] 151-158 (1961).

[6] H.J. Eichorn, "Reaction Behavior of Arsenic in Simple Glass Batches in Dynamical Thermal Conditions", Silikattechnik, **26** [1] 28 (1975).

[7] S. Bajo, "Volatalization of Arsenic (III, V), Antimony (III, V) and Selenium (IV, VI) from Mixtures of Hydrogen Fluoride and Perchlorid Acid Solution: Application to Silicate Analysis", Anal. Chem., **50** [4] 649-651 (1978).

[8] M. Cable, "Study of Refining I", Glass Technol., **1** [4] 144-154 (1960).

[9] M. Cable, "Study of Refining II", Glass Technol., **2** [2] 60-70 (1961).

[10] M. Cable, A.R. Clarke and M.A. Haroon, "The Effect of Arsenic on the Composition of the Gas in Seed During the Refining of Glass", Glass Technol., **10** [1] 15-21 (1969).

[11] M. Cable and M.A. Haroon, "The Action of Arsenic as a Refining Agent", Glass Technol., **11** [2] 48-53 (1970).

[12] L. Nemec, "Refining in the Glass Melting Process", J. Am. Ceram. Soc., **60** [9-10] 436-440 (1977).

[13] H.O. Mulfinger, "Use of Gas Analysis to Follow the Refining Process in Crucible and Tank", Glastechn. Ber., **49** [10] 232-245 (1976).

[14] K.C. van Erk, E. Papanikolau and W. van Pelt, pp. 137-146 in Glass 1977 Vol. IV, Edited by J. Goetz, North Holland Publishing Co., Amsterdam, 1977.

[15] C.H. Greene and D.R. Platts, "Behavior of Bubbles of Oxygen and Sulfur Dioxide in Soda-Lime Glass", J. Am. Ceram. Soc., **52** [2] 106-109 (1969).

[16] C.H. Greene and H.A. Lee, "Effect of As_2O_3 and $NaNO_3$ on the Solution of O_2 in Soda-Lime Glass", J. Am. Ceram. Soc., **48** [10] 528-533 (1965).

[17] W. Vogel, Glas Chemie, Deutscher Verlag für Grundstoffen Industrie Leipzig, 1979.

[18] H. Verweij, H. van den Boom and R.E. Breemer, "Raman Scattering of Carbonate Ions Dissolved in Potassium Silicate Glasses", J. Am. Ceram. Soc., **60** [11-12] 529-534 (1977). Thesis: page 8.

[19] H. Verweij, H. van den Boom and R.E. Breemer, "Raman Spectroscopic Study of the Reactions in a Potassium Carbonate-Silica Glass-Forming Batch", J. Am. Ceram. Soc., **61** [3-4] 118-121 (1978). Thesis: page 14.

[20] H. Verweij, "Raman Study of the Reactions in a Glass-Forming Mixture with Molar Composition: 30 K_2CO_3-70 SiO_2-1 As_2O_3", J. Am. Ceram. Soc., **62** [9-10] 450-455 (1979). Thesis: page 18.

[21] H. Verweij, "Raman Study on Glasses and Crystalline Compounds in the System K_3AsO_4 – $KAsO_3$", Appl. Spectr., **33** [5] 509-515 (1979). Thesis: page 24.

[22] J. Hornstra and H. Verweij, "Structure of Potassium Arsenate $K_5As_3O_{10}$" Acta Cryst. **B36**, in press (1980). Thesis: page 31.

[23] H. Verweij en J.G. van Lierop, "Raman Spectra of Crystalline Compounds and Glasses in the System K_2O – As_2O_3", J. Phys. Chem. Glasses, submitted for publication. Thesis: page 33.

[24] H. Verweij, "Raman Spectra of Arsenic-Containing Potassium Silicate Glasses", J. Am. Ceram. Soc., submitted for publication. Thesis: page 39.

[25] M.L. Pearce, "Solubility of Carbon Dioxide and Variation of Oxygen Activity in Soda-Silica Melts", J. Am. Ceram. Soc., **47** [7] 342-347 (1964).

Reprinted from the Journal of The American Ceramic Society, Vol. 60, No. 11-12, November-December, 1977

Raman Scattering of Carbonate Ions Dissolved in Potassium Silicate Glasses

H. VERWEIJ, H. VAN DEN BOOM, and R. E. BREEMER

Philips Research Laboratories, Eindhoven, The Netherlands

Raman spectra of glasses, prepared from a mixture of K_2CO_3 and SiO_2, give evidence for the presence of almost isolated planar CO_3^{2-} ions, dissolved in the glass. It appears that measurement of the Raman spectra is a useful nondestructive method for the determination of the CO_3^{2-} concentration in glasses.

I. Introduction

A STUDY of potassium silicate glasses by Pisarchik *et al.*[1] indicated that after SiO_2 and K_2CO_3 were melted to a glass,

Received February 2, 1977; revised copy received May 30, 1977.

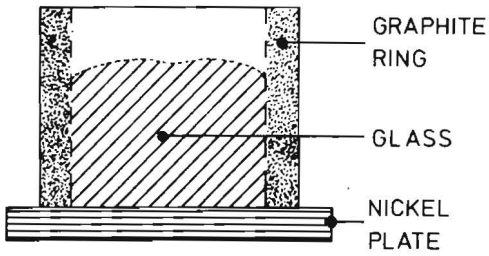

Fig. 1. Setup for pouring glass samples with flat surfaces.

large quantities of CO_3^{2-} remained. They assigned the absorption band at 1400 to 1500 cm^{-1} (observed in the ir spectrum of a glass prepared from 50 mol% K_2CO_3 and 50 mol% SiO_2) to vibrations within CO_3^{2-} groups dissolved in the glass.

Weil[2] and Kroeger and Goldmann[3] measured the CO_2 concentrations of alkali-silicate glasses by vacuum extraction. Pearce[4] measured CO_2 concentrations in soda-silica melts using C^{14}-enriched CO_2. All the investigators[1-4] observed a strong increase of CO_2 solubility in alkali-silicate glasses on increase of the alkali content. Recent testing with Raman spectroscopy[5] showed that carbonate-rich glasses (with CO_3^{2-} concentrations >1 mol%) occurred as an intermediate product during the glassmelting process in a $30K_2CO_3$-$70SiO_2$ batch. A detailed Raman study of carbonate-containing glasses was begun because: (1) We are interested in the molecular structure of CO_3^{2-}, dissolved in glass, and (2) Raman spectroscopy is a nondestructive analytical tool with a high spatial resolution[6] (<10 μm) which can be used to determine CO_3^{2-} concentrations as a function of position in the glass. The present study measured glasses with batch composition $xK_2CO_3(1-x)SiO_2$ with $x=0.40$, 0.45, and 0.50 mol.

II. Experimental Procedure

The glasses were prepared by mixing K_2CO_3* (purity >99.9%) and SiO_2 (ground rock crystal; mean particle size 250 μm, purity >99.999%); this mixture was melted in an Al_2O_3† crucible in air. The reacting mixtures were very foamy. The batches, which had a total weight of 50 g, were introduced in 5-g portions at intervals of at least 5 min. After the last portion was introduced, the melt was allowed to stand in the oven for 1 h, with the temperature kept constant within 1°C.

This glassmelt was poured into a preheated graphite ring placed on a nickel plate which was polished to optical flatness (Fig. 1); the temperature of both was ≈400°C. In this way, a glass sample with a cylindrical shape and a sufficiently flat surface was obtained. The sample was tempered in a dry oxygen flow. The Raman measurements were performed with an exciting wavelength of 5145 Å (argon-laser).‡ The apparatus is described in Refs. 7 and 8. During the measurements the sample was placed in a dry CCl_4-filled cell (Fig. 2). Because the samples were very hygroscopic, all sample handling at room temperature was performed in a dry nitrogen-filled glove bag.§

For comparison, Raman polarization measurements were performed on a solution of K_2CO_3 and KOH in water. The KOH was added to ensure that no HCO_3^- ions were present in the solution. The measurements were made with a special rotating cell which made it possible to eliminate the water bands from the spectrum (Ref. 9). The Raman spectra of some water-free carbonates were obtained from powdered, thoroughly dried samples contained in a capillary 1 mm wide. Some ir spectra were also taken, using the KBr technique. The CO_2 content of the glass samples was determined by extraction at 1000°C in O_2, followed by a conductometric determination (Table IV).

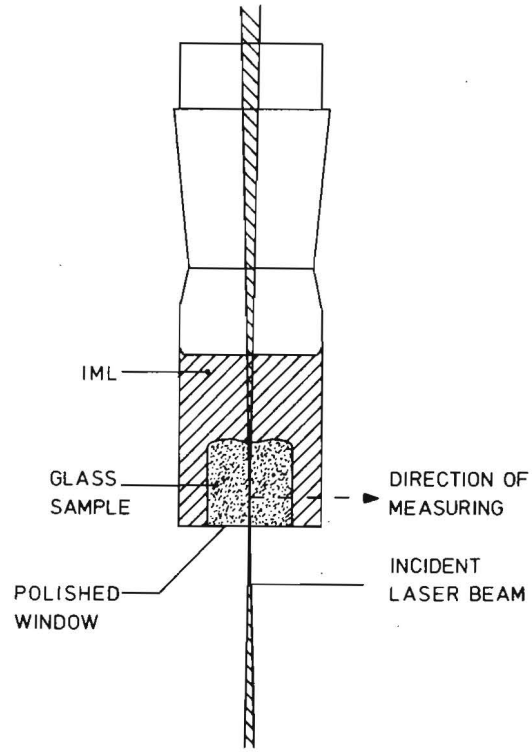

Fig. 2. Cell for polarization measurements.

III. Experimental Results

Figures 3(*A*) and (*B*) show the Raman spectra (optical measuring geometry: *X(ZZ+ZX)Y*, according to Ref. 10; in our case *X* is the direction of the primary beam; *Y* is the direction of observation; *Z* is the direction perpendicular to the *XY* plane) of glasses melted from $xK_2CO_3(1-x)SiO_2$ with $x=0.40$, 0.45, and 0.50 mol, at a melting temperature of 1100°C. The assignment of most of the observed peaks has been described in the literature.[11,12] Peaks at 1100, 590, and 550 cm^{-1} have been assigned to a disilicate network occurring in crystalline $K_2O{\cdot}2SiO_2$. Peaks at 940 and 590 cm^{-1} have been assigned to a metasilicate network occurring in crystalline $K_2O{\cdot}SiO_2$. The peak at 830 cm^{-1} is assigned to an isolated SiO_4^{4-} tetrahedron occurring in various orthosilicates. The disilicate network has 1 nonbridging oxygen ion (NBO); the metasilicate chain has 2 NBO's and the SiO_4^{4-} tetrahedron has 4 NBO's. The Raman spectra of the glasses also clearly show peaks at 1040, 680, 1428, and 1770 cm^{-1}, which so far have not been related in the literature[11,12] to vibrations in a silicate network. Figures 4(*A*) and (*B*) give the Raman spectra (optical measuring geometry: *X(ZZ+ZX)Y*) of glasses with batch composition $50K_2CO_3$-50 SiO_2, melted at 1000°, 1100°, and 1200°C. The relative intensity of the peaks at 1770, 1428, 1040, and 680 cm^{-1} is seen to decrease as melting temperature increases, although the relative intensity of the 830 cm^{-1} peak (orthosilicate) increases with melting temperature.

Polarization properties of the Raman spectrum of a glass with $x=0.50$, melted at 1100°C, were measured. Spectra with optical measuring geometries *X(ZZ)Y* and *X(ZX)Y* are given in Figs. 5(*A*) and (*B*) in which it can be observed that the silicate peaks at 940, 830, and 590 and the peaks at 1040 and 1770 cm^{-1} are strongly polarized, while the peaks at 1428 and 680 cm^{-1} are depolarized. Experimentally the corrected depolarization ratio ($\rho=I_{ZX}/I_{ZZ}$) of the peak at 1428 cm^{-1} is found to be 0.8 ± 0.1. The correction for systematic errors has been performed, with the aid of the 318 cm^{-1} line of CCl_4. The depolarization ratio of the 1770 cm^{-1} line is very close to zero. The exact values of the depolarization ratio for the

*E. Merck AG, Darmstadt, Federal Republic of Germany.
†Quality A123. Degussa, Frankfurt, Federal Republic of Germany.
‡CR52, Cohe iation, Palo Alto, Calif.
§Model 1[2]-R, Instruments for Research and Industry, Cheltenham, Pa.

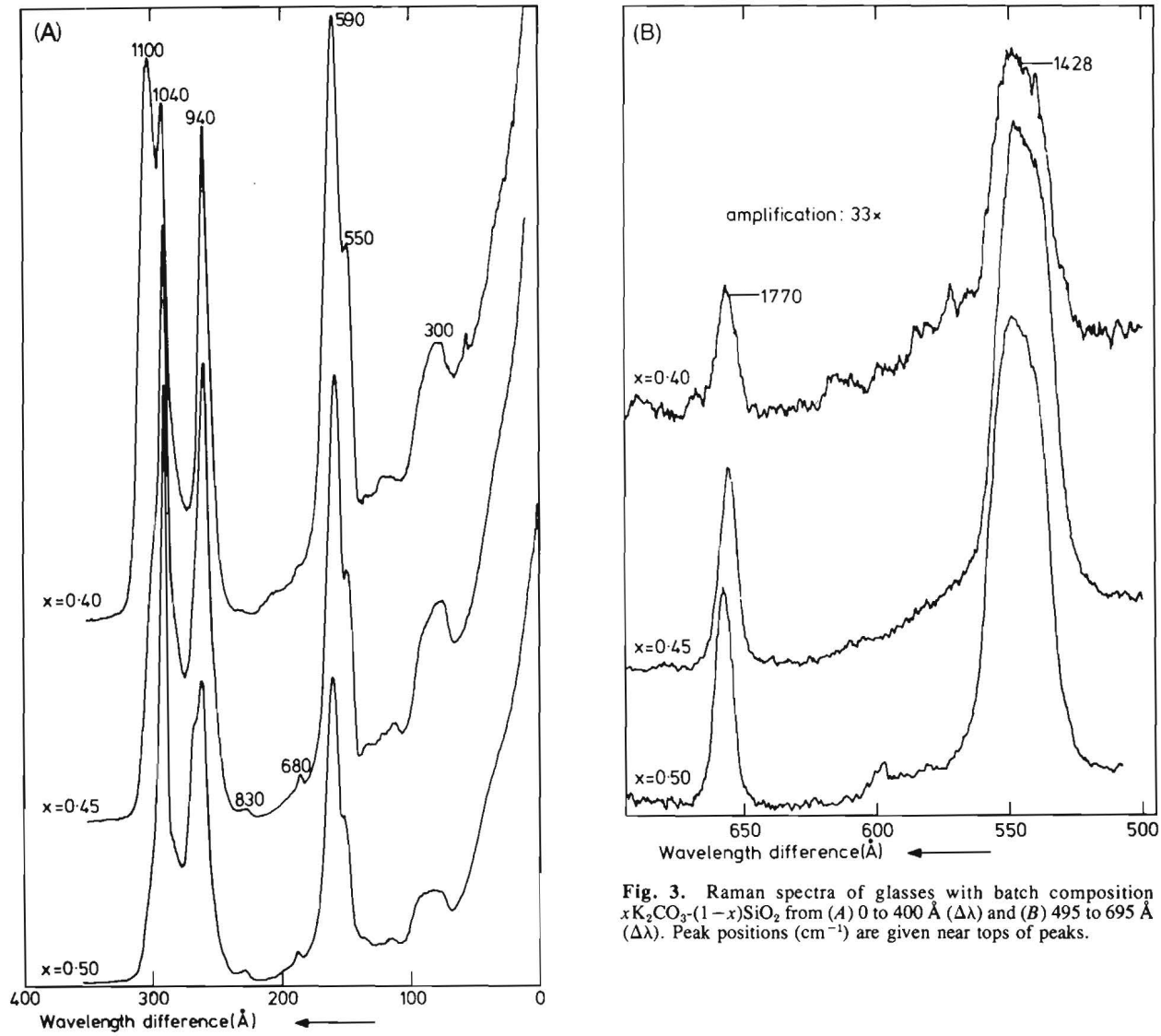

Fig. 3. Raman spectra of glasses with batch composition xK_2CO_3-$(1-x)SiO_2$ from (*A*) 0 to 400 Å ($\Delta\lambda$) and (*B*) 495 to 695 Å ($\Delta\lambda$). Peak positions (cm^{-1}) are given near tops of peaks.

Table I. Observed Vibrational Modes (cm^{-1}) of Various Waterfree Carbonates*

	A_1' mode		A_2'' mode	E′ mode		E′ mode		$A_2''\times A_2$ mode	Reference	
Compound	Raman	ir	ir	Raman	ir	Raman	ir	Raman	Raman	ir
Li_2CO_3	1088s	1090w	865m	1458w	1450s +1510s	708w +747w	720m +740w	1769w	om	13
Na_2CO_3	1076s		880m	1425w	1450s	697w		1764w	om	13
K_2CO_3	1053s	1060w	880m	1396w	1450s	678w	710m	1759w	om	13
$RbCO_3$	1052s	1050w	876m	1391w	1380s	683w	778m	1763w	om	om
$CsCO_3$	1034s	1050w	877m	1378w	1350s	671w	673m 677m	1755w	om	om
$CaCO_3$ (calcite)	1081s		875m	1431w	1450s	707m	715m	1744w	om	13
$SrCO_3$	1067s	1070w	860m	1444w	1450s	696m	700m 710m	1765w	om	13
$BaCO_3$	1057s	1060w	860m	1419w	1450s	689m	695m	1768w	om	13

*s = strong, m = medium, w = weak, om = own measurements.

peaks at 1040 and 680 cm^{-1} cannot be determined, owing to the background, although it is clearly seen that the line at 1040 cm^{-1} has a depolarization ratio near zero, whereas the line at 680 cm^{-1} is depolarized.

Measurements of a solution of K_2CO_3 in water showed 1 strongly polarized peak at 1064 cm^{-1} ($\rho = 0.07 \pm 0.01$) and 2 relatively weak depolarized peaks at 1420 and 686 cm^{-1}. The depolarization ratio of these peaks at 1420 and 686 could not be measured with accuracy, due to their very low intensity.

IV. Discussion of the Results

In this section it is shown that in the Raman spectra of glasses with batch composition $xK_2CO_3(1-x)SiO_2$ with $x = 0.40$, 0.45, and 0.50, peaks at 1770, 1428, 1040, and 680 cm^{-1} can be ascribed to the CO_3^{2-} ion dissolved in the glass. Table I gives observed Raman and ir bands of various crystalline carbonates. It can be seen that the peak positions are almost independent of the cation type and there is a striking similarity between the Raman lines of the crystalline carbonates and the carbonate lines observed in the glass. The sym-

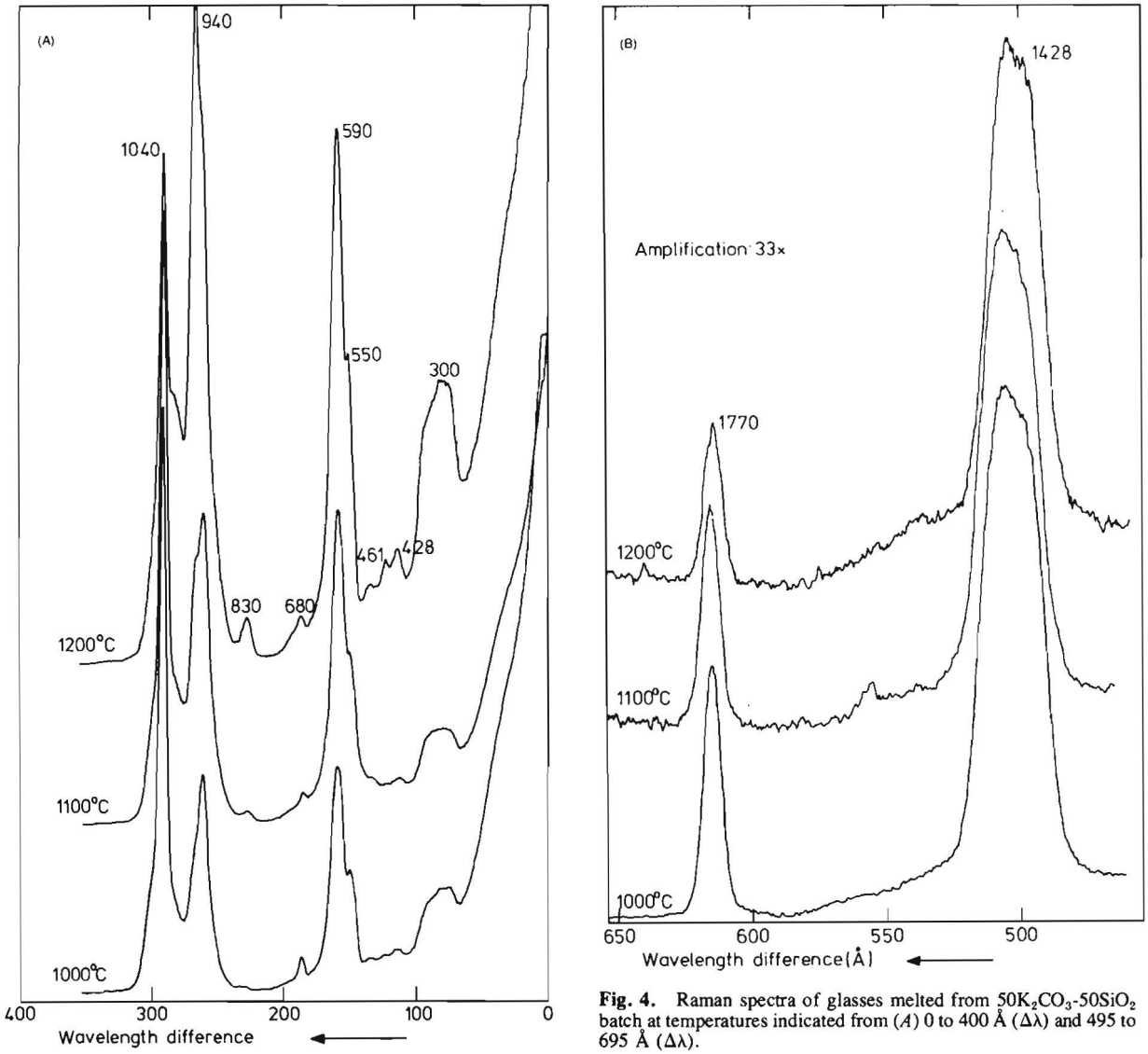

Fig. 4. Raman spectra of glasses melted from $50K_2CO_3$-$50SiO_2$ batch at temperatures indicated from (*A*) 0 to 400 Å ($\Delta\lambda$) and 495 to 695 Å ($\Delta\lambda$).

Table II. Vibrational Modes of D_{3h} CO_3^{2-} (Refs. 14, 16)*

Mode	Symmetry	Raman	Polarization	ir	Assignment
ν_1	A_1'	a(s)	p	ia	C-O sym. stretch
ν_2	A_2''	ia		a(m)	CO_3 out of plane deformation
ν_3	E′	a(w,broad)	dp	a(s)	C-O assym. stretch
ν_4	E′	a(w,m)	dp	a(m)	In-plane deformation
$2\nu_2$	A_1'	a(w)	p	ia	Overtone

*a = active, ia = inactive, s = strong, m = medium, w = weak, p = polarized, dp = depolarized.

metry of the free CO_3^{2-} ion is D_{3h}. The vibrational modes are given in Table II.[14,15] For D_{3h} CO_3^{2-}, Herzberg[16] calculated the frequencies to be $\nu_1=1063$, $\nu_2=879$, $\nu_3=1415$, and $\nu_4=680$ cm^{-1}; ν_1 is polarized and ν_3 and ν_4 are depolarized. Poulet and Mathieu[15] pointed out that the first overtone of the ir-active vibration ν_2 (symmetry A_2'', Table II) might be Raman active and has symmetry A_1' ($A_2''\times A_2''=A_1'$ for D_{3h} symmetry). This overtone is to be expected at $\approx$1760 cm^{-1} and is expected to be polarized. In the glasses with batch composition $0.50K_2CO_3$-$0.50SiO_2$, it is observed (Fig. 5) that the peaks at 1040 and 1770 cm^{-1} are strongly polarized and that the peaks at 1428 and 680 cm^{-1} are depolarized. In a perfect D_{3h} symmetry the depolarization ratio (I_x/I_z) can have any value between 0 and 0.75 for the peaks at 1040 cm^{-1} and 1770 cm^{-1} and should be 0.75 for the peaks at 1428 and 680 cm^{-1}.[17]

From measurements on the free CO_3^{2-} ion in aqueous solution, it appears that the depolarization ratio for the symmetrical stretch vibration (symmetry A_1') at 1064 cm^{-1} is 0.07, which is in good quantitative agreement with the observed depolarization ratio in the glass. The lines at 1420 and 686 cm^{-1} are depolarized. From these results we conclude that the carbonate ion dissolved in glass is comparable with a carbonate ion dissolved in water and has symmetry D_{3h}.

In Table III the results of the measurements on the $50K_2CO_3$-50 SiO_2 glass, the crystalline K_2CO_3 powder, the aqueous solution, and the calculations by Herzberg[16] are compared. In Figs. 4(*A*) and (*B*), where the dependence of the melting temperature on the spectra of the glasses is demonstrated, it is observed that the relative intensity of the orthosilicate (4 NBO's) peak at 830 cm^{-1} increases and the relative intensity of the carbonate peaks decreases with increasing melting temperature, so the number of NBO's increases with an

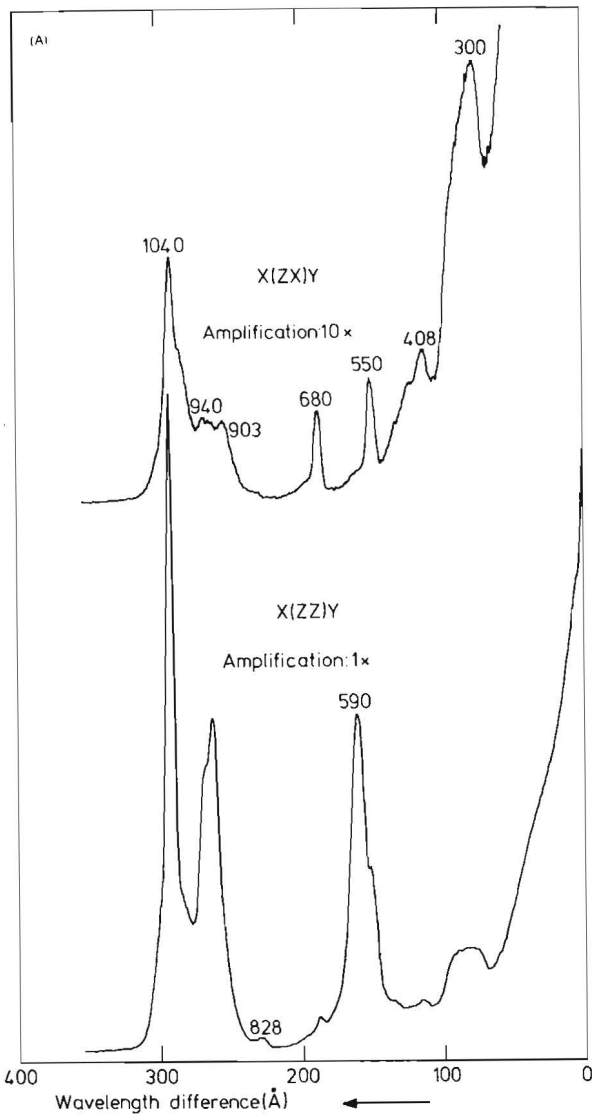

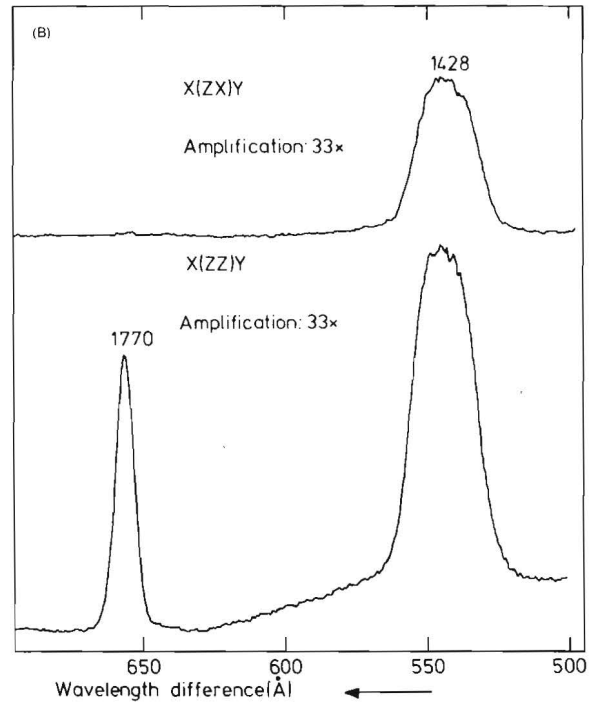

Fig. 5. Raman spectra of $50K_2CO_3$-$50SiO_2$ glass melted at 1100°C obtained using different optical measuring geometries from (*A*) 0 to 400 Å ($\Delta\lambda$) and (*B*) 495 to 695 Å ($\Delta\lambda$).

increase of melting temperature. From this observation we conclude that the carbonate ions take some potassium away from the network.

Figures 3(*A*) and 4(*A*) show that the shape of the silicate band around 575 cm^{-1} is almost the same for all compositions, so for rough estimates the height of this band may be used as an internal intensity standard. In Table IV the relative peak heights of the carbonate peaks at 1420 and 1770 cm^{-1} are compared with the CO_2 concentrations as determined by chemical analysis. It can be seen from Table IV that there is good agreement between the data. From this fact and from the fact that no Raman peaks were found that can be ascribed to other forms of dissolved CO_2, we may conclude that the major part of the CO_2 is dissolved as CO_3^{2-}

V. Final Remarks

In the preceding section the conclusion was drawn that in the glasses with batch composition $xK_2CO_3(1-x)SiO_2$ with $x=0.40$, 0.45, and 0.50 the major part of the CO_2 is dissolved as planar CO_3^{2-}. However, it is not quite clear to what degree CO_3^{2-} ions are isolated from their environment. In this paper we looked at glasses containing more than 1 mol% CO_2 (Table IV). In these glasses the

Table III. Comparison of the Raman Data of $50K_2CO_3$-$50SiO_2$ Glass, K_2CO_3 Powder, CO_3^{2-} Solution, and the Calculations by Herzberg[15]

Mode	Sym.	Glass energy (cm^{-1})	Dep. ratio	K_2CO_3† energy(cm^{-1})	CO_3^{2-} in H_2O energy(cm^{-1})	Dep. ratio	Calc. by Herzberg Energy(cm^{-1})	Calc. by Herzberg Dep. ratio
ν_1	A_1'	1040	≈0.0*	1053	1064	0.07±0.01	1063	p
ν_3	E'	1420	0.8±0.1	1396	1420	dp*	1415	0.75
ν_4	E'	680	dp*	678	696	dp*	680	0.75
$2\nu_2$	A_1'	1760	0.00	1759	Not present			

*Cannot be measured with accuracy. †Dep. ratio cannot be measured on powders.

Table IV. Comparison of Chemical Analysis of CO_2 Content and Raman Data

Sample	Temp. (°C)	Analyzed CO_2 (mol/mol SiO_2)	Idem related to sample 1	$I_{(1428)}/I_{(575)}$ ($\times 10^{-2}$)	Idem related to sample 1	$I_{(1770)}/I_{(575)}$ ($\times 10^{-2}$)	Idem related to sample 1
$50K_2CO_3$-$50SiO_2$	1000	0.27	1	7.2	1	3.6	1
$50K_2CO_3$-$50SiO_2$	1100	.20	0.75	4.8	0.68	2.3	0.66
$50K_2CO_3$-$50SiO_2$	1200	.094	.35	3.0	.41	1.1	.31
$45K_2CO_3$-$55SiO_2$	1100	.091	.34	3.6	.50	1.5	.43
$40K_2CO_3$-$60SiO_2$	1100	.052	.19	1.6	.23	0.8	.22

intensities of the peaks caused by CO_3^{2-} are of the same order of magnitude as the intensities of the silicate peaks.

Investigators are studying the usefulness of Raman spectroscopy for the quantitative determination of CO_2 concentrations in practical glasses. An attempt will be made to use the 1428 cm^{-1} and 1770 cm^{-1} peaks, which are very well isolated from the silicate peaks, for a space-resolved nondestructive analytical determination for the CO_2 concentration.

Acknowledgment: Thanks to A. Meyer and D. Verspaget for performing the chemical analysis and to T. W. Bril for useful suggestions.

References

[1] N. M. Pisarchik, V. D. Mazurenko, and B. K. Bogush, "IR and X-Ray Studies of Crystallization in Some K_2CO_3·$CaCO_3$·SiO_2 System Glasses," *Zh. Prikl. Spektrosk.*, **15** [2] 278–82 (1971).

[2] Woldemar Weyl, "Reactions of Carbon Dioxide with Silicates Under High Pressure," *Glastech. Ber.*, **9** [12] 641–60 (1931).

[3] C. Kroeger and N. Goldmann, "Solubility of Carbon Dioxide in Glasses," *ibid.*, **35** [11] 459–66 (1962).

[4] M. L. Pearce, "Solubility of Carbon Dioxide and Variation of Oxygen Ion Activity in Soda-Silica Melts," *J. Am. Ceram. Soc.*, **47** [7] 342–47 (1964).

[5] H. Verweij and H. van den Boom; pp. 529–34 in Reactivity of Solids 8. Edited by J. Wood, O. Lindqvist, C. Helgesson, and N-G. Vannerberg. Plenum, New York, 1977.

[6] J. J. Barrett and N. I. Adams, "Laser-Excited Rotation-Vibration Raman Scattering in Ultrasmall Gas Samples," *J. Opt. Soc. Am.*, **58** [3] 311–19 (1968).

[7] J. H. Haanstra and A. T. Vink, "Localized Vibrations in GaP Doped with Mn or As," *J. Raman Spectrosc.*, **1** [1] 109–15 (1973).

[8] H. van den Boom and J. H. Haanstra, "Raman Spectra of Vibrational Modes in Spinel $CdIn_2S_4$," *ibid.*, **2** [3] 265–74 (1974).

[9] H. van den Boom and R. E. Breemer, "Simple Setup for Raman Difference Spectroscopy," *Rev. Sci. Instrum.*, **46** [12] 1664–66 (1976).

[10] T. C. Damen, S. P. S. Porto, and B. Tell, "Raman Effect of Zinc Oxide," *Phys. Rev.*, **142** [2] 570–74 (1966).

[11] W. L. Konijnendijk and J. M. Stevels, "Raman Scattering Measurements of Silicate Glasses and Compounds," *J. Non-Cryst. Solids*, **21** [3] 447–53 (1976).

[12] S. A. Brawer and W. B. White, "Raman Spectroscopic Investigation of the Structure of Silicate Glasses: I," *J. Chem. Phys.*, **63** [6] 2421–32 (1975).

[13] R. A. Nyquist and R. O. Kagel, Infrared Spectra of Inorganic Compounds. Academic Press, New York and London, 1971.

[14] B. M. Gatehouse, S. E. Livingstone, and R. S. Nyholm, "Infrared Spectra of Some Simple and Complex Carbonates," *J. Chem. Soc.*, **1958**, No. 8–10, pp. 3137–42.

[15] H. Poulet and J. P. Mathieu, Vibrational Spectra and Symmetry of Crystals; p. 338. Gordon & Breach, Paris, 1970 (in Fr.).

[16] Gerhard Herzberg, Molecular Spectra and Molecular Structure, Vol. II, 2d ed.; p. 178. Van Nostrand, Princeton, N.J., 1945.

[17] J. A. Koningstein, Introduction to the Theory of the Raman Effect; pp. 125–30. D. Reidel Publishing, Boston, Mass., 1972.

Reprinted from the Journal of The American Ceramic Society, Vol. 61, No. 3-4 March-April, 1978

Raman Spectroscopic Study of the Reactions in a Potassium Carbonate-Silica Glass-Forming Batch

H. VERWEIJ, H. VAN DEN BOOM, and R. E. BREEMER

Philips Research Laboratories, Eindhoven, The Netherlands

Raman investigation results are presented for the reaction products formed in a glass-forming batch. With Raman spectroscopy it is possible to identify the various glassy and crystalline phases which occur during the reactions. This is demonstrated on a batch containing 30 mol% K_2CO_3 and 70 mol% SiO_2. It is also shown that CO_2 gas is released via an intermediate glassy product. A qualitative description of the reaction process is given.

I. Introduction

STUDIES OF glass-forming reactions are important for a better understanding of the total process of glassmaking, including melting, fining, and homogenization. Most studies on glass-forming reactions have been performed on Na_2CO_3-$CaCO_3$-SiO_2

Received May 9, 1977; revised copy received August 16, 1977.

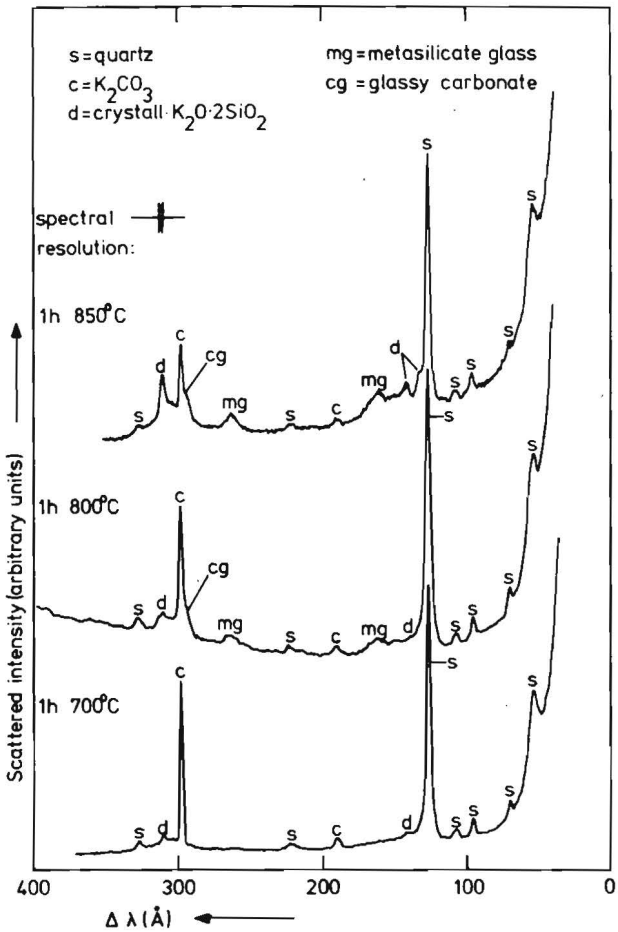

Fig. 1. Raman spectra of incompletely reacted $30K_2CO_3$-$70SiO_2$ batches.

glass-forming batches,[1] generally using X-ray diffraction and thermal analysis methods.

X-ray diffraction gives information about crystalline components, which are present in concentrations of >5 mol%, but information about glassy components or about the reaction path of low-concentration additives cannot be obtained with it.

Thermal analysis techniques give indirect structural information only. With thermogravimetry the CO_2 emission can be studied and differential thermal analysis gives information about thermal effects. Therefore, for glass-forming batches, the thermal analysis techniques do not give direct information about the reaction components or products that are actually present. These techniques are useful, but a complete picture of the glassmelting process cannot be obtained from them. For these reasons, Raman spectroscopy was used for identification in the present study. Raman spectra of crystalline and glassy compounds are highly characteristic and very well resolved. Many examples of Raman spectra of vitreous and crystalline borates and silicates are given in Ref. 2.

It is also possible to obtain semiquantitative information about the reaction products by measuring the relative peak intensities of specific peaks in the spectrum. It might even be possible to obtain quantitative information with the aid of standards.

The present writers studied glass formation using a batch with composition 30 mol% K_2CO_3-70 mol% SiO_2. This composition was chosen because the silicon content is about the same as in practical glasses, the system is relatively simple compared with the usual multicomponent systems, and Raman spectra of potassium silicate glasses are well known in the literature.[2,3]

II. Experimental Procedure

Materials were α-quartz (milled rock crystal) with a sieve fraction of 180 to 250 μm and K_2CO_3* dried at 300°C for 24 h. The components were mixed by ball-milling; 10-g portions were used for each experiment.

Samples were fired in cylindrical Pt10Rh crucibles (70 mm high, 30 mm in diam.) in an electrically heated furnace with temperature control within 0.5°C. The mixtures were heated at various temperatures for varying times, then quenched in vitreous silica vessels which were subsequently evacuated. Samples were crushed and ground in an agate mortar and the resulting material was transferred into sample tubes (50 mm long, 1 mm ID). Because the samples were hygroscopic, they were handled at room temperature inside a nitrogen-filled glove bag.† Raman spectra were measured using an argon ion laser‡ operating at a wavelength of 5145 Å. Power on the sample was ≈600 mW. To get rid of unwanted plasma lines a Fabry-Perot etalon§ was used, set at a free spectral range of 50 cm^{-1}. A more detailed description of the laser Raman apparatus is given in Ref. 4.

Table I. Raman Data for Crystalline SiO_2, K_2CO_3, $K_2O·SiO_2$, $K_2O·2SiO_2$, and $K_2O·4SiO_2$

SiO_2 (Ref. 6)			K_2CO_3 (Ref. 7)		
cm^{-1}	Δλ* (Å)	I†	cm^{-1}	Δλ (Å)	I
207	55	w	678	186	w
356	96	w	1053	295	s
401	108	w	1396	398	w
464	126	s	1759	512	w
697	191	w	$K_2O·SiO_2$ (Ref. 3)		
795	219	w	490	133	m
807	223	w	563	153	w
1072	300	w	585	160	m
1085	304	w	963	268	s
1162	327	w	1015	283	w
$K_2O·2SiO_2$ (Ref. 3)			$K_2O·4SiO_2$ (Ref. 8)		
245	66	w	305	82	m
280	75	w	340	92	m
365	98	w	420	114	s
490	133	m	510	139	m
520	141	m	525	143	m
1105	310	s	1075	301	m
			1110	312	m
			1160	327	m

*λ = 5145 Å, †w = 0 to 10% of the strongest peak (underlined), m = 10 to 50% of the strongest peak (underlined), and s = 50 to 100% of the strongest peak (underlined).

III. Results

Figure 1 gives the Raman spectra of powdered samples, fired for 1 h at various temperatures. Three crystalline compounds and three types of molecules in the vitreous state can be identified in these spectra. The identification is based on position, relative intensity, and shape (width) of the peaks.

For identification, Raman data of crystalline compounds and glasses in the system K_2O-CO_2-SiO_2 are important. From the crystalline compounds K_2CO_3, SiO_2 (α-quartz), $K_2O·4SiO_2$ (Ref. 5), $K_2O·2SiO_2$ (Ref. 5), and $K_2O·SiO_2$ (Ref. 5) are of interest. The most relevant Raman data for these compounds are given in Table I.

As far as we know, no ternary compounds in the system K_2O-CO_2-SiO_2 have been reported in the literature; Raman spectra of K_2O-SiO_2 glasses are well known.[2,3,8] A study of CO_2-containing glasses in the system K_2O-CO_2-SiO_2 is given in Ref. 7, which also shows that, in glasses melted from K_2CO_3-SiO_2 batches containing 40 to 50% mol K_2CO_3, CO_2 is dissolved in the form of planar CO_3^{2-} ions in concentrations of >1 mol%. These CO_3^{2-} ions give Raman peaks at 679, 1036, 1428, and 1770 cm^{-1}; these CO_3^{2-} ions in the vitreous state are called vitreous carbonate.

*E. Merck AG, Darmstadt, Federal Republic of Germany.
†Model 12R, Instruments for Research and Industry, Cheltenham, Pa.
‡Model 52, Coherent Radiation, Palo Alto, Calif.
§Model CL 100, Tropel, Inc., Fairport, N.Y.

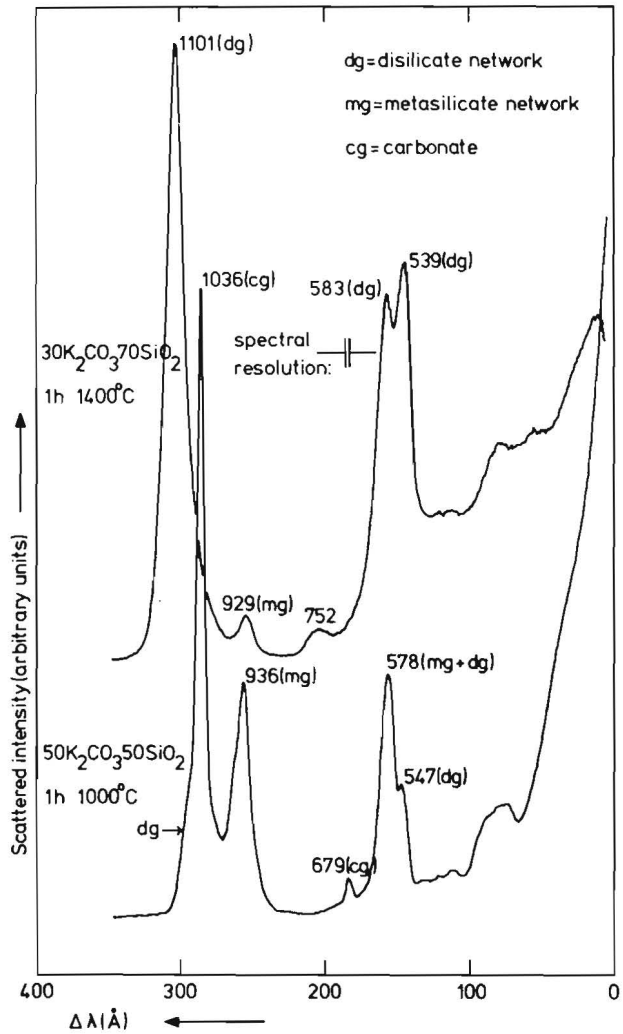

Fig. 2. Raman spectra of glasses fired from $30K_2CO_3$-$70SiO_2$ and $50K_2CO_3$-$50SiO_2$ batches.

Figure 2 gives two examples of Raman spectra of glasses that can be melted from a K_2CO_3-SiO_2 batch. The upper spectrum is for a glass with a batch composition of 30 mol% K_2CO_3-70 mol% SiO_2. The silicate network of this glass is mainly disilicate (vitreous $K_2O{\cdot}2SiO_2$[2,3,8]). The lower spectrum is for a glass with a batch composition of $50K_2CO_3$-$50SiO_2$. The silicate network of this glass is mainly metasilicate (vitreous $K_2O{\cdot}SiO_2$[2,3,7,8]). Furthermore, a large quantity of dissolved CO_3^{2-} (vitreous carbonate (0.27 mol CO_3^{2-}/mol SiO_2 (Ref. 7)) is present in this glass.

Crystalline SiO_2 (α-quartz) is identified in each of the spectra of Fig. 1. Crystalline K_2CO_3 is found in the spectra of the samples fired at 700°, 800°, and 850°C and crystalline $K_2O{\cdot}2SiO_2$ is identified in each spectrum. Peaks which can be ascribed to vitreous carbonate, vitreous K_2O-SiO_2, $K_2O{\cdot}2SiO_2$ are clearly observed in some of the spectra of Fig. 1. It is not certain how many separate vitreous phases are present in the incompletely reacted batches. In Section IV a reaction model is presented with one vitreous phase having a K^+ concentration gradient. From measurements on samples fired at the same temperature for various times it appears that the concentration of vitreous carbonate goes through a maximum in time.

Figure 3 gives spectra of $30K_2CO_3$-$70SiO_2$ mixtures fired at 900°C for various times. From the relative peak intensities in the spectra it is obvious that the vitreous carbonate concentration is already decreasing. The concentration of vitreous $K_2O{\cdot}SiO_2$ appears to be coupled with the vitreous carbonate concentration. The present writers found that the spectra of the fired $30K_2CO_3$-$70SiO_2$ mixtures are derived entirely from the spectra of the observed components.

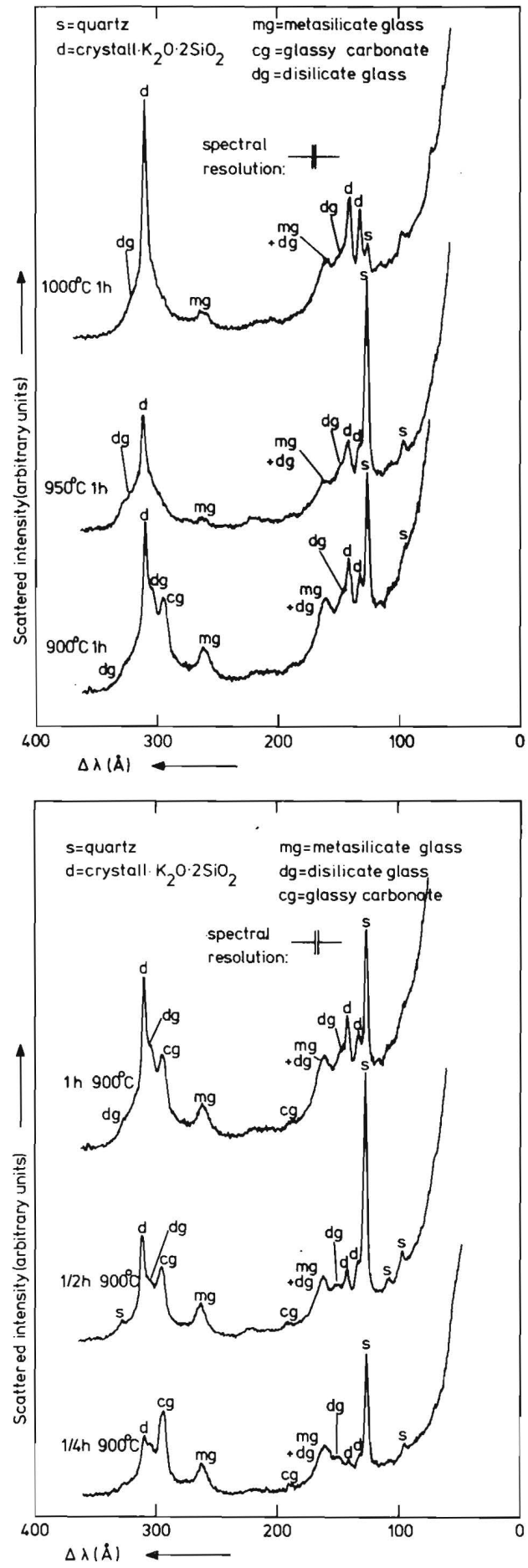

Fig. 3. Raman spectra of incompletely reacted $30K_2CO_3$-$70SiO_2$ batches fired at 900°C for varied times.

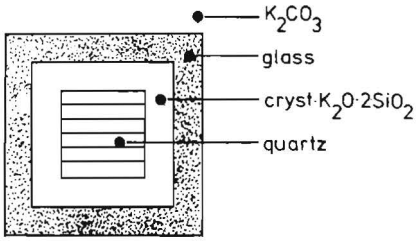

Fig. 4. Schematic of SiO_2 grain which has undergone attack.

IV. Discussion

By using the previously obtained results, a qualitative description of the reaction process in a $30K_2CO_3$-$70SiO_2$ batch at 700° to 1000°C can be derived.

The reaction products observed in the spectra are crystalline $K_2O \cdot 2SiO_2$, vitreous $K_2O \cdot SiO_2$, vitreous $K_2O \cdot 2SiO_2$, and vitreous carbonate. These results indicate a reaction in which different phases are formed in layers around the SiO_2 grains present in the batch and in which the K^+ ions, supplied by the K_2CO_3, are much more mobile than the Si^{4+} ions.

The first layer around the SiO_2 consists of crystalline $K_2O \cdot 2SiO_2$, whereas the second layer (around the $K_2O \cdot 2SiO_2$ layer) should contain the vitreous $K_2O \cdot SiO_2$, vitreous carbonate, and vitreous $K_2O \cdot 2SiO_2$ since the K^+ concentration must decrease continuously as it moves to the center of the attacked grain.

Figure 4 is a schematic of an attacked SiO_2 grain. The glass layer is probably not homogeneous in composition; at the interface of the glass and the crystalline $K_2O \cdot 2SiO_2$ the K_2O concentration in the glass will be $\approx$33 mol% (vitreous $K_2O \cdot 2SiO_2$) whereas the K_2O concentration at the outside of the glass layer may be as much as 50 mol% (vitreous $K_2O \cdot SiO_2$ together with vitreous carbonate). The CO_3^{2-} in the glass layer may vary from concentrations of the order of 0.1 mol CO_3^{2-}/mol SiO_2 at the alkali-rich side[7] to very low concentrations at the interface with the crystalline $K_2O \cdot 2SiO_2$.

Below 1015°C (melting point of $K_2O \cdot 2SiO_2$) the glass phase is an intermediate reaction product. This is consistent with the fact that the concentration of vitreous carbonate goes through a maximum. As long as K_2CO_3 is present the vitreous carbonate concentration will increase, but when the K_2CO_3 has disappeared the K^+ ions will diffuse out of the glass until a total concentration of $\approx$33 mol% K_2O in the glass is reached. When the K_2O concentration in the glass is lowered, the CO_2 solubility decreases drastically and the total vitreous carbonate concentration will decrease.

V. Summary

At 700° to 1000°C crystalline $K_2O \cdot 2SiO_2$ is the first phase formed in a $30K_2CO_3$-$70SiO_2$ batch and an intermediate glassy phase is formed, which contains large quantities of dissolved CO_3^{2-}. In the present paper only a qualitative description of the reactions is given. In future, standards will be used to gain a more quantitative insight into the reactions so that they may be compared with quantitative solid state reaction models.

References

[1] Glass-Making (Melting and Fining). Bibliographic Review; pp. 267 and 157. Union Scientifique Continentale du Verre, Charleroi, Belgium, 1973.

[2] W. L. Konijnendijk, "Structure of Borosilicate Glasses," *Philips Res. Rep. Suppl.*, **1975**, No. 1 (thesis); 243 pp.

[3] S. A. Brawer and W. B. White, "Raman Spectroscopic Investigation of the Structure of Silicate Glasses: I," *J. Chem. Phys.*, **63** [6] 2421–32 (1975).

[4] J. H. Haanstra and A. T. Vink, "Localized Vibrations in GaP Doped with Mn or As," *J. Raman Spectrosc.*, **1** [1] 109–15 (1973).

[5] F. C. Kracek, N. L. Bowen, and G. W. Morey, "Equilibrium Relations and Factors Influencing Their Determination in the System K_2SiO_3-SiO_2," *J. Phys. Chem.*, **41** [9] 1183–93 (1937).

[6] J. F. Scott and S. P. S. Porto, "Longitudinal and Transverse Optical Lattice Vibrations in Quartz," *Phys. Rev.*, **161** [3] 903–10 (1967).

[7] H. Verweij, H. van den Boom, and R. E. Breemer, "Raman Scattering of Carbonate Ions Dissolved in Potassium Silicate Glasses," *J. Am. Ceram. Soc.*, **60** [11–12] 529–34 (1977).

[8] H. Verweij and W. L. Konijnendijk, "Structural Units in K_2O-PbO-SiO_2 Glasses by Raman Spectroscopy," *ibid.*, **59** [11–12] 517–21 (1976).

Reprinted from the Journal of the American Ceramic Society, Vol. 62, No. 9-10 September-October, 1979

Raman Study of the Reactions in a Glass-Forming Mixture with Molar Composition: $30K_2CO_3$-$70SiO_2$-$1As_2O_3$

HENK VERWEIJ*

Philips Research Laboratories, Eindhoven, The Netherlands

The results of a study of the reactions in a glass-forming batch with molar composition $30K_2CO_3$-$70SiO_2$-$1As_2O_3$ are given. Laser Raman spectroscopy was used for nondestructive identification of silicate, carbonate, arsenite (As^{3+}), and arsenate (As^{5+}) ions in the vitreous or crystalline state, occurring in quenched reaction mixtures. It is shown that in the first stage of melting a potassium-rich liquid phase is formed, containing metasilicate chains $(SiO_3^{2-})_\infty$ and carbonate ions, in which all arsenic is present in the pentavalent state as AsO_4^{3-} ions. When this liquid phase reaches the final product glass composition the AsO_4^{3-} ions condense to $As_2O_7^{4-}$ (As^{5+}) ions and AsO_2^- (As^{3+}) groups, during which process O_2 is formed. The preliminary results of studies on crystalline and vitreous potassium arsenates and arsenites and of arsenic-containing potassium silicate glasses are given for identifying arsenate and arsenite groups. It is argued that the reaction mechanism found describes the effectiveness of As_2O_3 as a fining agent. Contrary to the current view in the literature for the fining action of As_2O_3, which states that an O_2 evolution which is triggered by a temperature increase causes fining, an important effect is found in the O_2 evolution triggered by alkali oxide concentration variations during melting.

I. Introduction

One of the major problems in glassmelting technology is the occurrence of small gas bubbles with diameters of 20 to 1000 μm.[1-3] Quality demands regarding bubble content of the final glass products are becoming increasingly stringent, especially for flat glass, optical glass, and glass for television tubes.

Besides the application of ever higher melting temperatures, many methods have been proposed and applied to shorten the time needed for glassmelts to become bubble-free[1-3] (i.e. to speed up the fining process), since the normal rise of bubbles to the surface of the melt takes too long. Among these methods are physical methods, such as stirring, control of glass streams, and application of low pressure or ultrasound, and chemical methods like bubbling oxygen and the addition of the so-called fining agents, the most important of which are sulfates in combination with carbon and halides and the compounds As_2O_3 and Sb_2O_3 in combination with nitrates. These compounds are widely used in the glass industry. Our interest was to investigate the reactions of arsenic (As_2O_3) in silicate glass-forming batches in relation to the fining process.

The total melting process can be divided into two stages: (1) reaction of the batch components, during which the carbonates are decomposed and the silica grains dissolve until a glassmelt which is very inhomogeneous and contains many gas bubbles is formed, and (2) fining and homogenization of the glassmelt. These two processes occur at about the same time; the rise of large bubbles to the surface of the melt contributes largely to the homogenization. The sources of bubbles are usually gases, developed during the melting reactions, especially from the decomposition of carbonates or from trapped air. However, the fining process of the glassmelt is coupled to the chemical reactions in the first stages of melting[4]; to obtain a complete picture of the glassmelting process the chemical reactions of batch components and fining must be studied.

Presented at the 80th Annual Meeting, The American Ceramic Society, Detroit, Michigan, May 9, 1978 (Glass Division No. 37 G 78). Received November 27, 1978; revised copy received February 5, 1979.

* Member, the American Ceramic Society.

The present paper gives a Raman spectroscopic study of the behavior of As_2O_3 during melting in a glass-forming system. A model system was chosen with a batch composition of $30K_2CO_3$-$70SiO_2$-$1As_2O_3$, which is compatible to the system chosen in Ref. 5 (see Section I (1)).

(1) Survey of Studies of Reactions of Batch Components With and Without As_2O_3

Glass-forming reactions have been studied primarily in the system Na_2CO_3-$CaCO_3$-SiO_2 using X-ray diffraction (XRD) or thermal analysis techniques.[1,3,4] In a review of studies of batch component reactions, Cable[4] stated that the information obtained is not very useful to the glass manufacturer, probably because it is usually too limited. Identification of liquid intermediate products, which play an important role in the melting process, was not possible in the studies reported.

However, this difficulty can be overcome by using laser Raman spectroscopy as an identification technique.[5] A study of batch component reactions in a model glass-forming system with molar composition $30K_2CO_3$-$70SiO_2$ is reported in Ref. 5, where vitreous and crystalline phases occurring in the batches were identified by Raman spectra of mixtures which were quenched after firing for different times at various temperatures. The reaction products were identified from peak positions, peak widths, and relative intensities in the Raman spectra of powdered reaction mixtures.

From the experimental results a reaction scheme was proposed for the region of 700° to 1000°C, in which two layers of reaction product are formed around the SiO_2 grains present in the batch. The first layer, directly surrounding the SiO_2 grains, consists of crystalline $K_2O \cdot 2SiO_2$ and the layer surrounding the $K_2O \cdot 2SiO_2$ consists of a liquid phase (vitreous at room temperature) which is very rich in potassium and contains large amounts of dissolved CO_3^{2-} in the first stages of the reaction, when large amounts of K_2CO_3 are still available. As the reaction proceeds, K^+ ions diffuse out of the liquid layer through the $K_2O \cdot 2SiO_2$ layer into the SiO_2 grains. The reduction in the K_2O concentration in the liquid layer (until the final product glass composition is reached) drastically decreases the CO_2 solubility, and CO_2 must escape. As a consequence the final CO_2 emission, which causes the major part of bubble formation, occurs at about the same time as the final product glass composition is reached in $30K_2CO_3$-$70SiO_2$ glass-forming batches.

No structure-identification studies have been reported for the behavior of small As_2O_3 additions to glass-forming batches during the chemical reaction of batch components. Cable[6] studied the reaction products of a mixture of molar composition $3Na_2CO_3$-$1As_2O_3$ heated at various temperatures. He concluded that Na_3AsO_4 forms at ≈700°C and that some elemental As forms at lower temperatures. Karch[7] postulated that the following reactions occur at 1000°C:

$$5As_2O_3 \rightarrow 4As + 3As_2O_5 \quad (1)$$

$$2As + {}^3/_2O_2 \rightarrow As_2O_3 \quad (2)$$

$$As_2O_5 + 3Na_2CO_3 \rightarrow 2Na_3AsO_4 + 3CO_2\uparrow \quad (3)$$

and at the glassmelting temperature (1400°C):

$$2Na_3AsO_4 + 3SiO_2 \rightarrow 3Na_2SiO_3 + As_2O_3 + O_2\uparrow \quad (4)$$

The formation of Na_2SiO_3 in this formula is probably symbolic of the formation of the final product glass; the evaporation of As_2O_3

contradicts the observations reported by many writers, which show that arsenic remains in the glass, even at 1400°C.[6,8,9]

The low-temperature reactions proposed by Karch[7] were corrected by Eichorn[10] to:

$$5As_2O_3 + 5Na_2CO_3 \xrightarrow{180-350°C} 10NaAsO_2 + 5CO_2 \uparrow \quad (5)$$

$$10NaAsO_2 + 4Na_2CO_3 \xrightarrow{300-500°C} 6Na_3AsO_4 + 4CO_2 \uparrow + 4As \quad (6)$$

Elemental As is probably reoxidized by O_2 from the air or by nitrates added to the batch. Both writers studied mixtures of Na_2CO_3 and As_2O_3 using XRD for identification.

(2) Studies of the Fining Mechanism of As_2O_3

The fining mechanism of As_2O_3 has been the subject of many studies for several years, the most important recent ones being those by Cable *et al.*,[6,11-14] Greene *et al.*,[9,15] Nemec,[16] and Mulfinger.[17]

Cable and coworkers studied glasses with molar batch composition $16.5Na_2CO_3$-$10CaCO_3$-$73.5SiO_2$ with and without As_2O_3, Na_2O_2, or $NaNO_3$ as refining agents. Cable[12] stated that large bubbles disappear from the melt by rising to the surface and that small bubbles disappear by a dissolution mechanism. He also stated[6] that good refining requires that bubbles formed in the early stages of melting must be very rich in oxygen. Cable *et al.*[13] showed that the optimum concentration of refining agents corresponds to a maximum in the O_2 content of the bubbles formed.

When As_2O_3 or Sb_2O_3 are used as refining agents, the O_2/CO_2 ratio in bubbles increases with the melting time from which a bubble growth mechanism by O_2 in-diffusion or CO_2 dissolution, considered less probable, is concluded. Furthermore, some N_2 bubbles are found after long melting times.

A bubble growth mechanism by oxygen in-diffusion was also proposed by Mulfinger,[17] Van Erk *et al.*,[18] who studied gas bubble content as a function of melting time, and Nemec,[16] who used direct observation of large bubbles at melting temperatures. These writers also suggested that O_2 bubbles are resorbed in the cooled melt. This suggestion is supported by the investigations of Greene and Lee,[9] and Greene and Platts,[15] who studied the dissolution of O_2 bubbles in well-refined glasses. They found that O_2 bubbles dissolved rapidly at temperatures below that at which the glass was melted.

When the mechanism of bubble growth by O_2 in-diffusion at increasing temperatures, followed by O_2 resorption at decreasing temperatures, is valid there must be a shift of the As^{3+}/As^{5+} ratio as a function of temperature. The present writer knows of no systematic study of the As^{3+}/As^{5+} ratio as a function of temperature, perhaps because chemical analysis of As^{3+}/As^{5+} in glass is rather difficult.

(3) Conclusions

The existing literature data give a reasonably consistent picture of the function of arsenic during the refining of glass, although an accurate analysis of As^{3+}/As^{5+} as a function of temperature is still needed to prove the proposed mechanisms. Few data are available regarding the reactions of As_2O_3 during the glassmelting reactions and its relation with fining.

It is proposed that: (1) Arsenic is present mainly in the pentavalent state at relatively low temperatures; (2) a temperature increase triggers an O_2 evolution, caused by an increase of the As^{3+}/As^{5+} ratio, the O_2 diffusing into and inflating the bubbles so that they may easily rise to the surface of the melt; and (3) O_2 bubbles resorb on cooling.

An accurate analysis of As^{3+}/As^{5+} in glassmelts as a function of temperature and atmosphere is still needed to prove the proposed mechanisms. Few data are available concerning the behavior of As_2O_3 during the glassmelting reactions and the relation with the fining process.

II. Experimental Procedure

The materials used were α-quartz* (milled rock crystal, sieve fraction 180 to 250 μm), K_2CO_3† (reagent grade, dried at 300°C for 24 h, coarse grains ≈ 1 mm), and As_2O_3† (reagent grade sublimated).

Samples of molar composition $30K_2CO_3$-$70SiO_2$-$1As_2O_3$ were mixed mechanically by tumbling for 20 h. For each experiment 10-g portions were fired in air in cylindrical Pt10Rh crucibles (70 mm high by 30 mm in diam.) inside an electrically heated furnace. Temperature measurement was accurate within 2°C; temperature was controlled by a proportional band (PID) controller in combination with a thyristor unit and was constant within 1°C. The mixtures were heated for 1 h at 700° to 1100°C. At 1100°C a clear glass was formed, containing many bubbles. The reacting mixtures were very foamy. After heating, the crucibles containing the reacted mixture were quenched in vitreous silica vessels which were subsequently evacuated. These samples were crushed and ground in an agate mortar and the powder was transferred into vitreous silica sample tubes (5.8 by 4.2 mm in diam. and ≈40 mm long) provided with stoppers. After filling, the tubes were sealed. Because the samples were very hygroscopic, all handling at room temperature was done inside nitrogen-filled glove bags.‡

The Raman spectra of the powdered samples were measured with the sample tube rotating at ≈1000 rpm to average out sample inhomogeneity. The spectra were excited using a 4 W continuous Ar^+ laser,§ operating at a wavelength of 5145 Å with a light output stabilization of 0.5%. A 10 Å bandpass interference filter¶ was placed in the primary beam to avoid unwanted plasma lines. Power on the sample was ≈200 mW and the spot size of the laser beam at the sample was ≈50 μm.

The spectrometer‖ used consisted of a double monochromator with concave holographic gratings, a step-motor drive, a Peltier-cooled photo multiplier tube,** a dc amplifier†† in combination with a double RC filter set to a time constant of 5 s, and a recorder.‡‡ A polarization scrambler (¼-wave plate) was mounted at the entrance of the monochromator to remove the effects of polarization-dependent system response. Scanning speed was 20 cm^{-1}/min. The monochromator slits were set to 300 μm, corresponding to a spectral bandwidth of ≈3 cm^{-1}. The accuracy was ± 1 cm^{-1}.

No peaks due to fluorescence or Raman effects of the vitreous silica tubes were found in the Raman powder spectra. This result was checked by running a blank consisting of a sample tube filled with NaCl which has no first-order Raman spectrum. No OH-stretching modes were found in the powder spectra at ≈3600 cm^{-1} nor bending modes at ≈1600 cm^{-1}, indicating that the preparation procedure, as described, did not give water-contaminated samples.

III. Interpretation of the Raman Spectra of Reaction Mixtures

To identify vitreous and crystalline arsenic compounds in the powdered $30K_2CO_3$-$70SiO_2$-$1As_2O_3$ reaction mixtures, Raman studies were conducted on glasses and crystalline compounds in the systems $KAsO_3$-K_3AsO_4[19] and K_3AsO_3-As_2O_3[20] and on potassium silicate glasses containing small amounts of As_2O_3 in the batch.[21] Data for identifying silicates and carbonates were obtained from Refs. 5 and 22. The following sections give preliminary results of the studies on arsenites and arsenates.[19-21]

(1) Crystalline and Vitreous Potassium Arsenates (Ref. 19)

All crystalline potassium arsenates contain chains of AsO_4 tetrahedra with various chain lengths (i.e. γ-$KAsO_3$ contains chains of infinite length, $K_5As_3O_{10}$ of three tetrahedra, $K_4As_2O_7$ two tetrahedra, and K_3AsO_4 isolated AsO_4 tetrahedra). Vitreous potassium arsenates can be prepared in the composition region $K_4As_2O_7$-γ-$KAsO_3$; like the crystalline compounds, the glasses contain chains of AsO_4 tetrahedra which vary in length from two to infinity.

The ν_s§§ AsO_n modes are found in the energy region from 800 to 950 cm^{-1}, ν_s AsOAs modes from 600 to 400 cm^{-1}, and the deformation modes are all <450 cm^{-1}. The ν_s modes are strongly polarized

*Heraeus-Amersil, Inc., Hanau, Federal Republic of Germany.
†E. Merck AG, Darmstadt, Federal Republic of Germany.

‡Model I²-R, Instruments for Research and Industry, Cheltenham, Pa.
§Coherent Radiation, Palo Alto, Calif.
¶No. 5145-11, Oriel Corp. of America, Stamford, Conn.
‖Ramanor HG 2S, Jobin Yvon, Long Jumeau, France.
**FW 130, International Telephone and Telegraph Co., Rochester, N.Y.
††Keithley Instruments, Inc., Cleveland, Ohio.
‡‡PM 3222, Philips Gloeilampenfabrieken N. V., Eindhoven, The Netherlands.
§§Notations used for vibrational modes are ν = stretch, δ = bending, and (a)s = (anti)symmetrical.

Table I. Raman Data for Crystalline Arsenates (Ref. 19) and Arsenites (Ref. 20) at 700 to 1000 cm^{-1}

Compound	Peak position (cm^{-1})	Peak width (cm^{-1})	I/I_0	Assignment
γ-$KAsO_3$	969	4	9	ν_{as},ν_{as}' AsO_2
	950	5	11	
	917	5	100	$\nu_s AsO_2$
	896	5	0.6	$\nu_s' AsO_2$
	839	12	1.5	ν_{as}' AsOAs
	817	9	0.7	
	715	10	5	ν_{as}AsOAs
$K_5As_3O_{10}$	954	7	8	$\nu_{as} AsO_2$
	908	4	2.5	
	900	5	3	$\nu_{as}\nu_{as} AsO_3$
	875	4	6.5	
	887	8	100	$\nu_s AsO_2$
	849	6	56	$\nu_s\nu_s' AsO_3$
	806	12	29	ν_{as}' AsOAs
	742	14	3.5	ν_{as}AsOAs
$K_4As_2O_7$	900		<1	
	885		<1	
	879		<1	$\nu_{as}\nu_{as}' AsO_3$
	854		<1	
	840		<1	
	859	14	100	$\nu_s\nu_s' AsO_3$
	845	6	9	
	728	5.5	1.5	ν_{as}AsOAs
α-K_3AsO_4	843	6	4.5	
	827	6	4.5	$\nu_{as} AsO_4$
	800	6	4.5	
	814	8	100	$\nu_s AsO_4$
$KAsO_2$	830	10	100	$\nu_s AsO_2$
K_3AsO_3	782	20	100	$\nu_s AsO_3$
	715	14	50	

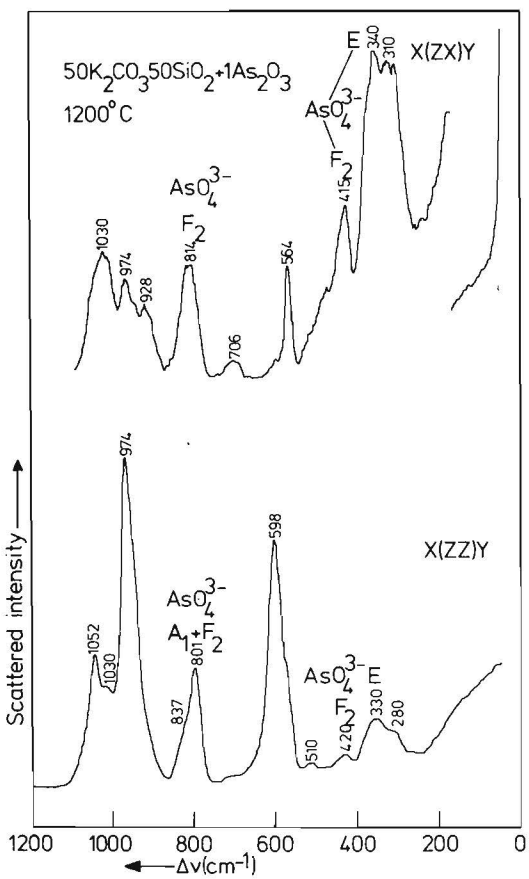

Fig. 1. Polarized and depolarized Raman spectra of a glass with batch composition $50K_2CO_3$-$50SiO_2$-$1As_2O_3$, melted at 1200°C; scattering geometries $X(ZZ)Y$ and $X(ZX)Y$ according to Ref. 24.

and the ν_{as} and deformation modes are generally depolarized. The ν_s and ν_{as} AsO_n modes are most suitable for identification in silicate glass batches or glasses. The most important Raman data are given in Table I.

(2) Crystalline and Vitreous Potassium Arsenites

The fact that crystalline and vitreous potassium arsenites are still under investigation[20] does not affect the conclusions reached in the present study. The crystalline compounds $KAsO_2$ and K_3AsO_3 were identified. Potassium arsenite glasses can be formed in the composition region $KAsO_2$-As_2O_3. The structural building unit throughout the system is an irregular AsO_3 pyramid which forms two-dimensional networks in the case of As_2O_3, infinite chains in $KAsO_2$, and is present as an isolated ion in K_3AsO_3. The ν AsO_n vibrations are found at 700 to 850 cm^{-1}, ν_s AsOAs vibrations between 450 and 600 cm^{-1}, and the deformation modes at <450 cm^{-1}. As in the case of the arsenates, the ν AsO_n modes are most suitable for identification. The most important Raman data are given in Table I.

(3) Arsenite and Arsenate Groups in Potassium Silicate Glasses

Konijnendijk and Buster[23] gave an interpretation of the Raman peaks caused by small amounts of arsenic in various disilicate-type glasses. A peak observed in the Raman spectra at ≈830 cm^{-1}, caused by the presence of arsenic, was ascribed to isolated AsO_4^{3-} tetrahedra in glass. The present study, however, shows that this peak is probably due to $As_2O_7^{4-}$ and AsO_2^- ions. It appears that the state of arsenic in potassium silicate glasses depends strongly on the alkali content.

When the glass contains 35 to 50 mol% K_2O, arsenic is mainly present as isolated AsO_4^{3-} ions in a T_D symmetry. For example, Fig. 1 gives the polarized and depolarized Raman spectra of a glass with batch composition $50K_2CO_3$-$50SiO_2$-$1As_2O_3$, melted at 1200°C (scattering geometrics $X(ZZ)Y$ and $X(ZX)Y$, according to Ref. 24). The ν_s AsO_4 (A_4 species) mode is found as a polarized peak at 801 cm^{-1} and the ν_{as} AsO_4 (F_2) mode is found at 814 cm^{-1} as a depolarized peak. The δ_{as} (F_2) and δ_s (E) modes are found as depolarized peaks at 420 and 330 cm^{-1}, respectively. The peak positions and intensities of peaks caused by AsO_4^{3-} in potassium-rich silicate glasses agree very well with those of crystalline α-K_3AsO_4 (Table 1, Ref. 19). Furthermore, chemical analysis shows that in glass with batch composition $50K_2CO_3$-$50SiO_2$-$1As_2O_3$ all arsenic is present in the pentavalent state.[21] The other peaks observed in the spectra of Fig. 1 are caused by metasilicate or carbonate groups, the assignment of which is given in Ref. 22.

In glass containing less K_2O (0 to 35 mol%) the situation becomes completely different. Chemical analysis of these glasses (melted at 1200° to 1400°C) shows that ≈10% of the arsenic is in the trivalent state.[21,23] The Raman spectra of a glass with batch composition $30K_2CO_3$-$70SiO_2$-$1As_2O_3$ melted at 1400°C are given in Fig. 2.

As described in Ref. 23, As_2O_3 in the batch causes peaks at 880 and 826 cm^{-1}. That at 880 cm^{-1} is completely depolarized and can be ascribed with certainty to ν_{as} AsO_3 of an $As_2O_7^{4-}$ group; this assignment is based on the study of crystalline and vitreous potassium arsenates.[19] The peak at 826 cm^{-1}, which is completely polarized, is probably composed of ν_s AsO_3 of $As_2O_7^{4-}$ and ν AsO_2 of AsO_2^-.

The other peaks observed in the spectra in Fig. 2 are mainly caused by disilicate networks present in the glass. Assignment of the peaks is given in Refs. 25, 26, and 27. It appears that the high valency of arsenic is favored when much alkali is present; at lower alkali concentrations, when fewer charge-compensating alkalis are present, more condensed arsenate structures and lower-valency arsenite structures are stable. The most important observation is that the As^{3+}/As^{5+} ratio depends on the alkali content.

IV. Results of Glass Formation Experiments on $30K_2CO_3$-$70SiO_2$-$1As_2O_3$ Batches

Figures 3 and 4 give the Raman spectra of powders prepared from samples fired for 1 h at various temperatures. Peaks caused by K_2CO_3 and SiO_2, or their reaction products, are labeled by symbols

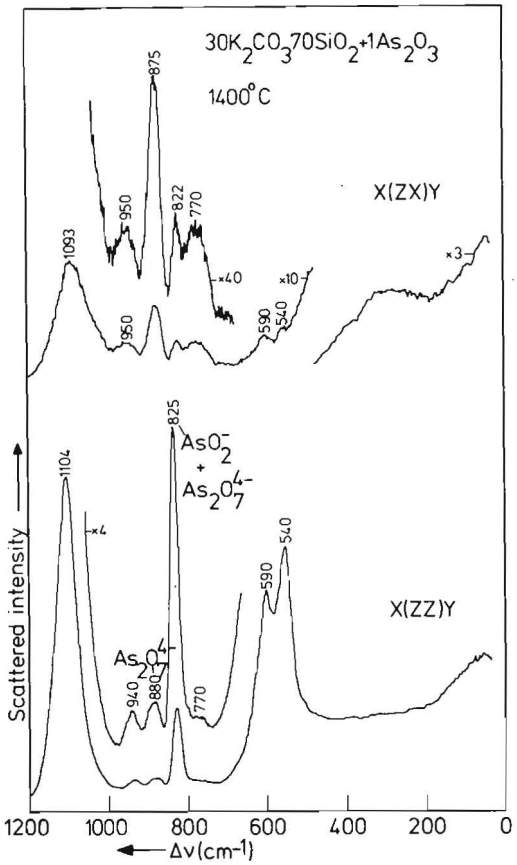

Fig. 2. Polarized and depolarized Raman spectra of a glass with batch composition $30K_2CO_3$-$70SiO_2$-$1As_2O_3$, melted at 1400°C; scattering geometries $X(ZZ)Y$ and $X(ZX)Y$ according to Ref. 24.

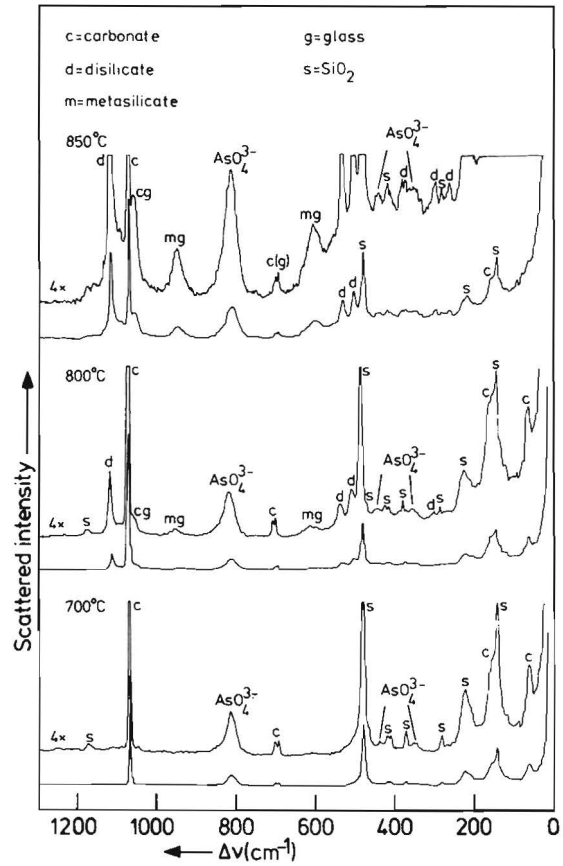

Fig. 3. Raman spectra of powdered $30K_2CO_3$-$70SiO_2$-$1As_2O_3$ mixtures fired for 1 h at 700°, 800°, and 850°C.

(c,d,m,g,s); peaks caused by arsenic are labeled by the anion part of the arsenate and arsenite structures formed.

(1) Batch Fired at 700°C (Fig. 3)

The presence of a sharp peak at 810 cm^{-1} and the absence of other peaks which may be caused by arsenic indicate that arsenic is completely present in the pentavalent state as K_3AsO_4. No reaction products of SiO_2 and K_2CO_3 are observed in the spectrum. The linewidth of the K_3AsO_4 peak is somewhat larger than that observed in the spectrum of crystalline α-K_3AsO_4 (Ref. 19); this difference is ascribed to a particle size effect. After firing at 700°C, arsenic is thus present as finely divided K_3AsO_4 particles.

(2) Batch Fired at 800°C (Fig. 3)

The peak at 810 cm^{-1} is again observed, although somewhat broadened. This additional broadening is ascribed to the fact that AsO_4^{3-} is now dissolved in a potassium-rich liquid phase which contains CO_3^{2-} and metasilicate chains[5,22]; at room temperature this phase is present as a glass in the mixture (see Section III (3) and Fig. 1*). Besides the formation of the potassium-rich liquid phase, the formation of crystalline $K_2O{\cdot}2SiO_2$ is concluded from the spectrum.

(3) Batch Fired at 850°C (Fig. 3)

The potassium-rich liquid phase, consisting of metasilicate, carbonate, and AsO_4^{3-}, is again observed. Crystalline $K_2O{\cdot}2SiO_2$ is also observed. The situation is qualitatively the same as for a batch fired at 800°C, but the concentration of reaction products has increased somewhat.

(4) Batch Fired at 900°C (Fig. 4)

Crystalline carbonate has disappeared, which is consistent with

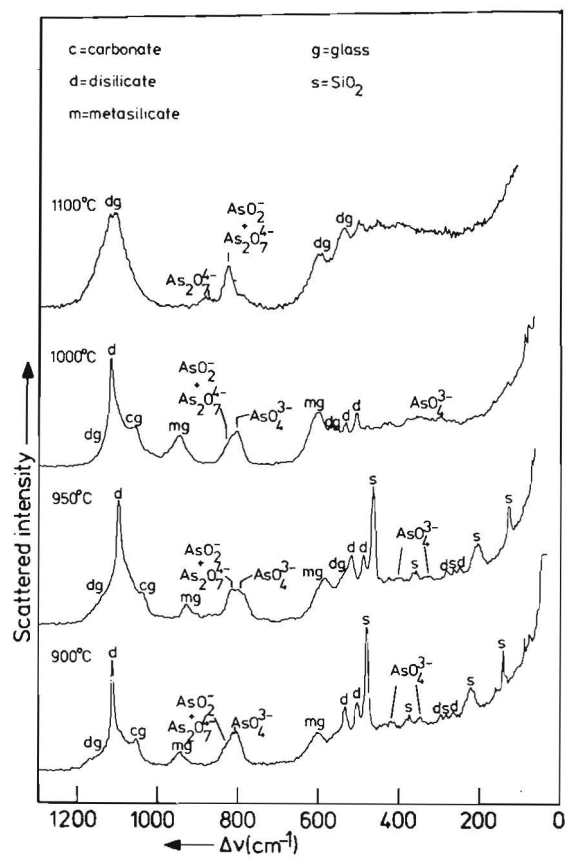

Fig. 4. Raman spectra of powdered $30K_2CO_3$-$70SiO_2$-$1As_2O_3$ mixtures fired for 1 h at 900°, 950°, 1000°, and 1100°C.

*For identifying glasses in powdered mixtures, the polarized spectrum of the glass can be used, as it closely resembles the powder spectra.

the fact that the melting point of K_2CO_3 is 891°C.[28] Crystalline SiO_2 is still present, along with a large proportion of crystalline $K_2O{\cdot}2SiO_2$. The first formation of disilicate structures in the liquid-phase reaction product is concluded from the broadening at the base of the $K_2O{\cdot}2SiO_2$ peak at 1104 cm^{-1}. The formation of $AsO_2^-/As_2O_7^{4-}$ structures is also concluded from the spectrum, which means that the formation of As^{3+} occurs first at ≈900°C. The $AsO_2^-/As_2O_7^{4-}$ structures are stable in glasses with a K_2O concentration <35 mol% (Section III (3)) and seem to be coupled with the occurrence of disilicate structures in the liquid phase. The Raman spectra of a glass with batch composition $30K_2CO_3$-$70SiO_2$-$1As_2O_3$ are given in Fig. 2. It cannot be concluded from the Raman spectra of Fig. 3 whether the liquid phase is homogeneous.

(5) Batch Fired at 950°C (Fig. 4)

Compared with the mixture fired at 900°C, the proportion of disilicate in the liquid phase has increased, together with the proportion of $AsO_2^-/As_2O_7^{4-}$ groups. Carbonate in the liquid phase has decreased. Crystalline SiO_2 and $K_2O{\cdot}2SiO_2$ are still present.

(6) Batch Fired at 1000°C (Fig. 4)

The spectrum of the batch fired for 1 h at 1000°C differs from what would be expected from an extrapolation of the results for the batches fired at 900° and 950°C. Relatively large amounts of crystalline $K_2O{\cdot}2SiO_2$ and potassium-rich glass are present, whereas SiO_2 has disappeared and little disilicate is present in the liquid phase. The explanation may be that the temperature has been so close to the melting point of $K_2O{\cdot}2SiO_2$ (1015°C)[28] that $K_2O{\cdot}2SiO_2$ has grown rapidly.

(7) Batch Fired at 1100°C (Fig. 4)

Crystalline SiO_2 and $K_2O{\cdot}2SiO_2$ have disappeared and no carbonate peak can be found in the spectrum. All silicate is present as disilicate liquid, and arsenic as $AsO_2^-/As_2O_7^{4-}$. The glass-forming reaction has been completed. The spectrum closely resembles that of a glass with batch composition $30K_2CO_3$-$70SiO_2$-$1As_2O_3$ fired at 1400°C (Fig. 2).

V. Discussion

(1) Description of the Reaction Process

Comparing the present results with those of reactions in a $30K_2CO_3$-$70SiO_2$ batch (without As_2O_3 (Ref. 5)), it can be concluded that As_2O_3 has no significant influence on the kinetics of the carbonate-silica reactions.

For the description of the total reaction process in a $30K_2CO_3$-$70SiO_2$-$1As_2O_3$ glass-forming batch, three temperature regions can be distinguished, aside from the fining region of the silicate melt at >1100°C.

(A) Region of Room Temperature to 700°C: In this region K_2CO_3 and SiO_2 do not react with each other significantly. The As_2O_3 is converted to K_3AsO_4, probably by the mechanism proposed by Eichorn[10] (see also Section I (1)). At 700°C all arsenic is present in the pentavalent state in K_3AsO_4, probably as very small particles on the surface of the K_2CO_3 grains.

(B) 700°C to 850°C: In this region the SiO_2 grains are attacked by K_2CO_3 and two layers of reaction product are formed around them[5]; Fig. 5 (*A*) is a schematic diagram of such an attacked SiO_2 grain. The first layer around the grain consists of crystalline $K_2O{\cdot}2SiO_2$ and the second layer of a potassium-rich liquid containing CO_3^{2-} and metasilicate chains. At <850°C, crystalline K_2CO_3 is still present. Arsenic is completely present in the pentavalent state as AsO_4^{3-}; at lower temperatures it is present as crystalline K_3AsO_4 and at higher temperatures it is dissolved in the liquid layer.

(C) 850° to 1100°C: Figure 5(*B*) is a schematic of an attacked SiO_2 grain. At 850° to 1000°C the crystalline $K_2O{\cdot}2SiO_2$ layer grows at the expense of the SiO_2 grain and the potassium-rich liquid layer until it finally melts at 1015°C. Thus the potassium-rich liquid layer gradually loses K_2O and is transformed into a potassium disilicate liquid layer, which corresponds to the final product composition. In this potassium disilicate liquid the CO_2 solubility is extremely low[29] and CO_2 originally present as CO_3^{2-} in the potassium-rich liquid layer must escape. The formation of potassium disilicate liquid is accompanied by the condensation of AsO_4^{3-} to $As_2O_7^{4-}$, which in turn decomposes partly to AsO_2^-. This process has to be accompanied by an O_2 evolution. When the potassium-rich layer which is formed at lower temperatures is written as $K_2O{\cdot}xCO_2{\cdot}ySiO_2$ with $x+y\approx1$, the overall reactions between 850° and 1000°C become:

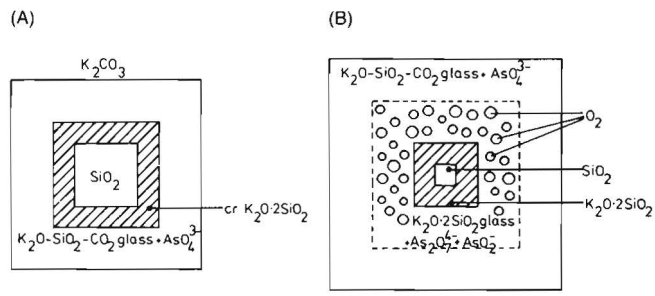

Fig. 5. Schematic drawing of SiO_2 grains attacked by K_2CO_3 in temperature regions (*A*) 700°–850°C and (*B*) 850°–1000°C.

$$K_2O{\cdot}xCO_2{\cdot}ySiO_2(l)+(2-y)SiO_2(s)\rightarrow K_2O{\cdot}2SiO_2(l)+xCO_2(g) \quad (7)$$

$$2K_3AsO_4(l)+2SiO_2(s)\rightarrow K_4As_2O_7(l)+K_2O{\cdot}2SiO_2(l) \quad (8)$$

and ≈10% of the $K_4As_2O_7$ decomposes as:

$$K_4As_2O_7(l)+2SiO_2(s)\rightarrow K_2O{\cdot}2SiO_2(l)+2KAsO_2(l)+O_2(g) \quad (9)$$

in which *g* and *s* refer to the gaseous and the solid state and *l* refers to the liquid formed during the reactions; this liquid is vitreous at room temperature. When the $30K_2O$-$70SiO_2$($1As_2O_3$) composition is approached during melting, the CO_2 development gradually decreases, whereas the O_2 development increases. This result explains the heterogeneous bubble nucleation at the surface of dissolving SiO_2 grains, as observed by Nemec,[16] and the very high concentrations of oxygen found in bubbles in glasses melted for short times at ≈1400°C.[13,17,18]

(2) Consequences for the Fining Process

In the discussion of the reaction mechanism in the model system used it was concluded that the O_2 and CO_2 developments occur at different positions around attacked SiO_2 grains; CO_2 is developed on the outside of the liquid silicate layer and O_2 is developed more on the inside, where the liquid layer contacts $K_2O{\cdot}2SiO_2$ or SiO_2 (at higher temperatures). Furthermore, the maximum evolution of O_2 will come after the maximum in CO_2 evolution during the reactions.

At the stage of first-product glass formation the reacting batch contains a large proportion of CO_2 (and N_2) in the pores. In a batch containing potassium carbonate, CO_2 in particular causes a great deal of trouble, because its release is delayed in the first stage of melting by the formation of a potassium-rich liquid phase which contains a large proportion of CO_3^{2-}.

When, at the final stage of melting, the K_2O concentration decreases in the liquid phase, CO_2 is gradually released and this may cause many small bubbles. However, as the K_2O concentration decreases, an O_2 evolution is triggered (Section V (1)). In the ideal case the large amount of O_2 which is developed sweeps other gases away and finally only O_2 bubbles remain. These bubbles disappear easily from arsenic-containing silicate glass melts, probably through a dissolution mechanism operating during temperature decrease.[9,15]

As indicated in Section I (2), a current view for the fining action of As_2O_3, based on previous literature, is that an O_2 evolution, triggered by a temperature increase, causes fining by means of bubble inflation followed by ascension. In the present study it was found that the variations in alkali oxide concentration in the silicate liquid formed during the melting process trigger an O_2 evolution. The decrease in alkali oxide concentration in the silicate liquid, due to the solution of SiO_2, triggers at the right moment and at the right place the evolution of O_2, which may be the reason for the effectiveness of arsenic.

VI. Conclusions

It has been shown by Raman spectroscopy that in the first stage of melting in a reacting $30K_2CO_3$-$70SiO_2$-$1As_2O_3$ glass-forming batch, all the arsenic is in the pentavalent state, dissolved as AsO_4^{3-} in a potassium-rich liquid phase, which contains metasilicate and carbonate. The high oxidation state of arsenic is then stabilized by the high potassium oxide concentration. When the reactions proceed and the product glass composition is reached, the melt becomes more acidic and part of the arsenic goes into the trivalent state, causing an oxygen evolution at the right place and time.

References

[1] G. Rindone, "Fining: I." *Glass Ind.*, **38** [9] 489–93, 516, 526, 528 (1957).

[2] Glass-Making (Melting and Fining): Bibliographic Review, Union Scientifique Continentale du Verre, Charleroi, Belgium, 1973.

[3] J. Stanek, "New Aspects in Melting of Glass," *J. Non-Cryst. Solids*, **26** [1–3] 158–78 (1977).

[4] M. Cable, "Glass Making, The Melting Process," *Glastek. Tidskr.*, **24** [6] 147–52 (1969).

[5] H. Verweij, H. van den Boom, and R. E. Breemer, "Raman Spectroscopic Study of the Reactions in a Potassium Carbonate-Silica Glass-Forming Batch," *J. Am. Ceram. Soc.*, **61** [3–4] 118–21 (1978).

[6] M. Cable, "Study of Refining: III," *Glass Technol.*, **2** [4] 151–58 (1961).

[7] Z. Karch, "Theoretical Principles and Practical Observations About Fining and Decolorizing of Flat Glass with Arsenic Compounds," *Sprechsaal*, **103** [10] 427–28, 430, 432, 434 (1970).

[8] E. M. Firth, F. W. Hodkin, W. E. S. Turner, and F. Winks, "The Function of Arsenic in Soda-Lime-Silica Glass: III," *J. Soc. Glass Technol.*, **11** [42] 205–14 (1927).

[9] C. H. Greene and H. A. Lee, Jr., "Effect of As_2O_3 and $NaNO_3$ on the Solution of O_2 in Soda-Lime Glass," *J. Am. Ceram. Soc.*, **48** [10] 528–33 (1965).

[10] H. J. Eichorn, "Reaction Behavior of Arsenic in Simple Glass Batches in Dynamic Thermal Conditions," *Silikattechnik*, **26** [1] 28 (1975).

[11] M. Cable, "Study of Refining: I," *Glass Technol.*, **1** [4] 144–54 (1960).

[12] M. Cable, "Study of Refining: II," *ibid.*, **2** [2] 60–70 (1961).

[13] M. Cable, A. R. Clarke, and M. A. Haroon, "The Effect of Arsenic on the Composition of the Gas in Seed During the Refining of Glass," *ibid.*, **10** [1] 15–21 (1969).

[14] M. Cable and M. A. Haroon, "The Action of Arsenic as a Refining Agent," *ibid.*, **11** [2] 48–53 (1970).

[15] C. H. Greene and D. R. Platts, "Behavior of Bubbles of Oxygen and Sulfur Dioxide in Soda-Lime Glass," *J. Am. Ceram. Soc.*, **52** [2] 106–109 (1969).

[16] L. Nemec, "Refining in the Glassmelting Process," *ibid.*, **60** [9–10] 436–40 (1977).

[17] H. O. Mulfinger, "Use of Gas Analysis to Follow the Refining Process in Crucible and Tank," *Glastech. Ber.*, **49** [10] 232–45 (1976).

[18] K. van Erk, E. Papanikolau, and W. van Pelt; pp. 137–46 in Glass 1977, Vol. IV. Edited by J. Goetz. North-Holland Publishing Co., Amsterdam, 1977.

[19] H. Verweij, "Raman Study of Glasses and Crystalline Compounds in the System $KAsO_3$-K_3AsO_4": to be published in *Journal of Applied Spectroscopy*.

[20] H. Verweij and J. G. van Lierop; unpublished work.

[21] H. Verweij; unpublished work.

[22] H. Verweij, H. van den Boom, and R. E. Breemer, "Raman Scattering of Carbonate Ions Dissolved in Potassium Silicate Glasses," *J. Am. Ceram. Soc.*, **60** [11–12] 529–34 (1977).

[23] W. L. Konijnendijk and J. H. J. M. Buster, "Raman Scattering Measurements of Silicate Glasses Containing AsO_4^{3-} Ions," *J. Non-Cryst. Solids*, **22** [2] 379–89 (1976).

[24] T. C. Damen, S. P. S. Porto, and B. Tell, "Raman Effect of Zinc Oxide," *Phys. Rev.*, **142** [2] 570–74 (1966).

[25] S. A. Brawer and W. B. White, "Raman Spectroscopic Investigation of the Structure of Silicate Glasses: I," *J. Chem. Phys.*, **63** [6] 2421–32 (1975).

[26] H. Verweij and W. L. Konijnendijk, "Structural Units in K_2O-PbO-SiO_2 Glasses by Raman Spectroscopy," *J. Am. Ceram. Soc.*, **59** [11–12] 517–21 (1976).

[27] H. Verweij, "Raman Study of the Structure of Alkali Germanosilicate Glasses: II," *J. Non-Cryst. Solids*, **33**, 55–69 (1979).

[28] Handbook of Chemistry and Physics, 51st ed. Edited by R. S. Weast. Chemical Rubber Publishing, Cleveland, Ohio, 1970.

[29] M. L. Pearce, "Solubility of Carbon Dioxide and Variation of Oxygen Ion Activity in Soda-Silica Melts," *J. Am. Ceram. Soc.*, **47** [7] 342–47 (1964).

Raman Study on Glasses and Crystalline Compounds in the System K_3AsO_4-$KAsO_3$

H. VERWEIJ

Philips Research Laboratories, Eindhoven, The Netherlands

Raman and IR spectra of the crystalline compounds α-K_3AsO_4 $K_4As_2O_7$, $K_5As_3O_{10}$, and γ-$KAsO_3$ are given together with tentative assignments in terms of symmetrical and antisymmetrical As—O^- and As—O—As bond-stretching and bond-bending vibrations. Comparison of the Raman spectra of crystalline arsenates with those of vitreous arsenates, stabilized with Al_2O_3, in the composition region $KAsO_3$-$K_4As_2O_7$ is used to deduce the molecular structure of these glasses. It appears that in the glasses chains of AsO_4 tetrahedra are present.

Index Headings: **Infrared; Light scattering; Molecular structure; Optics; Raman spectroscopy.**

INTRODUCTION

The study presented here is part of a research program in which the reactions of As_2O_3 additions to silicate glass

Received 30 December 1978; revision received 9 March 1979.

batches during melting are studied.[1] In this program Raman spectroscopy is used as a nondestructive identification method for molecular structures in the vitreous or crystalline state which occur in partly or completely reacted silicate glass-forming mixtures.

One of the central problems is the assignment of Raman peaks caused by the presence of arsenite or arsenate structures. In order to be able to make these assignments with sufficient certainty Raman peak position, intensity, and depolarization data of arsenate (and arsenite) groups are needed. The present study reports on arsenate groups occurring in crystalline and vitreous potassium arsenates.

The phase diagram of the K_3AsO_4-$KAsO_3$ system[2] indicates that at room temperature there are four stable compounds: α-K_3AsO_4; $K_4As_2O_7$; $K_5As_3O_{10}$; and β-$KAsO_3$. No x-ray diffraction structure studies on potassium arsenates have been reported in the literature.

α-K_3AsO_4 is likely to contain AsO_4^{3-} tetrahedra. A vibrational study on the AsO_4^{3-} ion in aqueous solution has been done.[3, 4]

$K_4As_2O_7$ probably contains $As_2O_7^{4-}$ groups of two tetrahedra sharing corners as in $Na_4As_2O_7$.[5] The infrared spectrum of a $Na_4As_2O_7$ melt together with an interpretation in terms of bond-stretching and -bending vibrations is given in Ref. 6. A normal coordinate analysis of $As_2O_7^{4-}$ is given in Ref. 7.

$K_5As_3O_{10}$ probably contains linear $As_3O_{10}^{5-}$ chains of three tetrahedra sharing corners as in $H_5As_3O_{10}$.[8, 9]

From chromatographic studies[10, 11] it was concluded that β-$KAsO_3$ consists of $As_3O_9^{3-}$ rings and that γ-$KAsO_3$, metastable at room temperature, consists of $(AsO_3^-)_\infty$ chains of AsO_4 tetrahedra sharing corners. $NaAsO_3$ consists of $(AsO_3^-)_\infty$ chains with a chain period of three AsO_4 tetrahedra[12]; the same is also true for $LiAsO_3$ with a chain period of two tetrahedra.[13] An interpretation of the vibrational spectra of β-$KAsO_3$ is given by Griffith,[14] who concluded a "chair" conformation for the $As_3O_9^{3-}$ rings.

Vitreous potassium arsenates have not been reported in the literature although glass formation in As_2O_3-based systems has been described.[15]

I. EXPERIMENTAL

A. Preparation. Crystalline potassium arsenates were prepared by high temperature solid state reaction of KH_2AsO_4 (Alfa products, Ventron, Beverly, MA) and K_2CO_3 (E. Merck, Darmstadt, W. Germany) in a dry O_2 stream. The reaction time was 20 h, and the temperatures were 600°C for γ-$KAsO_3$ and $K_5As_3O_{10}$, 650°C for $K_4As_2O_7$, and 850°C for α-K_3AsO_4. After the reaction no special cooling was applied. Vitreous potassium arsenates of composition $xK_2O \cdot As_2O_5$ (x = 1, 1.2, 1.4, 1.6, 1.667, 1.8 and 2.0) were prepared by melting in Al_2O_3 crucibles (Degussa, Frankfurt, W. Germany) for 1 h in air inside an electrically heated furnace at temperatures varying from 900 to 1000°C. The melts were poured between water-cooled steel rollers; in this way flat pieces of clear glass were obtained with a thickness varying from 2 mm (x = 1) to 0.5 mm (x = 2), depending on the crystallization rate of the glasses. The glasses with x = 1.8 and 2.0 were slightly yellow. When SiO_2 crucibles were used all efforts to make glass failed which indicates that Al^{3+} which dissolves from the Al_2O_3 crucible stabilizes the vitreous state. For x > 2 crystallization occurs in all cases. The results of a wet chemical analysis of the glasses are given in Table I.

B. Raman Measurements. The Raman spectrometer used was a commercially available instrument. (Raman, H. G. 2S, Jobin Yvon, Long Jumeau, France) For excitation an Ar^+ laser (Coherent Radiation model 52, Palo Alto, CA) was used, tuned to a wavelength of 514.5 nm; the maximum laser power was about 1 W and the light output stability was better than 0.5%. The monochromator was equipped with two concave holographic gratings and a controlled step motor drive. The detector consisted of a Peltier-cooled photomultiplier tube (ITT, FW 130, Rochester, NY). The spectra were recorded using a dc amplifier (Keithley, 117 picoammeter, Cleveland, OH) in combination with a double RC filter and a recorder. Wavelength checks were made, using non-lasing emission lines from the Ar^+ laser.

The Raman spectra of the crystalline powders were measured on samples contained in rotating sealed sample tubes (length 50 mm; inner diameter 1 mm). The laser power was reduced to 500 mW to avoid thermally induced phase transitions, which were especially serious for $K_5As_3O_{10}$ and α-K_3AsO_4. The spectral resolution was set to 2 cm^{-1}. In order to measure the Raman spectra of the very hygroscopic glass samples they were mounted inside a sample holder which was placed inside a square glass vessel, having optically polished windows. The glass vessel was filled with an index-matching liquid (IML) to protect the sample from atmospheric attack and to avoid surface depolarization effects. The refractive index of the IML was carefully matched to the refractive index of the glass samples using a modified version of a method described in Ref. 16. The IML consisted of a mixture of C_6H_5Br and paraffin oil. The sample holder was constructed in such a way that the very strong Raman scattering from the IML was completely shielded. A laser power of 500 mW was applied so that no thermal defocussing in the IML or pyrolysis of the IML at the glass-liquid interface occurred. The primary beam was polarized using a Glan-Thompson prism. Polarized and depolarized spectra were measured in the geometries Y(ZZ)X and Y(ZY)X respectively[17]; Y is the direction of the laser beam and X is the direction of measurement. As a check, the depolarization ratios of the 318 and 459 cm^{-1} bands of CCl_4 were measured, using an empty sample holder. The measured depolarization ratios were found to be close to the theoretical values, so no corrections were made to the measured depolarization ratios of the glass samples. The optical path length of the scattered light in the glass samples was reduced as much as possible to avoid internal depolarization effects. The spectral resolution used for the glasses was set to 5 cm^{-1}.

All Raman spectra were run with a time constant of 5 s and a scan speed of 20 cm^{-1}/min.

TABLE I. As^{3+} and Al^{3+} content of the potassium arsenate glasses $xK_2O \cdot As_2O_5$ as determined by wet chemical analysis.

x	As^{3+} (wt, %)	Al^{3+} (wt, %)
1.0	1.82	3.8
1.2	0.54	3.1
1.4	0.14	3.9
1.6	0.14	3.3
1.667	0.11	4.4
1.8	0.05	4.1
2.0	0.01	5.0

C. Infrared Measurements. Infrared spectra of the crystalline compounds in the region 200 to 1300 cm^{-1} were obtained, using standard apparatus (Hitachi types EPI-G2 and EPI-I, Tokyo, Japan). Wavelength checks were made by recording a standard polyethylene foil. The samples were pressed in KBr and polyethylene discs.

All sample handling at room temperature occurred inside nitrogen-filled glove bags (I^2R, Cheltenham, PA).

II. RESULTS AND DISCUSSION

Except for α-K_3AsO_4 the assignments in this paper are approximative in character and are generally made following the empirical method of interpretation of Ref. 18. The following "rules of thumb" are used: (1) symmetrical vibrations with small oscillating dipoles are strong in Raman and weak in IR, and (2) antisymmetrical vibrations are strong in IR and weak in Raman.

A. α-K_3AsO_4. In Fig. 1 the Raman and IR powder spectra of crystalline α-K_3AsO_4 are given. Spectral data together with assignments are given in Table II. The AsO_4^{3-} tetrahedron for which we assume a pseudo T_D symmetry has as Raman active species: $A_1 + E + 2F_2$; the F_2 species is also IR active.[19] The A_1 species is found as a very strong peak in the Raman spectrum of α-K_3AsO_4; the two F_2 modes are found in the IR spectrum as strong absorptions; in the Raman spectrum removal of the three-fold degeneracy of the two F_2 species is observed. This removal of degeneracy is not observed in the IR spectrum; this is apparently caused by the large band width of the modes in the IR spectrum. The E species is also found in the Raman spectrum; removal of the two-fold degeneracy of the E species causes line-broadening.

The results are consistent with those for AsO_4^{3-} in aqueous solution,[3,4] in which case the A_1 and F_2 stretching modes are found at 818 and 791 cm^{-1} and the F_2 and E deformation modes at 405 and 350 cm^{-1}, respectively.

B. $K_4As_2O_7$. In Fig. 1 the Raman and IR powder spectra of crystalline $K_4As_2O_7$ are given. Spectral data together with tentative assignments are given in Table III.

For $As_2O_7^{4-}$ in a C_{2v} symmetry we may expect $7A_1 + 4A_2 + 4B_1 + 6B_2$ vibrations; the A_2 is not IR active.[18] In the region of stretching frequencies $2\nu_{as}$ AsO_3, $2\nu'_{as}$ AsO_3, $1\nu_s$ and $1\nu'_s$ AsO_3, $1\nu_{as}$ and $1\nu_s$ AsOAs are expected; with $\nu_{as} > \nu_s$.[18] From the deformation modes $1\delta_s$ AsO_3, $1\delta'_s$ AsO_3, $2\delta_{as}$ AsO_3, and $2\delta'_{as}$ AsO_3 are expected between 300 and 450 cm^{-1}; the region where the δ AsO_4 modes in K_3AsO_4 are also found (Table I). The strong peaks at 261 and 248 cm^{-1} may be ascribed to a δ AsOAs vibration. While 21 Raman active fundamentals were expected for $As_2O_7^{4-}$, 17 maxima are actually observed in the Raman spectrum of $K_4As_2O_7$ and were all assigned to internal vibrations of the $As_2O_7^{4-}$ group. The remaining 4 fundamentals which were not observed in the Raman spectrum are of the rocking type[18] and can be expected at very low frequencies (where also lattice modes and K—O stretching modes can be expected) because of the large rotational freedom of the As—O—As bonds in $As_2O_7^{4-}$ ions.

The number of maxima in the IR spectrum of $K_4As_2O_7$ is less certain because of the large bandwidth of the absorptions. While 17 IR active fundamentals were ex-

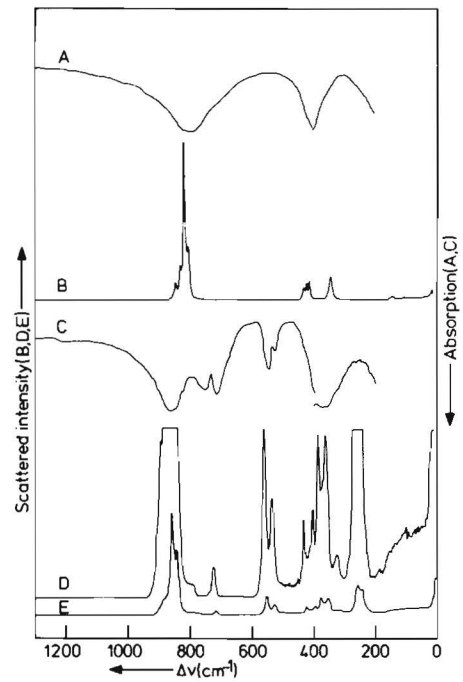

FIG. 1. Raman and IR powder spectra of α-K_3AsO_4 and $K_4As_2O_7$. A, α-K_3AsO_4 (IR); B, α-K_3AsO_4 (Raman); C, $K_4As_2O_7$ (IR); D, $K_4As_2O_7$ (Raman 10×); E, $K_4As_2O_7$ (Raman 1×).

TABLE II. Raman and IR data and assignments for α-K_3AsO_4

Raman				Infrared					
Peak position (cm^{-1})	Relative peak height	Peak width (cm^{-1})	Relative intensity[a]	Absorption (cm^{-1})	Relative absorption depth	Absorption width (cm^{-1})	Relative absorption[a]	Assignment[b]	T_D[c]
843	6	6	4.5						
827	6	6	4.5	815	100	210	100	ν_{as} AsO_4	F_2
800	6	6	4.5						
814	100	8	100					ν_s AsO_4	A_1
418	7	7	6						
409	9	7	8	397	90	160	70	δ_{as} AsO_4	F_2
399	11	7	10						
330	13	14	23					δ_s AsO_4	E

[a] Intensity and absorption are calculated as: peak height × width or absorption depth × width; because of the technique used the IR absorptions are not very accurate. sh = shoulder.

[b] In this paper we use the following nomenclature for vibrations: ν = stretch-, δ = bending-, γ = torsion- or rocking-, (a)s = (anti)symmetric, a prime denotes an antiphase movement of adjacent groups.

[c] Corresponding symmetry species for an AsO_4 tetrahedron in T_D symmetry.

TABLE III. Raman and IR data and assignments for $K_4As_2O_7$.[a]

Raman				Infrared				Assignment	T_D	C_{2v}
Peak position (cm^{-1})	Relative peak height	Peak width (cm^{-1})	Relative intensity	Absorption (cm^{-1})	Relative absorption depth	Absorption width (cm^{-1})	Relative absorption			
900	sh		<1							
885	sh		<1							
879	sh		<1	878	100	145	100	ν_{as}, ν'_{as} AsO_3	F_2	A_1, A_2, B_1, B_2
854	sh		<1							
840	sh		<1							
859	100	14	100					ν_s AsO_3	A_1	A_1
845	20	6	9	838	20	20	3	ν'_s AsO_3	A_1	B_1
				765	20	35	5			
728	4	5.5	1.5	730	100	80	60	ν_{as} AsOAs	F_2	B_1
564	18	12	15	557	70	30	15			
540	9	15	9	537	40	20	6	ν_s AsOAs	A_1	A_1
433	5	5	1.5							
401	4	6	1.5							
384	11	10	8							A_1, B_1
372	7	10	5	400–350	80	120	69	δ_s, δ'_s, δ_{as}, δ'_{as} AsO_3	$E + F_2$	A_1, A_2, B_1, B_2
360	9	14	9							
324	2	10	1.5							
261	28	18	36							
248	22	20	31					δ AsOAs		A_1

[a] See footnotes a, b, and c of Table II for explanation.

pected for $As_2O_7^{4-}$ in a C_{2v} symmetry 7 maxima were actually found which were all assigned to internal vibrations of the $As_2O_7^{4-}$ group.

In the region of the ν_{as} AsO_3 vibrations 5 maxima are found in the Raman spectrum while $2\nu_{as}$ and $2\nu'_{as}$ modes are expected for isolated $As_2O_7^{4-}$. In the spectra the ν_{as} AsOAs mode is split up; this splitting is not found in the IR spectrum of $Na_4As_2O_7$[6,7] where a strong absorption band is found instead, which envelopes the ν_{as} As—O—As bands in the IR spectrum of $K_4As_2O_7$. Furthermore 2 peaks in the Raman spectrum are assigned to δ AsOAs for which only one mode is to be expected.

The observations above point to an important interaction between two neighboring $As_2O_7^{4-}$ groups (Davydov splitting[20]). The ν_{as} AsO_3, the δ AsOAs, and especially the ν_{as} As—O—As modes are relatively strongly dipolar in character and accordingly give rise to a relatively long interaction distance for the $As_2O_7^{4-}$ groups. This may explain why for the other vibrational modes observed in the Raman an IR spectra of $K_4As_2O_7$ no splitting up is found. As the exact structure of $K_4As_2O_7$ is not known, a more detailed explanation of the observed phenomena cannot be given.

C. $K_5As_3O_{10}$. Fig. 2 gives Raman and IR powder spectra of crystalline $K_5As_3O_{10}$. Spectral data together with tentative assignments are given in Table IV. The $As_3O_{10}^{5-}$ ion in a C_{2v} symmetry has $11A_1 + 6A_2 + 9B_1 + 7B_2$ species. The same number of ν AsO_3 and δ AsO_3 modes are present as in $As_2O_7^{4-}$ although the coupling between the two AsO_3 groups will be considerably less due to the presence of the AsO_2 group so that the separation between ν and ν' modes can be expected to be less than for $K_4As_2O_7$ and in fact not observable.

The AsO_2 group gives rise to $1\nu_{as}$ AsO_2, $1\nu_s$ AsO_2, 1δ AsO_2, and three AsO_2 rocking modes. Furthermore there are $1\nu_{as}$ AsOAs, $1\nu'_{as}$ AsOAs, $1\nu_s$ AsOAs; $1\nu'_s$ AsOAs, 2δ AsOAs, 1δ OAsO, and two AsOAs rocking modes.[18] The assignments for the AsO_3 groups are derived from those of $As_2O_7^{4-}$ (Table III). The ν_{as} AsO_2 mode is found as a

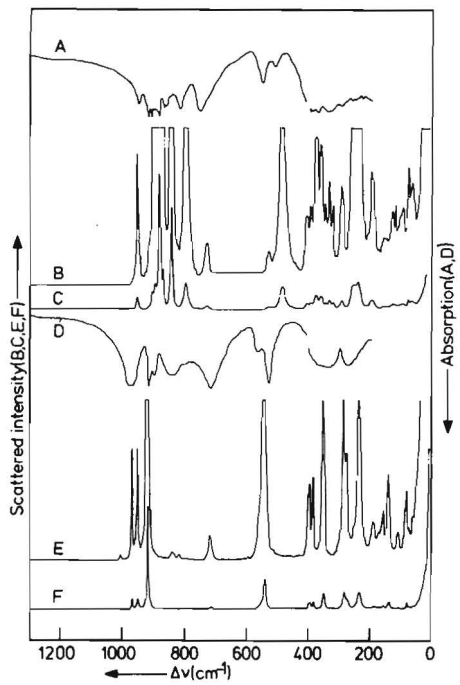

FIG. 2. Raman and IR powder spectra of $K_5As_3O_{10}$ and γ-$KAsO_3$. A, $K_5As_3O_{10}$ (IR); B, $K_5As_3O_{10}$ (Raman 10×); C, $K_5As_3O_{10}$ (Raman 1×); D, γ-$KAsO_3$ (IR); E, γ-$KAsO_3$ (Raman 10×); F, γ-$KAsO_3$ (Raman 1×).

single peak at 954 cm^{-1} in the Raman spectrum and as a strong band in the IR spectrum; ν_s AsO_2 is found as a very strong peak in the Raman spectrum at 887 cm^{-1}. The observation: ν $XO_2 > \nu$ $XO_3 > \nu$ XO_4 is consistent with what is found for many tetrahedrally coordinated networks, e.g., silicates,[21] germanates,[21] and phosphates.[18] ν'_{as} AsOAs belongs to the totally symmetrical representation and is found in the Raman spectrum as a relatively strong peak.

While 33 Raman active fundamentals can be expected for $As_3O_{10}^{5-}$, 27 maxima were actually found in the Raman spectrum and 21 were assigned to internal vibrations of

TABLE IV. Raman and IR data and assignment for $K_5As_3O_{10}$.[a]

Raman				Infrared				Assignment	T_D	C_{2v}
Peak position (cm^{-1})	Relative peak height	Peak width (cm^{-1})	Relative intensity	Absorption (cm^{-1})	Relative absorption depth	Absorption width (cm^{-1})	Relative absorption			
954	9	7	8	941	100	30	50	ν_{as} AsO_2	F_2	B_2
908	5	4	2.5	909	50	10	8	ν'_{as} AsO_3 + ν_{as} AsO_3	F_2	B_1, B_2
900	5	5	3	899	50	10	8			
883	sh		<1	890	25	10	4			
875	13	4	6.5	875	50	10	8		F_2	A_1, A_2
887	100	8	100					ν_s AsO_2	A_1	A_1
				858	25	10	4	ν'_s AsO_3	A_1	B_1
849	74	6	56	849	25	10	4	ν_s AsO_3	A_1	A_1
806	19	12	29	806	75	30	60	ν'_{as} AsOAs	$F_2 + A_1$	A_1
742	2	14	3.5	741	100	60	100	ν_{as} AsOAs	F_2	B_1
520	1	14	2	535	75	30	40	ν'_s AsOAs	$F_2 + A_1$	B_1
494	16	18	36	492	25	30	13	ν_s AsOAs	A_1	A_1
412	4, 5	10	5, 5							
400	2	8	2	392						
383	9	14	16	383				δ_{as}, δ'_s AsO_3 + δ_{as}, δ'_{as} AsO_3 + δ AsO_2	E	A_1B_1
363	9	16	18	368						
351	1.5	4	1		?				F_2	$A_1A_2B_1B_2$
338	4	16	8	335						
326	3	12	4.5						E	A_1
296	5	10	6.5	293						
256	16	18	36					δ AsOAs		A_1B_1
241	19	18	43							
197	5	13	8							
160	8	16	1.5							
125	2.5	10	2.0							
93	2	10	2.5					?		
74	4.5	18	10							
62	3.5	10	4.5							

[a] See footnotes a, b, and c of Table II for explanation.

the $As_3O_{10}^{5-}$ chain. The number of maxima in the IR spectrum of $K_5As_3O_{10}$ is less certain again; while 27 IR active fundamentals can be expected for $As_3O_{10}^{5-}$ in C_{2v} symmetry, 16 maxima could be distinguished which were all assigned to internal vibrations of the $As_3O_{10}^{5-}$ group. The peaks below 200 cm^{-1} in the Raman spectrum of $K_5As_3O_{10}$ are difficult to assign; they may be caused by lattice modes, deformation modes, or K—O modes.

D. γ-$KAsO_3$. In Fig. 2 the Raman and IR powder spectra of γ-$KAsO_3$ are given. Spectral data together with assignments are given in Table V. From X-ray powder diffraction it was concluded[22] that in γ-$KAsO_3$ chains of AsO_4 tetrahedra are present with a chain period of four, probably with an inversion center in the chain. The assignment given in Table V agrees with the assignment for β-$KAsO_3$[14] as far as the AsO_2 stretching modes are concerned. The AsOAs modes indicated as ring modes in Ref. 14 differ considerably from the AsOAs modes found for γ-$KAsO_3$; this may be explained by the strong angle dependence of these types of vibration.[21]

E. Depolarization Ratios. The ν_s AsO_4, AsO_3, and AsOAs (Tables II to V) modes are all expected to be strongly polarized as they are all related to ν_s AsO_4 in T_D symmetry, which is completely polarized. Furthermore, ν'_{as} AsOAs in $K_5As_3O_{10}$ and the δ AsOAs modes are expected to have a depolarization ratio ρ: $0 < \rho < 0.75$. The vibrations of other symmetry species are depolarized.[23]

F. $xK_2O \cdot As_2O_5$ Glasses. Fig. 3 gives polarized and depolarized Raman spectra of $xK_2O \cdot As_2O_5$ glasses with x = 1-2. Spectral data together with assignments are given in Table VI. It can be observed from Figs. 2 and 3 and read from Tables IV, V, and VI that the polarized Raman spectra of $K_2O \cdot As_2O_5$ and 1.67 $K_2O \cdot As_2O_5$ glasses are very similar to the Raman spectra of the crystalline compounds with the same composition: γ-$KAsO_3$ and $K_5As_3O_{10}$. The intense band at 908 cm^{-1} in the polarized spectrum of $K_2O \cdot As_2O_5$ glass consists of a polarized part which can be ascribed to a ν_s AsO_2 vibration and a depolarized part with a maximum at 935 cm^{-1} which can be ascribed to ν_{as} AsO_2 vibrations. At 770 cm^{-1}, a weak depolarized band is found which can be ascribed to a ν_{as} AsOAs vibration and at 570 cm^{-1} a broad polarized band due to ν_s AsOAs vibrations is found. The broadening and shifting of the ν_s AsOAs band from 534 cm^{-1} in crystalline γ-$KAsO_3$ toward 570 cm^{-1} in the glass can be explained by the fact that this type of vibration is highly sensitive to the AsOAs bonding angle.[21] Two depolarized bands at 404 and 360 cm^{-1} can be ascribed to δ_s and δ_{as} AsO_2 deformation modes and the partly polarized band at 254 cm^{-1} is ascribed to a δ AsOAs mode.

In the Raman spectrum of vitreous 1.67 $K_2O \cdot As_2O_5$ ($K_5As_3O_{10}$) the three polarized bands at 880, 825, and 816 cm^{-1} can be ascribed to ν_s AsO_2, ν_s AsO_3, and ν'_{as} AsOAs, respectively. The asymmetric depolarized band at 976 cm^{-1} consists of ν_{as} AsO_2 and ν_{as} AsO_3 bands. The depolarized band at 760 cm^{-1} can be ascribed to ν_{as} AsOAs and the polarized band at 547 and 484 cm^{-1} can be ascribed to ν_s AsOAs, the depolarized bands at 400 and 366 to δ_s and δ_{as} AsO_2, AsO_3 modes and the partly polarized band at 250 cm^{-1} to δ AsOAs.

From Fig. 3 it can be observed that the Raman spectra of glasses with composition intermediate between x = 1 and x = 1.67 gradually change as a function of x. The ν_s AsO_2 band shifts in position from 908 cm^{-1} (x = 1) to 880 cm^{-1} (x = 1.67), while the bandwidth decreases. The ν_s AsO_3 band can be observed first at x = 1.4.

In the region 800 to 950 cm^{-1} in the depolarized spectra

TABLE V. Raman and IR data and assignment for γ-$KAsO_3$.[a]

Raman				Infrared					
Peak position (cm^{-1})	Relative peak height	Peak width (cm^{-1})	Relative intensity	Absorption (cm^{-1})	Relative absorption depth	Absorption width (cm^{-1})	Relative absorption	Assignment	T_D
969	11	4	9	978	100	75	70	ν_{as}, ν'_{as} AsO_2	F_2
950	11	5	11	965					
917	100	5	100	911	60	10	5	ν_s AsO_2	A_1
896	0.5	5	0.6	894	30	15	5	ν'_s AsO_2	A_1
839	0.5	12	1.5	839	30	55	15	ν'_{as} AsOAs	F_2
817	0.5	9	0.7						
715	2.5	10	5	712	90	90	75	ν_{as} AsOAs	F_2
554	sh			557	40	30	10	ν'_s AsOAs	A_1
534	29	11	64	523	90	30	25	ν_s AsOAs	A_1
390	1.5	5	1.5						
386	7	5	7	400–300	90	120	100	δ AsO_2	E, F_2
374	7	5	7						
340	15	7	21						
274	16	10	32	280	80	80	60	γ AsO_2	
263	8.3	5	8.5						
224	15	13	39					δ AsOAs	
180	1.9	13	5						
160	0.2	5	0.2						
148	2.5	6	3						
132	6.2	8	10						
99	1.7	6	2					?	
73	5.8	8	9						
64	1.0	5	1						
51	0.6	5	0.6						

[a] See footnotes a, b, and c of Table II for explanation.

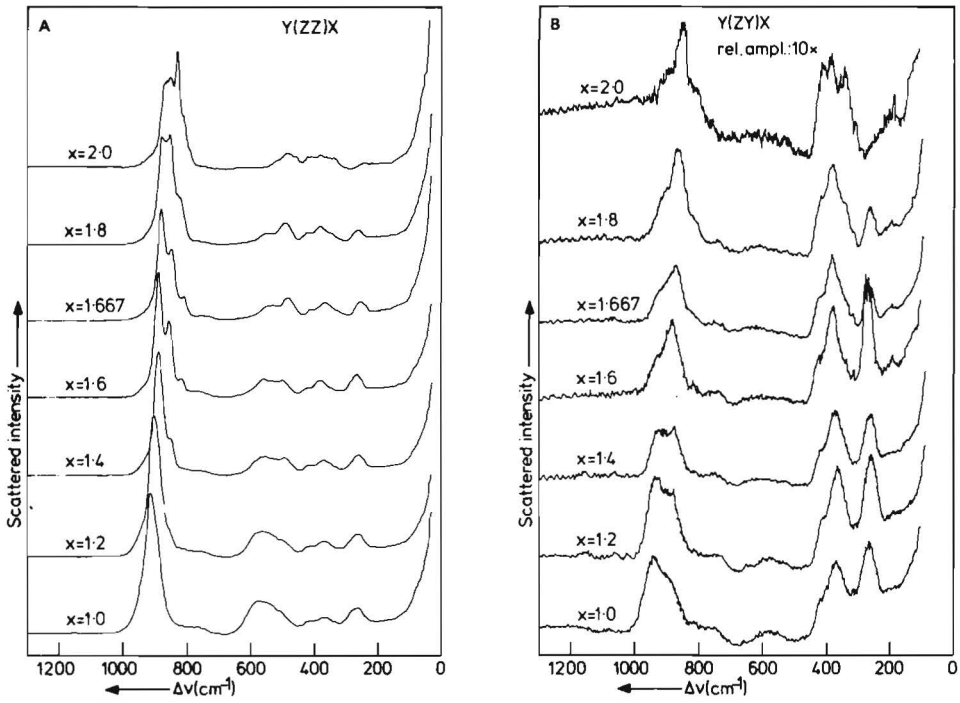

FIG. 3. Polarized (A) and depolarized (B) Raman spectra of xK_2O. As_2O_5 glasses.

we observe that the ν_{as} AsO_2 band at 935 cm^{-1} decreases in intensity and the ν_{as} AsO_3 band at about 876 cm^{-1} increases in intensity as the number of AsO_3 groups increases. The deformation modes remain at about the same position.

Although it is quite clear from the Raman spectra of glasses in the composition region $1 < x < 1.667$ that chains of AsO_4 tetrahedra occur, no conclusions on the chain length distribution can be drawn.

In the spectrum of 1.8 $K_2O \cdot As_2O_5$ glass ν_s AsO_2 is still present, but a new band at 830 cm^{-1} appears which must be ascribed to the formation of $As_2O_7^{4-}$ groups. According to the batch composition this glass should contain 50% $As_3O_{10}^{5-}$ and 50% $As_2O_7^{4-}$ groups. In the spectrum of $2K_2O \cdot As_2O_5$ glass, which theoretically must contain 100% $As_2O_7^{4-}$ groups, ν_s AsO_2 has disappeared and a sharp

TABLE VI. Raman data and assignment for $xK_2O \cdot As_2O_5$ glasses.

x	Peak position (cm^{-1})	Relative peak height	Peak width (cm^{-1})	Depolarization ratio (ρ)	Assignment
1.0	935	7	100	0.6–0.8	ν_{as} AsO_2
	908	100	52	0.0–0.1	ν_s AsO_2
	770	sh		0.6–0.8	ν_{as} AsOAs
	570	20	122	0.04	ν_s AsOAs
	404	5	66	0.72	δ_s, δ_{as} AsO_2
	360				
	254	10	52	0.35	δ AsOAs
1.2	932	5.5	99	0.6–0.8	ν_{as} AsO_2, AsO_3
	896	100	43	0–0.1	ν_s AsO_2
	760	sh		0.6–0.8	ν_{as} AsOAs
	560	16	122	0.05	ν_s AsOAs
	410	3.5	24	0.81	δ_s, δ_{as} AsO_4, AsO_3
	360	6.5	48	0.81	
	254	10	47	0.48	δ AsOAs
1.4	910	4.5	98	0.6–0.8	ν_{as} AsO_2, AsO_3
	880	100	33	0–0.1	ν_s AsO_2
	852	24	24	0–0.1	ν_s AsO_3
	760	sh		0.6–0.8	ν_{as} AsOAs
	552	13	88	0.4	ν_s AsOAs
	490	11	52	0.4	
	414	4		0.63	δ_s, δ_{as} AsO_2, AsO_3
	360	8	48	0.63	
	252	10	42	0.35	δ AsOAs
1.6	880	8	78	0.6–0.8	ν_{as} AsO_2, AsO_3
	882	100	32	0–0.1	ν_s AsO_2
	850	61	24	0–0.1	ν_s AsO_3
	760	sh		0.6–0.8	ν_{as} AsOAs
	550	13	60	0.04	ν_s AsOAs
	490	11	56	0.04	
	400	4.5	52	0.73	δ_s, δ_{as} AsO_2, AsO_3
	370	9.5	50	0.73	
	252	12	40	0.65	δ AsOAs
1.67	876	7	86	0.6–0.8	ν_{as} AsO_2, AsO_3
	880	100	28	0–0.1	ν_s AsO_2
	852	63	28	0–0.1	ν_s AsO_3
	816	20	24	0–0.1	ν'_{as} AsOAs
	760	sh		0.6–0.8	ν_{as} AsOAs
	547	10	58	0.03	ν_s AsOAs
	484	16	44	0.03	
	400	5.5	52	0.63	δ_s, δ_{as} AsO_2, AsO_3
	366	12	56	0.60	
	254	11	38	0.31	δ AsOAs
1.8	866	11.5	76	0.6–0.8	ν_{as} AsO_2, AsO_3
	868	100	54	0–0.1	ν_s AsO_2
	852				ν_s AsO_3
	830	43	24	0–0.1	ν_s AsO_3
	760	sh		0.6–0.8	ν_{as} AsOAs
	546	8	24	0.04	ν_s AsOAs
	494	15.5	48	0.04	
	410	5.5	36	0.62	δ_s, δ_{as} AsO_2, AsO_3
	370	12	23	0.62	
	250	8.5	38	0.32	δ AsOAs
2.0	860	14	44	0.6–0.8	ν_{as} AsO_3
	854	100	77	0–0.1	ν_s AsO_3
	832	55	11	0–0.1	
	480	17	66	0–0.01	ν_s AsOAs
	376	16	110	0.70	δ_s, δ_{as} AsO_3

* See footnotes a, b, and c of Table II for explanation.

band at 832 and a broad band at 860 cm^{-1} are present which are both polarized; these bands can both be ascribed to ν_s AsO_3.

It is not clear, however, why two polarized bands are present. A weak polarized band at 480 cm^{-1} can be ascribed to ν_s AsOAs; furthermore, deformation modes are present at 400, 376, and 200 cm^{-1}.

III. CONCLUSION

Raman spectra of vitreous $KAsO_3$ and $K_5As_3O_{10}$ are very similar to the spectra of the crystalline compounds γ-$KAsO_3$ and $K_5As_3O_{10}$ which suggests a structural similarity. The polarization behavior of the Raman bands of the glasses agrees with the assignments.

In the glasses $xK_2O \cdot As_2O_5$ with $1 < x < 1.67$ chains of AsO_4 tetrahedra are present. The interpretation of the spectra of $xK_2O \cdot As_2O_5$ glasses with x = 1.8 and 2.0 is somewhat uncertain. The appearance of two polarized ν AsO_3 bands cannot be explained yet.

The depolarized peak at 880 cm^{-1} observed in the Raman spectra of glass with batch composition $30K_2CO_3$ $70SiO_2$ $1As_2O_3$[1] can be ascribed to ν_{as} AsO_3 of a short chain arsenate group. At least part of the polarized band at 826 cm^{-1} can be ascribed to ν_s AsO_3. In order to complete the assignment of the "arsenic peaks" in silicate glass a detailed computer analysis of the Raman spectra of arsenic-containing silicate glasses is in preparation together with a study on crystalline and vitreous compounds in the K_2O-As_2O_3 system.

ACKNOWLEDGMENTS

The author thanks R. E. Breemer for assistance with the Raman measurements, J. L. C. Daams for x-ray diffraction measurements, and J. G. van Lierop for preparation of the glasses.

1. H. Verweij, J. Am. Ceram. Soc. accepted for publication.
2. E. M. Levin, C. R. Robbins, and H. F. McMurdie, *Phase Diagrams for Ceramics*, part 1 (The American Ceramic Society Columbus (1964); cited from M. Amadori, Atti Reale Ist. Veneto Sci. **73**(II), 1677 (1914).
3. F. K. Vansant, B. J. Van der Veken, H. O. Desseyn, J. Mol. Struct. **15,** 425 (1973).
4. F. K. Vansant and B. J. Van der Veken, J. Mol. Struct. **15,** 439 (1973).
5. K. Y. Leung, C. Calvo, Can. J. Chem. **51,** 2082 (1973).
6. W. Bues, K. Bühler, and P. Kuhnle, Anorg. Allg. Chem. **325,** 8 (1963).
7. N. A. Mazhenov , O. A. Mazhenova, and Z. M. Muldakhmetov, Inorg. Mater. **13,** 328 (1977); translated from: Izv. Ak. Nauk USSR, Neorg. Mater. **13,** 391 (1977).
8. K. H. Jost, H. Worzala, and E. Thilo, Acta Cryst. **21,** 808 (1966).
9. E. Thilo and A. Winkler, Mh. Deut. Acad. Wiss. Berlin **8,** 301 (1966).
10. E. Thilo and K. Dostál, Z. Anorg. Allg. Chem. **298,** 101 (1959).
11. I. Grunze, K. Dostál, and E. Thilo, Z. Anorg. Allg. Chem. **302,** 221 (1959).
12. F. Liebau, Acta Cryst. **9,** 811 (1956).
13. W. Hilmer and K. Dornberger-Schiff, Acta Cryst. **9,** 87 (1956).
14. W. P. Griffith, J. Chem. Soc. (A) 905 (1967).
15. H. N. Heaton and H. Moore, J. Soc. Glass Techn. **41,** 3 (1957).
16. C. A. Faick and B. Fonoroff, J. Res. Natl. Bur. Stand. **32,** 67 (1944).
17. T. C. Damen and S. P. S. Porto, Tell B. Phys. Rev. **142,** 570 (1966).
18. W. Bues and H. W. Gehrke, Z. Anorg. Allg. Chem. **288,** 291 (1956).
19. G. Herzberg, *Molecular Spectra and Molecular Structure*, 2nd ed. (Van Nostrand, Princeton, NJ, 1945), Vol II.
20. A. S. Davydov, *Theory of the Absorption of Light in Molecular Crystals* (Izd. An. Ukrainian SSR, Kiev, 1951).
21. A. N. Lazarev, "Vibrational spectra and structure of the silicates," Special Research Report, translated from Russian (Consultants Bureau, New York, 1972).
22. H. Verweij, to be published.
23. J. A. Koningstein, *Introduction to the Theory of the Raman Effect* (D. Reidel Publishing Co., Dordrecht, The Netherlands, 1972).

STRUCTURE OF $K_5As_3O_{10}$

by J. HORNSTRA AND H. VERWEIJ
Philips Research Laboratories, Eindhoven - The Netherlands

Accepted for publication in Acta Crystallographica

Abstract

$K_5As_3O_{10}$, orthorhombic, $P2_12_12_1$,
a = 7.98 (1), b = 7.97 (1), c = 19.30 (2) Å
V = 1227.5 Å^3, Z = 4, D_m = 3.06 cm^{-3},
D_C = 3.14 cm^{-3}, μ (Mo K_α, λ = 0.8107 Å) = 105 cm^{-1}.

The structure was solved by Patterson methods from X-ray single-crystal data. For 912 independent intensity data the final R = 0.04.
Each As atom is tetrahedrally surrounded by four O atoms. Groups of three tetrahedra, sharing corners, from strongly bent chains. The coordination of the K atoms varies from 6 to 9.
Tetragonal pseudosymmetry may lead to twinning.

Introduction

Structure data on potassium arsenates are needed for a study on arsenic-containing silicate glasses (Verweij, 1979). Condensed alkali arsenates generally contain chains or rings of AsO_4 tetrahedra, sharing corners.
So, $(LiAsO_3)_X$ (Hilmer & Dornberger – Schiff, 1956) and $(NaAsO_3)_X$ (Liebau, 1956) contain chains of infinite length, whereas $Na_4As_2O_7$ (Leung & Calvo, 1973) contains pyroarsenate groups, built up of two AsO_4 tetrahedra.

Compounds similar to the title compound are $Na_5As_3O_{10}$ (Thilo & Winkler, 1966) of unknown crystal structure, $Na_5P_3O_{10}$ (Corbridge, 1960) containing stretched chains of three tetrahedra, and $H_5As_3O_{10}$ (Jost, Worzala & Thilo, 1966) which contains ribbons consisting of AsO_4 tetrahedra and AsO_6 octahedra.

The phase diagram of the K_2O-As_2O_5 system (Levin, Robbins & McMurdie, 1964) shows four compounds stable at room temperature: α-K_3AsO_4, $K_4As_2O_7$, $K_5As_3O_{10}$ and γ-$KAsO_3$. The subject of this paper, $K_5As_3O_{10}$ melts incongruently at 630°C.
Single crystals were grown from a melt in a Pt-10% Rh crucible by cooling from 800°C at a rate of 0.14°C/min. The composition of the melt was 58 mole % K_2O and 42 mole % As_2O_5, which is between that of $K_5As_3O_{10}$ and the eutectic between γ-$KAsO_3$ and $K_5As_3O_{10}$ (Levin, Robbins & Mc Murdie, 1964), so that the title compound was the primary crystalline phase on cooling. The cooled mixture consisted of microscopic needles of γ-$KAsO_3$ (Thilo & Dostal, 1959) and (Grunze, Dostal & Thilo, 1959) and transparent, highly imperfect crystals of $K_5As_3O_{10}$. The crystals were very hygroscopic and had to be handled in a glove bag filled with dry nitrogen (I^2R, Cheltenham, Penn.).

An irregular, beam-shaped crystal of dimensions 0.32 x 0.20 x 0.08 mm was sealed in a glass capillary and mounted on a PW1100 computer-controlled four-circle diffractometer (Hornstra & Vossers, 1973). The crystal appeared homogeneous when inspected with a polarization microscope.

The reflections were obtained in ω scans with a stationary detector.
Many reflections showed a satellite at about 0.5° from the main reflection with an intensity about ten times lower. These satellites were included in the integrated intensity. The similarity of a and b axis suggested tetragonal symmetry; in addition many hkl-khl pairs had similar intensities. The 130 reflection, however, was three times stronger than the 310 reflection. This showed the structure to be orthorhombic.

Due to the irregular shape of the specimen, an exact absorption correction was impossible. Therefore, the intensity of the 123 reflection, a plane almost perpendicular to the φ axis, was measured at various azimuths. This showed how the intensity varied with φ and all intensities were corrected correspondingly. After this procedure the differences between symmetry-related reflections were comparable to the final R factor. By averaging over symmetry-related reflexions, 912 independent intensity data were obtained from 3796 individual measurements up to θ = 22°. The computer programs used for structure determination were by Braun, Hornstra and Leenhouts. The structure was solved from the Patterson function which showed pseudotetragonal symmetry. In the least squares refinement of the parameters the sum of $w(F_O-F_C)^2$ was minimized. The weighting system used was that described by Braun, Hornstra and Leenhouts (1970). Although the starting set of parameters of all K and As atoms had tetragonal symmetry (space group $P4_12_12$ with 4_1 along ¼ 0z), full-matrix refinement in $P2_12_12_1$ started without problems. A difference-Fourier synthesis gave all oxygen positions. These positions showed clearly that the crystal was not tetragonal.

The introduction of anisotropic thermal parameters reduced the reliability factor only from 4.2 to 3.8% and was therefore considered not to be significant. The final parameters are given in table 1. Because pseudosymmetry favours twinning, the list of observed and calculated structure factors and the final difference Fourier were carefully inspected since X-ray photographs would not reveal this type of twinning. They showed that at most ten per cent of the specimen was in the twinned orientation. Owing to this, some parameters may be in error by slightly more than 3 τ.

Table I Atomic parameters
Fractional coordinates (x 10^4) and isotropic thermal parameters. Estimated standard deviation between parentheses.

	x	y	z	B
As(1)	0720(1)	3253(2)	1242(1)	1.28(5)
As(2)	4730(1)	2778(2)	1471(1)	1.15(6)
As(3)	0183(2)	7294(2)	1060(1)	1.33(6)
K(1)	4930(3)	2425(3)	3769(2)	1.96(9)
K(2)	2646(4)	0064(4)	0054(1)	2.12(10)
K(3)	2451(4)	0006(3)	2526(1)	1.96(10)
K(4)	2526(4)	4581(4)	-296(1)	2.52(12)
K(5)	2261(4)	5273(4)	2669(1)	2.27(11)
O(1)	0127(11)	2536(11)	0476(5)	2.8 (3)
O(2)	0317(11)	2255(11)	1955(5)	3.1 (4)
O(3)	0396(11)	7133(11)	0197(4)	2.8 (3)
O(4)	0181(10)	0217(10)	3615(5)	2.8 (3)
O(5)	1617(10)	3186(11)	3725(5)	3.1 (4)
O(6)	1852(11)	7933(12)	1468(5)	3.5 (5)
O(7)	2848(9)	3822(11)	1180(5)	3.0 (4)
O(8)	3841(11)	9049(11)	3847(5)	3.3 (4)
O(9)	4640(10)	2812(10)	2331(4)	1.9 (3)
O(10)	4731(11)	0848(11)	1172(5)	3.4 (3)

Discussion

The structure may be described in terms of a body-centered subcell with dimensions a/2, b/2, c/4. If the origin is chosen at ¼ 00, all corners of the subcell are occupied by K atoms (see fig. 1). One quarter of these subcells have K(1) in their centre the others As. Oxygen atoms are found near the centres of the faces of these subcells.

Atom K(1) is surrounded by 6 oxygen atoms (see table 2) forming a nearly regular octahedron.

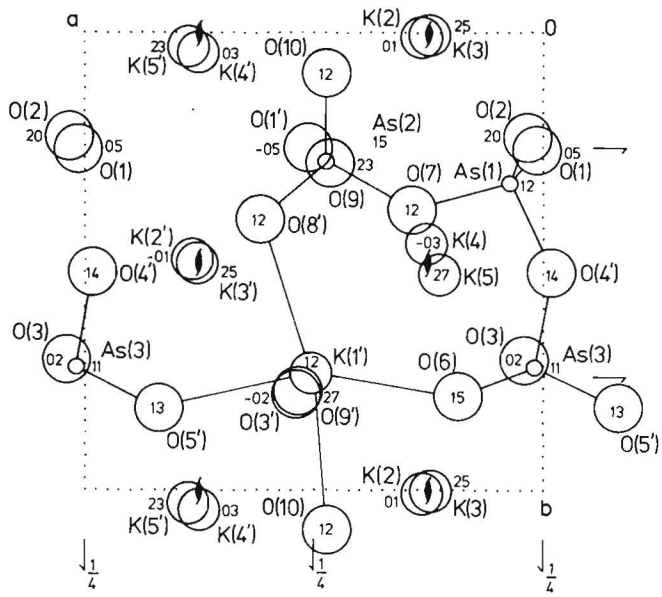

Fig. 1 Projection on (001) of the atoms with 0 < z < 0.27; the z coordinates are given in units of 0.01.

K(2) and K(3) have 8 oxygen neighbours forming a distorted dodecahedron. The six oxygen atoms around K(4) form an irregular octahedron and K(5) has 9 oxygen atoms at a distance below 3.35 Å.

The As atoms are surrounded by four oxygen atoms in almost regular tetrahedra, forming chains of three by sharing corners (see fig. 1).
The angles As(1) – O(7) – As(2) and As(1) – O(4) – As(3) have quite normal values of 131.4° and 134.9°, respectively. For the non-bridging oxygen atoms a mean As-O distance of 1.65 Å is found, and 1.78 Å for the bridging oxygen atoms, in agreement with other arsenates.
The strong bending of the chain is shown by the angle As(2) – As(1) – As(3), which is 105.0° only, compared with a corresponding angle of 173° in the chains of $Na_5P_3O_{10}$ (Corbridge, 1960).

Table II Short interatomic distances (Å)

As(1) – O(2)	1.62	K(2) – O(8)	2.71	K(4) – O(5)	2.68
As(1) – O(1)	165	K(2) – O(10)	2.80	K(4) – O(1)	2.70
As(1) – O(4)	1.75	K(2) – O(3)	2.85	K(4) – O(3)	2.82
As(1) – O(7)	1.76	K(2) – O(1)	2.93	K(4) – O(10)	2.82
As(2) – O(10)	1.64	K(2) – O(1)	2.94	K(4) – O(1)	2.92
As(2) – O(8)	1.64	K(2) – O(3)	2.96	K(4) – O(7)	2.92
As(2) – O(9)	1.66	K(2) – O(6)	3.28	K(5) – O(5)	2.68
As(2) – O(7)	1.81	K(2) – O(4)	3.28	K(5) – O(2)	2.69
As(3) – O(6)	1.63	K(3) – O(6)	2.67	K(5) – O(9)	2.81
As(3) – O(5)	1.66	K(3) – O(2)	2.71	K(5) – O(7)	3.13
As(3) – O(3)	1.68	K(3) – O(4)	2.78	K(5) – O(4)	3.15
As(3) – O(4)	1.79	K(3) – O(9)	2.86	K(5) – O(6)	3.16
K(1) – O(6)	2.64	K(3) – O(8)	2.88	K(5) – O(2)	3.18
K(1) – O(5)	2.71	K(3) – O(9)	2.92	K(5) – O(9)	3.20
K(1) – O(10)	2.74	K(3) – O(10)	3.25	K(5) – O(10)	3.31
K(1) – O(3)	2.79	K(3) – O(2)	3.27	As(1) – As(2)	3.25
K(1) – O(9)	2.80			As(1) – As(3)	3.27
K(1) – O(8)	2.83				

References

[1] Braun, P.B., Hornstra, J., Leenhouts, J. I. Computerprograms, Philips Research Laboratories, Eindhoven, Netherlands.
[2] Braun, P.B., Hornstra, J., Leenhouts, J.I., (1970). Acta Cryst. **B26**, 352-356.
[3] Corbridge, D.E.C., (1960). Acta Cryst. **13**, 263-269.
[4] Grunze, I., Dostal, K., Thilo, E., (1959). Z. Anorg. Allg. Chem. **320**, 221-229.
[5] Hilmer, W. von, Dornberger-Schiff, K., (1956). Acta Cryst. **9**, 87-88.
[6] Hornstra, J., Vossers, H., (1973). Philips Techn. Rev. **33**, 61.
[7] International Tables for X-ray Crystallography, (1974). Vol IV. Birmingham: Kynoch Press.
[8] Jost, K.H., Worzala, H., Thilo, E., (1966). Acta Cryst. **21**, 808-813.
[9] Leung, K.Y., Calvo, C., (1973). Can. J. Chem. **51**, 2082-2088.
[10] Levin, E.M., Robbins, C.R., McMurdie, F., (1964). Phase Diagrams for ceramists. Part 1, p. 88. Columbus Ohio: The American Ceramic Society.
[11] Liebau, F., (1956). Acta Cryst. **9**, 811-817.
[12] Thilo, E., Dostal., (1959). Z. Anorg. Allg. Chem. **298**, 100-115.
[13] Thilo, E., Winkler A., (1966) Monatsber. Deut. Akad. Berlin **8**, 301-304.
[14] Verweij, H., (1979). J. Am. Ceram. Soc. **62**, 450-455.

RAMAN SPECTRA OF CRYSTALLINE COMPOUNDS AND GLASSES IN THE SYSTEM $K_2O - As_2O_3$

by H. VERWEIJ and J.G. VAN LIEROP
Philips Research Laboratories, Eindhoven - The Netherlands

Submitted for publication to Physics and Chemistry of Glasses.

Abstract

The preparation of crystalline compounds and glasses in the K_2O-As_2O_3 system is described and Raman spectra are given. Mixtures of KOH and As_2O_3 of various composition were allowed to react in a N_2 atmosphere and the reaction products were inspected by their Raman spectra.
Compounds of stoichiometric composition KAs_3O_5, $KAsO_2$ and K_3AsO_3 were found in the mixtures.
Potassium arsenite glasses were prepared by melting $KAsO_2$ – As_2O_3 mixtures in vitreous silica tubes; polarized and depolarized Raman spectra of the glasses were taken. From these spectra it is concluded that the glass structures are similar to the structures of the compounds KAs_3O_5 and $KAsO_2$, which probably contain chains of As_3O_3 rings and AsO_3 pyramids respectively.

Introduction

Raman data of arsenites in the crystalline and the vitreous state are used for studies of melting and fining reactions of glass-forming batches containing As_2O_3.([1])
In these studies Raman spectroscopy is used as an identification technique for structures in crystalline and vitreous phases.
Studies of the vibrational spectra of the crystalline As_2O_3 modifications can be found in refs. 2, 3. Vibrational spectra of vitreous As_2O_3 are given in refs. 3, 4. A recent X-ray diffraction study of the structure of vitreous As_2O_3 is described in ref. 5.
In refs. 3, 4 and 5 the structure hypotheses for vitreous As_2O_3 are all based on networks of corner connected AsO_3 pyramids. In ref. 3, in which Raman and infrared spectra are studied, it is concluded that the structure of vitreous As_2O_3 contains both elements from the claudetite structure ([6]) and from the arsenolite structure ([7]). The claudetite structure contains folded layers of AsO_3 pyramids; in these layers interconnected rings of six pyramids can be distinguished clearly (cf. fig. 1A). The arsenolite structure can be regarded as a packing of cage-like As_4O_6 molecules which are also built up of AsO_3 pyramids. Rings of three AsO_3 pyramids can be seen in the As_4O_6 molecule (cf. fig. 1B).
Table I gives the Raman data of vitreous As_2O_3 together with the structural interpretation from ref. 3. The notations used are ([3]):

- R_2 = Rocking mode of the oxygen atoms: Out-of-plane motion of the oxygen atoms in the As-O-As bond.
- R_{23} = Rocking mode of the oxygen and arsenic atoms.

Table I Interpretation of Raman data of vitreous As_2O_3 according to ref. 3.

Frequency (cm^{-1})	Polarisation	Rel. Strength	Interpretation
255	Dep.	Weak	$Cld(R_2, R_{32})$
378	Pol.	Strong	$Ars(B_3 + (B_2))$
482	Pol.	Very strong	$Cld(B_2)$
527	Pol.	Medium	$Ars(B_2 - (B_3))$
610	Dep.	Weak shoulder	$Cld(B_2 - B_3)$
810	Dep.	Weak	$Cld(S_2 - D_3)$; $Ars(S_2 - B_3)$

- B_3 = Bending mode of the O-As-O bond: movement of the As atom along the bond angle bisector.
- B_2 = Bending mode of the As-O-As bond: Movement of the O atom along the bond angle bisector.
- S_2 = Antisymmetrical stretch mode: Movement of the O atom in the As-O-As bond in the direction of the As-As axis.
- S_3 = Antisymmetrical stretch mode: Movement of the As atom in the O-As-O bond in the direction of the O-O axis.
- D_3 = Cation motion with mixed B_3 and S_3 character.

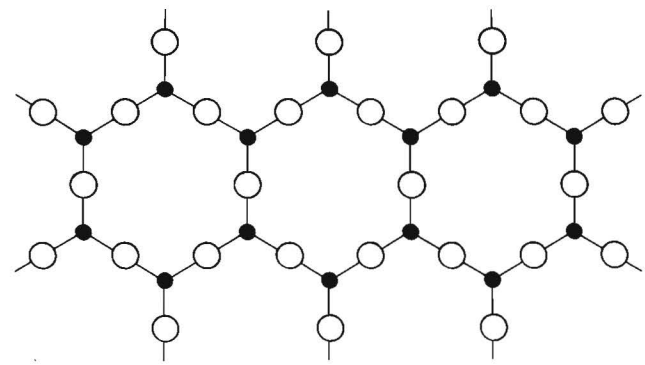

Fig. 1A Claudetite network

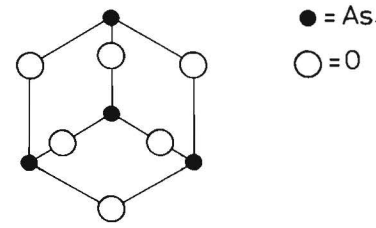

Fig. 1B As_4O_6 molecule

Enclosure between parentheses indicates a relatively small contribution and a minus sign denotes an antiphase movement. Cld is used for a claudetite-type structural element and Ars for an arsenolite-type network.

In ref. 5 an X-ray diffraction study of the structure of vitreous As_2O_3 is reported in which a layer network of As_3O_3 rings forming 6-membered rings is concluded (cf. fig. 2). This proposed structure is in a good agreement with the conclusions of ref. 3. The As_3O_3 rings can be regarded as arsenolite-type elements, while the bridges between the As_3O_3 rings can be regarded as claudetite-type elements (cf. fig. 2).

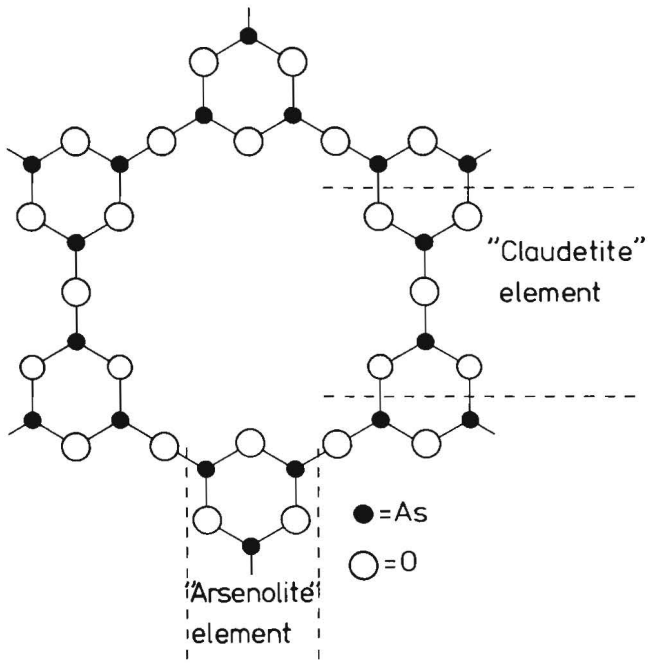

Fig. 2 Layer network structure as concluded for vitreous As_2O_3 in ref. 5.

Compound glasses based on As_2O_3 as the network-former are reported in refs. 8, 9. A study of the structure and properties of glasses in the Na_2O-As_2O_3 system is described in ref. 10 where IR spectra, density, refractive index and thermal expansion are given. In ref. 10 it is concluded that when Na_2O is introduced in As_2O_3 glass, networks are formed based on AsO_3 pyramids with one or two non-bridging oxygen atoms (NBO's). Furthermore it is concluded that glasses with 40-50 mole % Na_2O are structurally similar to crystalline $NaAsO_2$ ([11]).

Phase studies and structure determinations of crystalline alkali arsenites are scarce. The compound $NaAsO_2$ is reported to contain chains of AsO_3 triangles with one NBO, sharing corners ([11]). In ref. 12 a phase study of the K_2O-As_2O_3-H_2O system is reported in which a compound $K_2As_4O_7$ is postulated. The compounds K_3AsO_3 and $KAsO_2$ have been reported by various authors ([13,14]). In a phase study of the Na_2O-As_2O_3-H_2O system ([15]) a compound $NaAs_3O_5$ was found. Vibrational spectra of $KAsO_2$ have been given in ref. 13, of K_3AsO_3 in refs. 13 and 15, and of $NaAsO_2$ in ref. 16. Raman spectra of arsenites in solution have been given in refs. 14 and 16.

Experimental

The components, used for sample preparation, were resublimated, reagent grade As_2O_3 (> 99.5%) and reagent grade KOH pellets (86% by chemical analysis), both from E. Merck, Darmstadt. Pellets of molar composition xKOH-As_2O_3 were prepared by thoroughly mixing 5-gram quantities, using an agate mortar, followed by pressing in a 0.5" cylindrical mould. The parameter x was varied from 0 to 6 in steps of 0.5.

The pellets were heated in vitreous silica boats using a linear temperature increase from room temperature to 200°C at a heating rate of 3°C/hr, followed by a constant period of 60 hrs. After this treatment the samples were taken out of the furnace. Heating rates of more than 3°C/hr resulted in inhomogeneous reaction products with colours varying from yellow to black.

From inspection of the Raman spectra of the powdered reaction product it was concluded that the compounds KAs_3O_5, $KAsO_2$ and K_3AsO_3 were present in the mixtures in addition to some unreacted As_2O_3. The compounds $KAsO_2$ and K_3AsO_3 have been reported in refs. 13, 14; a compound $K_2As_4O_7$ as postulated in ref. 12 was not found. The compound KAs_3O_5 corresponds with the compound $NaAs_3O_5$, reported in ref. 15.

As the formation of KAs_3O_5 proved to be very sluggish, the following procedure was used to obtain it in a pure state. A concentrated solution of As_2O_3 and KOH in O_2-free destilled water was evaporated at 80°C. The product obtained was heated in a quartz boat to 210°C at a linear heating rate of 5°C/min, followed by a constant period of 75 hrs. The glassy reaction product was powdered in an agate mortar and pressed to a pellet. This pellet was heated again to 210°C with a linear rate of 3°C/hr followed by a constant period of 100 hrs. The Raman spectrum of the final reaction product showed no peaks belonging to compounds other than KAs_3O_5; the purity was estimated to be > 95%.

Potassium arsenite glasses with composition $K_2O.xAs_2O_3$ (x = 1, 2, 3) were prepared from mixtures of $KAsO_2$ and As_2O_3. Pellets, pressed from these mixtures, were sealed in vitreous silica tubes and melted by heating to 625°C at a linear rate of 14°C/min and a constant period of 2 hrs followed by air quenching. In this way glass fragments of several millimeters were obtained.

Raman spectra were taken in perpendicular scattering geometry using a Jobin Yvon Ramanor HG2S spectrometer with a Coherent Radiation 4W Ar^+ laser, a ITT FW130 photomultiplier tube and a Keithley 117 picoammeter.

For measurement of powder spectra an Oriel 5145-11 1 nm bandpass interference filter was placed in the laser beam to avoid unwanted plasma lines. Powders were sealed in vitreous silica tubes of 4 mm inner diameter which were rotated at a speed of 1000 rpm during the measurements. In this way sample decomposition due to laser heating was avoided.

Polarized and depolarized glass spectra were measured with a Glan-Thompson prism placed in the laser beam to obtain a linear polarization. The glass samples were cut, ground

and polished in oil to obtain two parallel surfaces and one perpendicular surface. They were measured in optical sample cells, filled with dry nitrogen.
The scan speed for all spectra was 20 cm^{-1}/min. The laser power was about 500 mWatt.
All sample preparation and manipulation took place in a glove box flowed with nitrogen which was purified using a gas purifier from ASM, Bilthoven, The Netherlands.

Results and discussion

Raman powder spectra of crystalline K_3AsO_3, $KAsO_2$ and KAs_3O_5 are given in fig. 3.

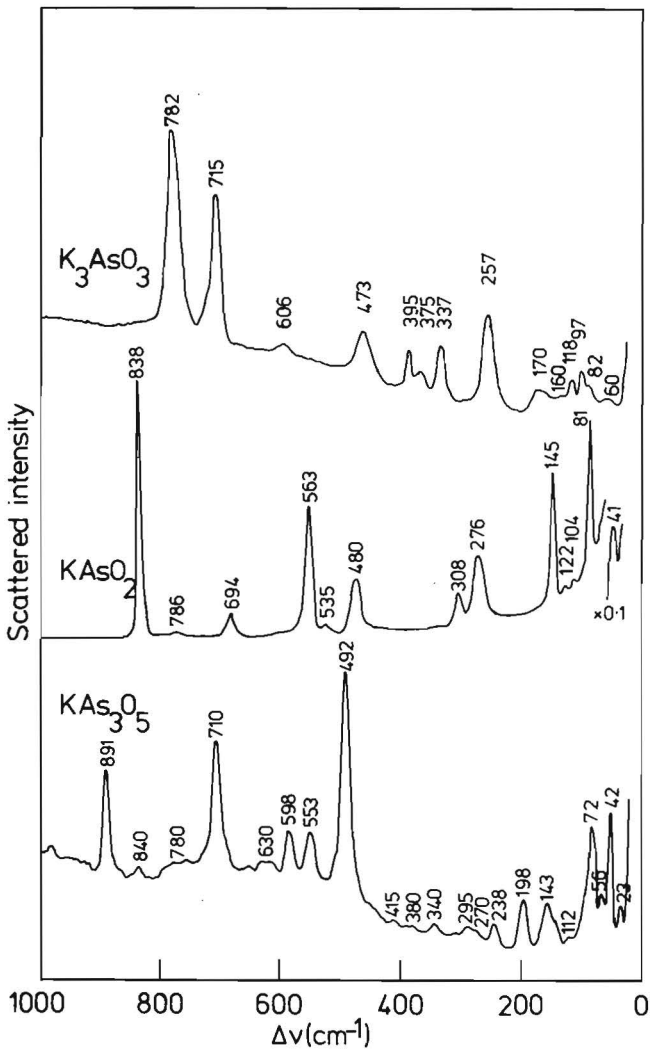

Fig. 3 Raman powder spectra of potassium arsenites. The spectral resolution is 5 cm^{-1}.

In the interpretation of the spectra use is made of the observation that arsenic atoms in arsenite structures are generally coordinated by three oxygen atoms forming pyramids of approximate C_{3v} symmetry; other coordinations are less probable because of the lone pair orbital of the As^{3+} ion. It is assumed that the Raman peaks above 200 cm^{-1} can only be ascribed to first order internal modes of the arsenite networks, in accordance with the findings for the various As_2O_3 phases ([2, 3, 4]).

The stoichiometry of the compound K_3AsO_3 suggests the presence of AsO_3^{3-} ions. In the Raman spectrum of K_3AsO_3 eight peaks are clearly distinguished above 200 cm^{-1}, whereas six internal vibrational modes, all Raman-active, are to be expected for an isolated AsO_3^{3-} ion ([17]). The extra peaks are probably caused by a significant interaction between the AsO_3^{3-} ions (Davydov splitting, ref. 18).
For an AsO_3^{3-} pyramid in C_{3v} symmetry $2A_1$ and 2E modes are expected ([17]) which can be described as symmetrical (A_1) and antisymmetrical (E) stretching and bending modes. If the symmetry of the pyramid is lowered the E modes are split up. Raman data together with an assignment for K_3AsO_3 are given in table II. The strong Raman peaks are assigned to A_1 modes and the peaks above 600 cm^{-1} are assigned to stretching modes by analogy with the As_2O_3 phases where the stretching (S) modes were all above 600 cm^{-1} ([3]).

Table II Raman data and assignment for K_3AsO_3

Freq. (cm^{-1})	Rel. height	Width (cm^{-1})	Rel. Int.	Assignment for $C_{3v}AsO_3^{3-}$
782	100	20	100	Symm. Stretch (A_1)
715	71	14	50	
606	7	20	7	Antisymm. Stretch (E)
473	21	26	27	Antisymm. Bending
395	17	9	8	(E)
375	7	20	7	
337	24	12	14	
257	43	22	47	Symm. Bending (A_1)
177	11	20	11	K-O, lattice modes
160	6	12	3	
118	13	12	8	
97	19	9	8	
82	11	12	6	
60	4	12	2	

The stoichiometry of the compound $KAsO_2$ points to the presence of rings of AsO_3 pyramids sharing corners, or chains as are present in crystalline $NaAsO_2$ ([11]). The Raman data for $KAsO_2$ agree very well with those given for $NaAsO_2$ ([16]) from which a structural similarity can be concluded. The Raman spectrum of $KAsO_2$ (cf. fig. 3) shows the general features of other chain-type compounds such as arsenates ([19]), germanates and silicates ([20]).
Raman data and assignments for $KAsO_2$ are given in table III. The weak peaks at 786 and 535 cm^{-1} are interpreted as Davydov partners of the strong peaks at 838 and 563 cm^{-1}. The strong peaks at 838 and 563 cm^{-1} are ascribed to symmetrical stretch vibrations of the NBO and of the As-O-As bond respectively.
NBO stretch vibrations give rise to strong peaks in the region of 800-950 cm^{-1} for chain-type arsenates, germanates and silicates; symmetrical X-O-X vibrations are found at

Table III Raman data and assignments for $KAsO_2$

Freq. (cm^{-1})	Rel. height	Width (cm^{-1})	Rel. Int.	Assignment for $(AsO_2^-)_\infty$ chains
838	50	6	50	As-O$^-$ stretch
786	1	10	2	
694	4	13	9	Antisymm. As-O-As stretch
563	24	11	45	Symm. As-O-As stretch
535	2	11	3	
480	10	13	22	Bending (B_2 of As_2O_3)
308	6	12	12	Bending (B_2 of As_2O_3)
276	13	21	45	
145	24	7	28	K-O, lattice modes
122	1	6	1	
104	1	7	1	
81	27	6	27	
41	100	6	100	

500-600 cm^{-1} for these compounds ([19, 20]). The weak peak at 694 cm^{-1} is ascribed to an antisymmetrical As-O-As stretch using the analogy with the S_2 vibration of vitreous As_2O_3([3]). In the same way the peaks at 480, 308 and 276 cm^{-1} are assigned to B_2 and B_3 type bending vibrations. From the stoichiometry of the compound KAs_3O_5 it can be calculated that in a network, based on AsO_3 pyramids, two thirds of the arsenic atoms should have no NBO's and one third should have one NBO. A hypothesis for the structure of the $As_3O_5^-$ network is given in fig. 4. This structure consists of chains of As_3O_3 rings connected by oxygen atoms with one NBO per ring which gives an average of 1/3 NBO per As atom. Support for the structure of fig. 4 can be obtained from the observation that As_3O_3 rings are also present in the arsenolite structure ([7]). Furthermore this structure can easily be formed from the vitreous As_2O_3 glass structure as concluded in ref. 5, by breaking part of the As-O-As bonds (cf. fig. 2).

Raman data and assignments for KAs_3O_5 are given in table IV. The peak at 891 cm^{-1} is ascribed to the stretching vibration of the NBO in correspondence with the 838 cm^{-1} peak, found for $KAsO_2$. The strong peak at 710 cm^{-1} is ascribed to a stretching mode of the As-O-As bonds between the As_3O_3 rings, comparable with the 694 cm^{-1} antisymmetrical As-O-As stretching mode of $KAsO_2$. The strong peak at 492 cm^{-1} corresponds to the strong peak at 461 cm^{-1} in the Raman spectrum of claudetite ([2]), and the peaks at 598 and 553 cm^{-1} correspond to the peak at 560 cm^{-1} in the Raman spectrum of arsenolite ([2]). These peaks are ascribed to B_2-type bending vibrations ([3]).

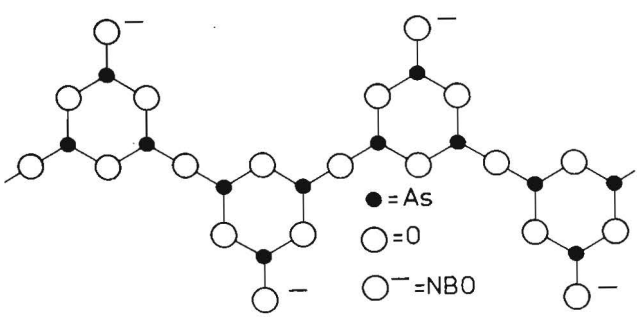

Fig. 4 Structure hypothesis for the $As_3O_5^-$ network in crystalline and vitreous KAs_3O_5.

Table IV Raman data and assignments for KAs_3O_5

Freq. (cm^{-1})	Rel. height	Width (cm^{-1})	Rel. Int.	Assigment for structure of fig. 4
891	47	10	34	
840	5	10	4	As-O$^-$ stretch
780	?	?	?	
710	57	13	53	As-O-As stretch
630	?	?	?	between the rings
598	18	14	18	Bending modes (B_2 of
553	20	17	24	As_2O_3)
492	100	14	100	Ring breathing modes
415	2	15	2	Bending + Rocking
380	2	15	2	modes
340	5	12	4	
295	6	12	5	
238	5	12	4	
238	10	14	10	
198	22	12	18	K-O + lattice modes
143	19	22	30	
112	2	10	2	
72	48	14	48	
56	17	10	12	
42	32	8	18	
23	8	6	3	

Polarized and depolarized Raman spectra of $K_2O.xAs_2O_3$ glasses are given in fig. 5. The polarized spectrum of $K_2O.As_2O_3$ glass is very similar to the powder spectrum of $KAsO_2$; the same applies to $K_2O.3As_2O_3$ glass and the compound KAs_3O_5. All observed Raman bands are polarized which points to symmetrical vibrations such as NBO stretching (800-900 cm^{-1}) and As-O-As stretching (400-750 cm^{-1}).

When alkali ions are introduced in vitreous As_2O_3, part of the bridging bonds in the network break up with the formation of NBO's. This apparently results in structures as are found in KAs_3O_5. If the structure hypothesis for KAs_3O_5, as given above, is valid, $K_2O.3As_2O_3$ glass should contain infinite chains of As_3O_3 rings (cf. fig. 4). The Raman spectrum of $K_2O.2As_2O_3$ glass shows bands at the same position as was found for $K_2O.3As_2O_3$ glass but with different intensities. This suggests that in the glass with x=2 chains of As_3O_3 rings are also present. According to the composition (x=2) an average length of four As_3O_3

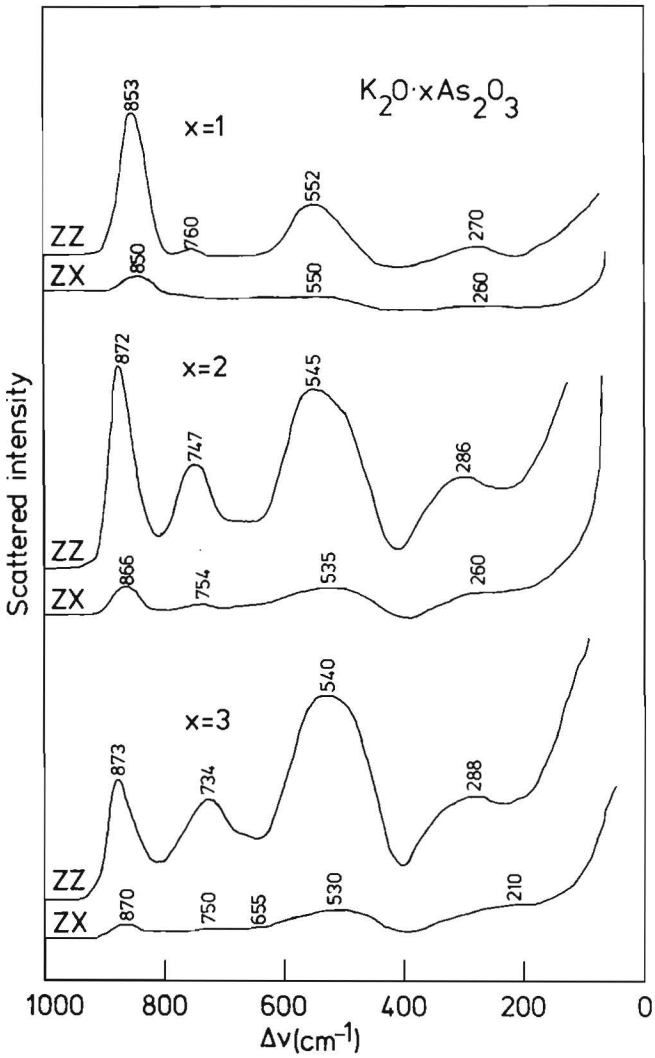

Fig. 5 Polarized (ZZ) and depolarized (ZX) Raman spectra of $K_2O.xAs_2O_3$ glasses with x = 1, 2, 3. The spectral resolution is 5 cm^{-1}.

rings can be expected for these chains. The relative increase of the intensity of the 872 cm^{-1} band with respect to the 747 cm^{-1} band in the Raman spectrum of $K_2O.2As_2O_3$ glass can easily be explained by the increase of the number of NBO's going from x=3 to x=2.

The bands at about 740 cm^{-1} in the Raman spectra of the glasses with x=3 and 2 correspond to the 710 cm^{-1} peak in the Raman spectrum of KAs_3O_5. This peak is ascribed to a stretch vibration of the As-O-As bonds between the As_3O_3 rings. The bands at about 870 cm^{-1} in the glass spectra correspond to the 891 cm^{-1} peak of KAs_3O_5 which is ascribed to an NBO stretch vibration.

In the present structure hypothesis for the glasses with x=3 and 2 the ratio of the number of NBO's to the number of As-O-As bonds between the As_3O_3 rings should be one for x=3 and two for x=2. Experimentally the intensity ratio of the 872 cm^{-1} (NBO) and 747 cm^{-1} (As-O-As) bands in the polarized Raman spectrum of $K_2O.2As_2O_3$ glass amounts to 1.7 times the corresponding ratio for $K_2O.3As_2O_3$. This gives further support for the present structure hypothesis for the glasses with x=2 and 3 and KAs_3O_5.

The Raman spectrum of $K_2O.As_2O_3$ glass is rather different, both in intensity and in peak position, from the Raman spectra of the glasses with x=2 and 3. From the glass composition and the correspondence of the polarized Raman spectrum to the powder Raman spectrum of $KAsO_2$, $(AsO_2^-)_n$ closed rings or chains with n very large can be expected. $As_3O_6^{3-}$ rings would be a logical consequence of the break up of the networks in the glasses with lower alkali concentration (x=2 and 3). These rings are less probable however because of the easy glass formation of $K_2O.As_2O_3$ glass which points to larger molecular units such as long chains.

The broad band at about 740 cm^{-1}, which was found in the Raman spectra of the glasses with x=2 and 3 is not found in the Raman spectrum of $K_2O.As_2O_3$ glass. The polarized NBO stretching band, found at about 870 cm^{-1} for x=2 and 3, is present at 853 cm^{-1} for x=1. A shift of the position of the NBO stretching band in oxide glasses towards lower frequencies is generally related with a depolimerization of the network.([19, 20]).

The broad bands which are found at about 545 cm^{-1} in all Raman glass spectra are probably built up of B_2-type vibrations as are found for vitreous As_2O_3 at 482 and 527 cm^{-1} and of symmetrical stretch vibrations of the As-O-As bonds as are found at 563 and 535 cm^{-1} in the Raman spectrum of crystalline $KAsO_2$.

Conclusions

It is concluded that the structure of potassium arsenite glasses $K_2O.xAs_2O_3$ is based on networks of connected As_3O_3 rings, as are probably present in vitreous As_2O_3([5]) and on chains of AsO_3 pyramids, as are present in crystalline $NaAsO_2$([11]). The rings are stable at $x < 1.5$; when the alkali content is increased ($x > 1.5$) they break up to form chains of simple AsO_3 pyramids with one NBO per As atom. In the As_3O_3 ring-based networks there may be one or two NBO's per ring.

References

[1] Verweij, H. (1979). J. Am. Ceram. Soc. **62** (9-10), 450.

[2] Flynn, E.J., Solin, S.A. & Papatheodorou, G.N. (1976). Phys. Rev. **13** (4), 1752.

[3] Lucovsky, G. & Galeener, F.L. (1980). J. Non-Cryst. Sol. **37**, 53.

[4] Papatheodorou, G.N. & Solin, S.A. (1975). Sol. State Comm. **16**, 5.

[5] Imaoka, M. & Hasegawa, H. (1980). Phys. Chem. Glass. **21** (2), 67.

[6] Becker, K.A. Pleith, K. & Stransky, I.M. (1954). Z. Anorg. Allgem. Chem. **275**, 297.

[7] Bozorth, R.M. (1923). J. Am. Chem. Soc. **45**, 1621.

[8] Heaton, H.M. & Moore, H. (1957). J. Soc. Glass Technol. **41**, 3T.

[9] Imaoka, M. (1962). Advances in Glass Technology Part I. Plenum Press, New York.

[10] Mochida, N. & Takahashi, K. (1975). J. Ceram. Soc. Japan **83**, 61.

[11] Menary, J.W. (1958). Acta Cryst. **11**, 742.

[12] Schreinemakers, F.A.H. & de Baat, W.C. (1920). Rec. Trav. Chim. **39**, 425.

[13] Szymanski, H.A., Marabella, L. Hoke, J. & Harter, J. (1968) Appl. Spectr. **22** (4), 297.

[14] Feher, F. & Morgenstern, G. (1937). Z. anorg. allgem. Chem. **232**, 169.

[15] Nelson, O.A. (1941). J. Am. Chem. Soc. **63**, 1870.

[16] Loehr, T.M. & Plane, R.A. (1968). Inorg. Chem. **7** (9), 1708.

[17] Herzberg, G. (1945). Molecular Spectra and Molecular Structure. Vol. II Van Nostrand, Priceton, New Jersey.

[18] Davydov, A.S. (1951). Theory of the Absorption of Light in Molecular Crystals. Izd. An. Ukrainian SSR, Kiev.

[19] Verweij, H. (1979). Appl. Spectr. **33** (5), 509.

[20] Verweij, H. (1979). J. Non-Cryst. Sol. **33**, 41.

RAMAN STUDY OF ARSENIC-CONTAINING POTASSIUM SILICATE GLASSES

by H. VERWEIJ
Philips Research Laboratories, Eindhoven - The Netherlands

Submitted for publication to the Journal of the American Ceramic Society

Raman spectra are given of potassium silicate glasses with batch composition x K_2CO_3-(100-x)SiO_2-0.5 As_2O_3 in which x varies from 10 to 50. To isolate the contribution of the As_2O_3 additions to the spectra from that of the silicate network, difference spectra were prepared from spectra of glasses with and without As_2O_3 added to the batch. In order to obtain a precision sufficient for this purpose, the spectral data were collected in multiple scans under full computer control using photon counting and a correction for laser source fluctuations.

It is concluded from the polarized and depolarized difference spectra that arsenic in potassium silicate glasses with $x > 35$ is mainly present in the pentavalent state as AsO_4^{3-} ions. For glasses with $x < 35$ it is concluded that As^{5+} is present in $As_2O_7^{4-}$ or $As_3O_{10}^{5-}$ ions and As^{3+} as $As_mO_{2m+1}^{-m-2}$ chains of AsO_3 pyramids. In these chains m increases with decreasing x. From the intensity ratio of Raman peaks, caused by arsenite (As^{3+}) and arsenate (As^{5+}) ions in the glasses it is concluded that there is a significant increase of the As^{3+}/As^{5+} ratio going from x = 50 to x = 10. The effect of melting temperature on the As^{3+}/As^{5+} ratio in $30K_2O$ $70SiO_2$ $0.5As_2O_3$ glasses in the range of 1300-1600°C was also studied.

No clear temperature effect could be concluded from the Raman spectra.

I. Introduction

The present study is part of a research program in which the fining action of As_2O_3 additions to silicate glassforming batches is investigated.

In a previous paper ([1]) a Raman study of the melting reactions in a model silicate glass-forming system with molar batch composition $30K_2CO_3$-$70SiO_2$-$1As_2O_3$ was reported.

In this study the preliminary results of the present paper were used. For a complete description of the melting and fining process in arsenic-containing silicate glass batches a detailed knowledge of Raman spectra of arsenate and arsenite structures as they occur in silicate glasses appeared to be of importance for two reasons:

I. Identification of arsenate and arsenite structures during melting reactions of silicate glass-forming batches.
II. Non-destructive analysis of As^{3+}/As^{5+} ratios in silicate glasses as a function of melting temperature, atmosphere and glass composition.

The present study sets out to give an interpretation of Raman spectra of arsenic-containing silicate glasses as detailed as possible over a wide composition range for identification purposes and for non-destructive analysis of As^{3+}/As^{5+} ratios as a function of temperature and composition. Raman spectra of arsenic-containing glasses were given earlier by Konijnendijk et al. ([2, 3]).

II. Experimental

The compounds used were:
- SiO_2 – α – quartz, milled rock crystal, sieve fraction 100-500 μ(A).
- K_2CO_3 , reagent grade, dried for two hours at 300°C(B).
- As_2O_3-arsenolite(B).

The batch compositions of the glasses studied were: xK_2CO_3-(100-x)SiO_2 with and without 0.5 As_2O_3. In this paper the notations Kx and KxA are used for the glasses with and without As_2O_3. The arsenic concentration was chosen to correspond to practical values and as a compromize between detectibility in the Raman spectra and minimization of alkali extraction from the network.

The batch components were mixed by tumbling for 1 hour in PVC containers. The glasses were melted inside an electrically heated vertical furnace and bubbled with O_2 for one hour for homogenization and equilibration. After bubbling, the melts were allowed to stand on the melting temperature for one hour to become bubble-free. The melting temperatures were 1400°C for the compositions with x = 20, 35, 40 and 50; 1300, 1400, 1500 and 1600°C for x = 30 and 1600°C for x = 10. The crucibles and bubble-pipes consisted of dense-sintered Al_2O_3 with purity > 99.5%(C). Chemical analysis of As^{3+} and As^{5+} was performed by dissolving the glasses in HF/$HClO_4$ mixtures, followed by iodometric titration of As^{3+} and total As.

The volatilization of As^{3+} as AsF_3([4]) led to badly reproducible results. Qualitatively it was found that about 50% of the originally added arsenic remained in the glass after melting. K50A appeared to contain no As^{3+} while K30A contained a quantity of As^{3+} of the order of 10% of total arsenic. Improvement of chemical analysis procedures for arsenic in silicate glasses is still under investigation. For the time being no drastic conclusions should be drawn from chemical analyses results.

For A35(A), A40(A) and A50(A) samples, suitable for obtaining polarized and depolarized Raman spectra, were prepared by pouring the melt into preheated graphite moulds followed by annealing in a dry O_2 stream. K30(A), K20(A) and K10(A), being less hygroscopic but much more viscous, were air quenched in the crucible and annealed under normal atmospheric conditions. Raman samples of these glasses were prepared by cutting, grinding and polishing

the appropriate surfaces. The dimensions of all samples were about 10 x 10 x 20 mm. During the Raman measurements the glass samples were positioned in a sample holder which was placed inside a square glass vessel built up from optical windows. This vessel could be closed with a stopper and was filled with dry nitrogen to protect the glass samples from atmospheric attack.

All sample-handling at room temperature occured inside a nitrogen-filled glove box. Accurate polarized and depolarized Raman spectra were obtained using a fully computerized Raman spectrometer system consisting of:

- A CR4, 4 Watt Ar^+ laser(D).
- An HG2S double monochromator with concave holographic gratings, a RAMANDIGIT 01 wavenumber display unit and a Ramanor L75 monochromator control unit (E).
- A FW130 photomultiplier tube (PMT).(F)
- A photon-counting system, consisting of a 1121 amplifier/discriminator and a 1109 counter. (G)

The computer system contained a PDP 11/04 computer(H) which controlled a SCORPIO 2000(I) MCA data collection and analysis system and a CAMAC modular interface system. The SCORPIO system is primarily designed for collection and analysis of nuclear gamma radiation spectra; in the present configuration only the spectrum analysis functions are used. The CAMAC system contains interface modules for computer control of the monochromator, of the photon counter and of a laser shutter and for selection of polarization filters. During the measurements under computer control the intensity data, obtained from the photon counter, are continuously checked for statistical significance in order to reject external interferences.

The laser intensity appeared to decrease considerably because of slow detuning during the long scans. To compensate for this effect a second PMT, type XP 1002(J) was used to monitor the intensity of the laser beam according to the method of ref. 5.

The pulses from the monitor PMT are processed by a second 1121 amplifier/discriminator(G) and serve as an external time base for the 1109 counter(G). The laser was tuned to a wave-length of 514.4 nm and set to an intensity of about 600 mW; the beam was linearly polarized using a coated Glan-Thompson prism(K). The scattered light was collected in a perpendicular direction in Y(ZZ)X (polarized) and Y(ZY)X (depolarized) geometries using a polaroid filter. The notation A(BC)D is according ref. 6; X is the direction of measurement, Y is the propagation direction and Z the polarization of the laser beam.

The Raman spectra were recorded in a step-scan mode in the wavenumber region of 20-2000 cm^{-1} using steps of 3 cm^{-1}. The spectrometer slits were set to 1000 μm, corresponding to a spectral resolution of about 10 cm^{-1}. For each spectrum 16 scans were performed, alternately in Y(ZZ)X and Y(ZY)X geometry. The measurement time per step was about 4s, giving a total measurement time of about 16 hrs. The precision of the largest intensities in the polarized spectra was of the order of 0.1%. To isolate the contribution of arsenic to the Raman spectra of the glasses, difference spectra were prepared by stripping the spectra of glasses without arsenic from the spectra of the arsenic-containing glasses with the same alkali content. For this purpose the SCORPIO 2000(I) spectrum analysis system was used.

III. Results and discussion

III.1 Polarized Raman spectra of glasses with batch composition K_2CO_3-(100-x)SiO_2-0.5As_2O_3(KxA)

Polarized Raman spectra of KxA are given in fig. 1. The contributions to the spectra caused by the presence of arsenic are marked with ⊕. According to refs. 7-9 the structure of K50A mainly consists of metasilicate chains which are built up of SiO_4 tetrahedra with two non-bridging oxygen atoms (NBO's) sharing corners. The strong polarized peaks at 968 and 953 cm^{-1} are ascribed to symmetrical stretch vibrations of the NBO's, the polarized peaks at 593 and 563 cm^{-1} to a symmetrical stretch vibration of the Si-O-Si bonds in the chains, and the weak depolarized peak at 710 cm^{-1} to an antisymmetrical Si-O-Si stretch vibration ([9]).

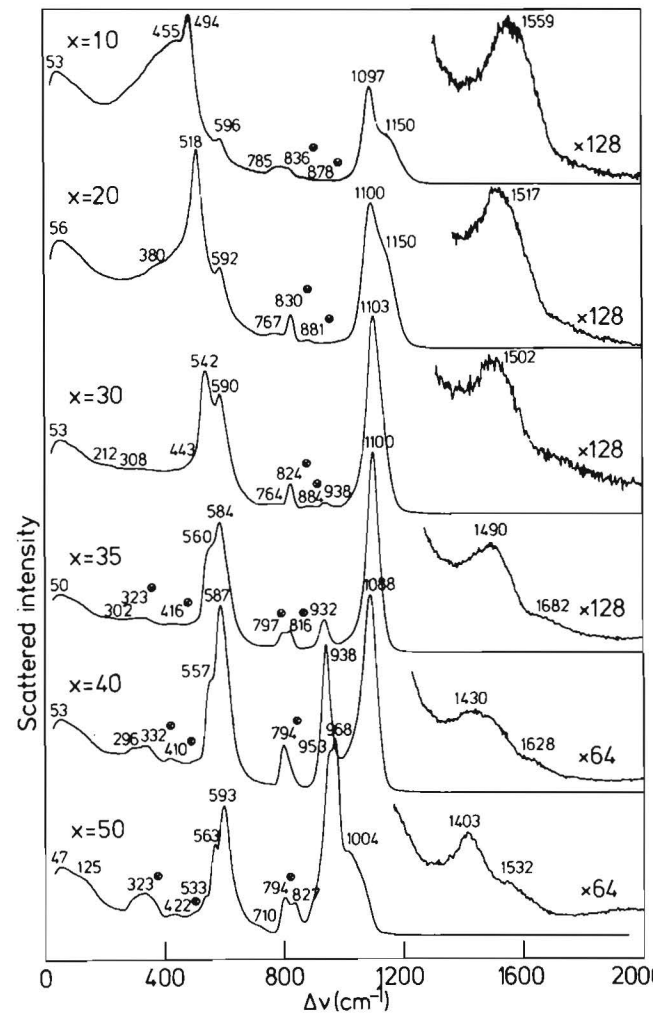

Fig. 1 Polarized Raman spectra of glasses with batch composition xK_2CO_3-(100-x)SiO_2-0.5 As_2O_3, melted at 1400°C (1600°C for x = 10).

The shoulder at 1004 cm^{-1} is probably caused by NBO stretch vibrations in disilicate type networks ([7, 10]) which are built up of SiO_4 tetrahedra with one NBO, sharing three corners. The polarized peak at 827 cm^{-1} in the Raman spectrum of the K50A is ascribed to the symmetrical stretch vibration of isolated SiO_4^{4-} tetrahedra ([7]). The very weak polarized bands at 1403 and 1532 cm^{-1} are probably combination or overtone bands. Raman peaks due to dissolved CO_3^{2-}, which are often found in spectra of metasilicate type glasses ([8, 10]), are not observed in the present spectra. K30A mainly consists of disilicate type network ([7, 10]). The strong polarized peak at 1103 cm^{-1} is ascribed to the NBO stretching vibration; the polarized peaks at 542 and 590 cm^{-1} to symmetrical Si-O-Si vibrations and the weak depolarized peak at 764 cm^{-1} to an antisymmetrical Si-O-Si vibration. The polarized peak at 938 cm^{-1} is ascribed to the symmetrical NBO stretch vibration of residual metasilicate chains ([10]). K35A and K10A contain silicate networks and more condensed networks of the kind found in crystalline $K_2O.4SiO_2$ ([11, 12]) and vitreous SiO_2 ([13]). Crystalline $K_2O.4SiO_2$ contains a silicate network with an average of 0.5 NBO's per silicon atom; the SiO_4 tetrahedra are connected to form a double-layer structure ([12]).

The polarized shoulder at 1150 cm^{-1} found in the spectra of K10A and K20A can be ascribed to the NBO stretch vibration in $K_2O.4SiO_2$ type networks. The broad polarized band at 455 cm^{-1} in the spectrum of K10A can be ascribed to the symmetrical Si-O-Si bending vibration of vitreous silica networks. In this vibration the bridging oxygen atom moves along the bisector of the Si-O-Si bond angle([14]).

In all spectra of fig. 1 very weak polarized overtone or combination bands are found at about 1500 cm^{-1}. These bands can be regarded as an overtone of the antisymmetrical Si-O-Si modes or as a combination of (symmetrical) NBO stretching and Si-O-Si stretching modes.

III.2 Difference spectra of glasses with batch composition xK_2CO_3 (100-x)SiO_2 with and without 0.5As_2O_3 (KxA and Kx)

Polarized and depolarized Raman difference spectra of KxA and Kx are given in figs. 2-4. The difference spectra for x=50 are given in fig. 2. The presence of arsenic in the glass causes weak depolarized peaks at 335 and 407 cm^{-1}, a strong polarized peak at 794 cm^{-1} and a weak depolarized peak at 808 cm^{-1} which is not observed in the polarized spectrum. The positions and intensities of the peaks at 335, 407, 794 and 808 cm^{-1} agree very well with the positions and intensities of peaks in the powder Raman spectrum of α-K_3AsO_4([20]). The peaks above 200 cm^{-1} in the Raman spectrum of this compound are ascribed to vibrations within an AsO_4^{3-} ion with approximate T_D symmetry. The peak at 330 cm^{-1} corresponds to the E species symmetrical bending mode of a perfect XO_4 tetrahedron, the peaks at 399, 409 and 418 cm^{-1} to the F_2 antisymmetrical bending modes, the peaks at 800, 827 and 843 cm^{-1} to the F_2 antisymmetrical stretching modes and the strong peak at 814 cm^{-1} to the A_1 symmetrical stretching mode. The degeneracy of the F_2 modes is removed as the real site symmetry of the AsO_4^{3-} ion in α-K_3AsO_4 is lower than T_D([20]). The E and F_2 type modes are expected to be depolarized and the A_1 mode to be completely polarized. From the difference spectra for x=50 it can be observed that the peaks that correspond to the E and F_2 type modes of α-K_3AsO_4 are depolarized and that the peak that corresponds to the A_1 type mode is strongly polarized. This provides strong evidence that isolated AsO_4^{3-} ions occur in K50A. No other arsenic-containing structures can be deduced from the glass spectra of fig. 2; the other peaks in the spectra are residual silicate peaks.

The difference spectra for x=40 are given in fig. 3. These spectra are very similar to those for x=50 from which it can be concluded that arsenic is mainly present at AsO_4^{3-} ions in K40A. The weak shoulders at 880 cm^{-1} in the polarized spectrum and at 884 cm^{-1} in the depolarized spectrum can be ascribed to more condensed arsenate structures. This will be discussed below.

The difference spectra for x=40 show relatively intense residual silicate peaks at 542, 584 and 1100 cm^{-1}. These peaks can very well be ascribed to vibrational modes within a disilicate network. Apparently there is more disilicate present in K40A than in K40. This can easily be explained

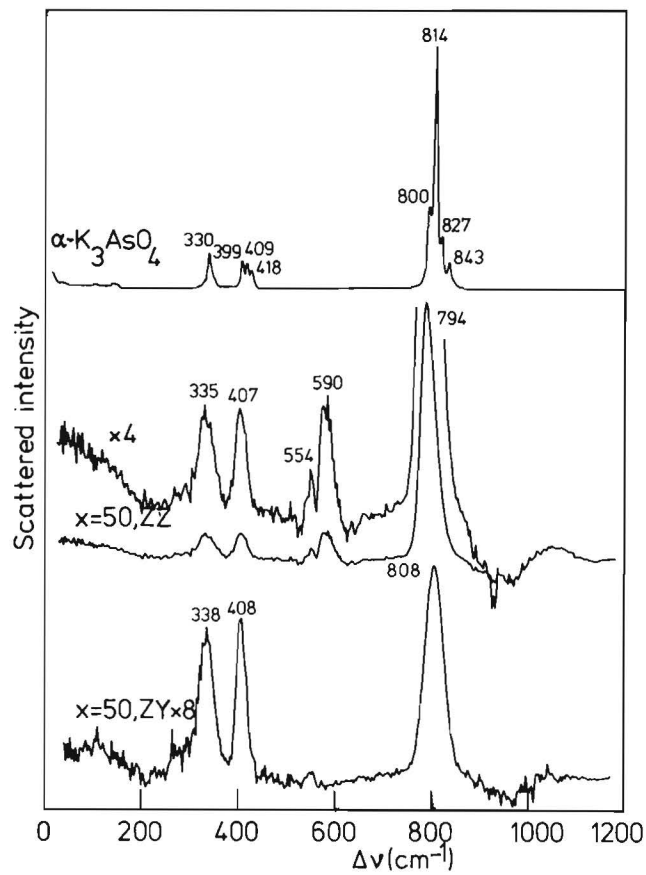

Fig. 2 Raman difference spectra for x=50 and Raman powder spectrum of crystalline K_3AsO_4([20]).

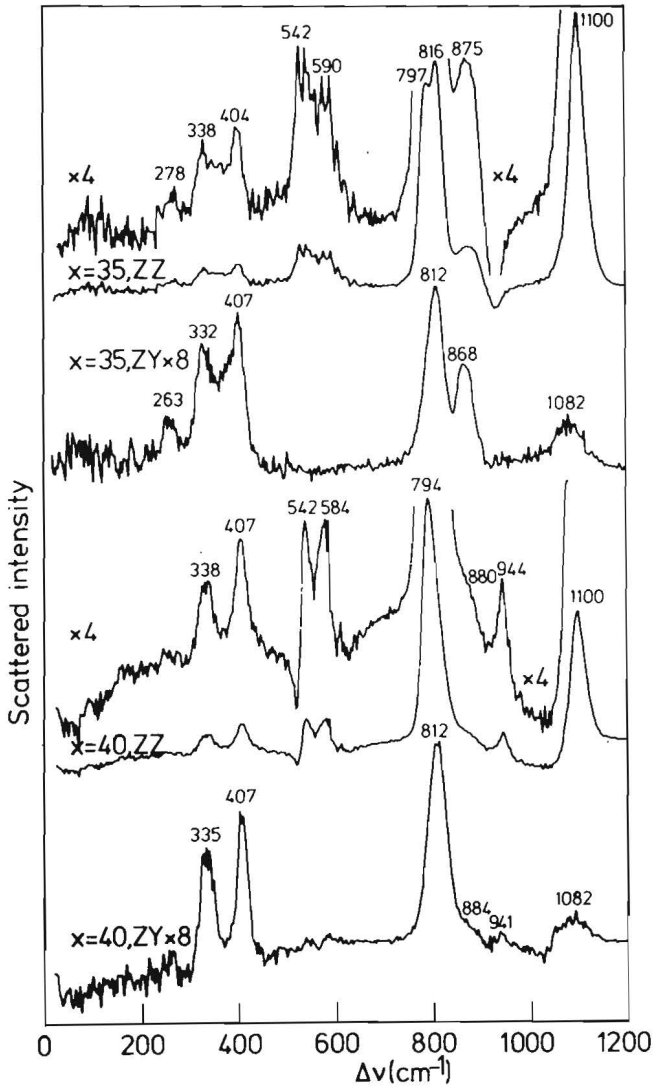

Fig. 3 Raman difference spectra for x=40 and x=30

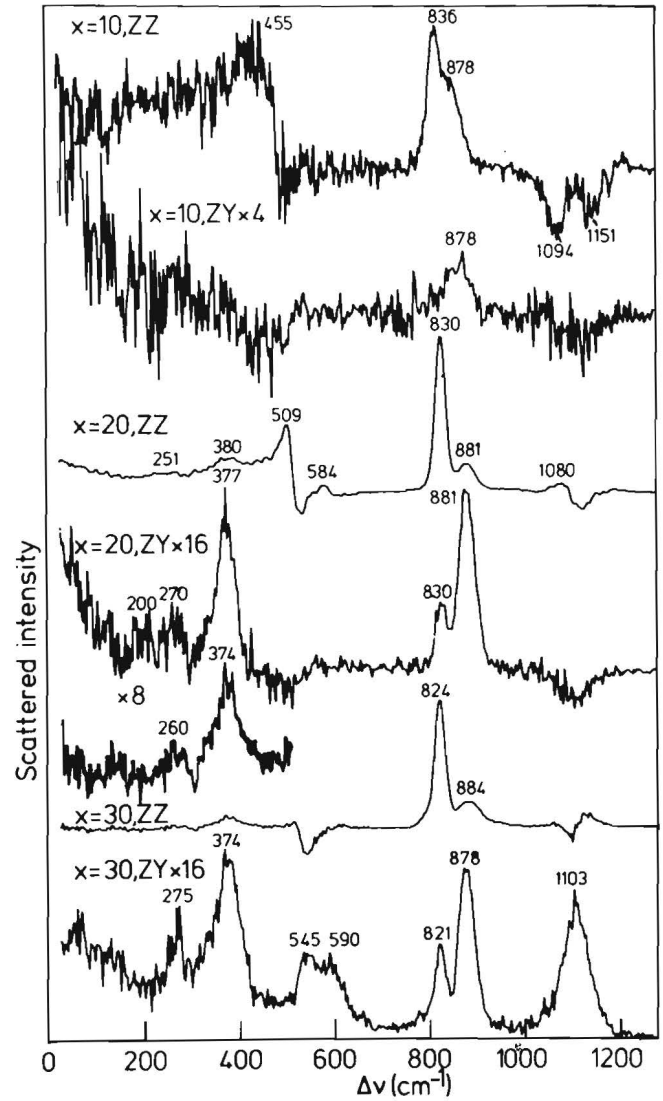

Fig. 4 Raman difference spectra for x=30, x=20 and x=10.

by the fact that arsenic extracts alkali ions from the silicate network to form the AsO_4^{3-} tetrahedra, which need three charge-compensating alkali ions per arsenic atom. When alkali is extracted from the silicate network disilicate structures which need only one charge-compensating alkali ion per SiO_4 tetrahedron are formed from metasilicate structures which need two charge-compensating alkali ions per SiO_4 tetrahedron.

For K50A the extraction of alkali from the network by arsenic has less consequences for the silicate part of the difference spectra as the total alkali concentration is larger; much alkali can be delivered by the isolated SiO_4^{4-} tetrahedra with their four charge compensating alkali ions. Only a small negative metasilicate peak is therefore found in the Raman spectra of K50A.

In the Raman difference spectra for x=35 (cf. fig. 3) peaks that point to the presence of AsO_4^{3-} ions are found again at 338, 404, 797 and 812 cm^{-1}. Other peaks caused by the presence of arsenic in the glass are found at 278, 816 and 875 cm^{-1}. The peak at 278 cm^{-1} is depolarized; the peak at 816 cm^{-1} is completely polarized and the peak at 875 cm^{-1} is partly polarized. The depolarized part of the 875 cm^{-1} peak is found at 868 cm^{-1} in the depolarized difference spectrum for x=35. The AsO_4^{3-} peaks at 332 and 407 cm^{-1} are superposed on a broad depolarized peak at 375 cm^{-1}. The difference spectrum for x=35 also shows residual polarized silicate peaks at 542, 590 and 1100 cm^{-1}.

In the difference spectra for x=30 (cf. fig. 4) peaks due to AsO_4^{3-} ions are not found anymore. Weak, depolarized peaks are found at 260 and 377 cm^{-1} besides a strong polarized peak at 824 cm^{-1} and a partly polarized peak at 884 cm^{-1}. The difference spectrum for x=20 shows qualitatively the same picture as the difference spectrum for x=30. Weak depolarized peaks are found at 270 and 377 cm^{-1}, an almost completely polarized peak at 830 cm^{-1} and a partly polarized peak at 880 cm^{-1}.

The difference spectrum for x=10 is very weak and shows a large scatter. A great deal of arsenic evaporated at the melting temperature (1600°C). A polarized peak at 836 cm^{-1} and a partly polarized peak at 878 cm^{-1} can be observed clearly in the difference spectra however. The residual silicate peaks in the difference spectra of x=10, 20

and 30 are much less intense than was the case for x=35 and 40. This is obviously connected with the formation of arsenic-containing structures that need a relatively low number of charge-compensating alkali ions per arsenic atom. The peaks at 545, 590 and 1103 cm^{-1} in the *depolarized* spectrum for x=30 correspond to the *polarized* peaks of the disilicate structures in the glass; this is probably caused by optical inhomogeneity of the sample. The broad polarized band at 455 cm^{-1} in the difference spectrum for x=10 can be ascribed to vitreous silica type structures without charge compensating ions.

Summarizing, the difference spectra show the following features, caused by the presence of arsenic in the batch:

- for x = 35-50 depolarized Raman peaks at about 330, 410 and 810 cm^{-1} together with a strongly polarized Raman peak at about 800 cm^{-1} which can very well be ascribed to AsO_4^{3-} ions.
- for x = 35-20 weak depolarized peaks at about 270 and 375 cm^{-1}.
- for x = 35-10 strong, almost completely polarized peaks at 816 to 836 cm^{-1}. The position of these peaks increases significantly with decreasing x.
- for x = 40-10 a partly polarized peak at about 880 cm^{-1}; the ratio of the intensity of the 875 cm^{-1} peaks in the depolarized difference spectra to the 880 cm^{-1} peaks in the polarized difference spectra is about 0.5 ± 0.1.

No unambigous assignment of the difference spectra of G35-10A in terms of a single arsenate ([15]) or arsenite structure([16]) can be made. In refs. 7, 8 the polarized peak at 824 cm^{-1} in K30A is assigned to the symmetrical stretch vibration of AsO_4^{3-} ions. This assignment cannot be correct as AsO_4^{3-} ions evidently only occur at higher alkali concentrations, giving a symmetrical stretch vibration peak at about 800 cm^{-1} as was shown above.

Using the present knowledge of Raman data of vitreous and crystalline potassium arsenates([15]) and arsenites([16]) two interpretations or the difference spectra for x=10-35 can be given:

I. The arsenic part of the difference spectra is completely due to the presence of $As_2O_7^{4-}$ ions. The strong polarized peaks at 816-836 cm^{-1} can then be ascribed to symmetrical AsO_3 stretch (ν_s AsO_3), the partly polarized peaks at 880 cm^{-1} to antisymmetrical AsO_3 stretch vibrations (ν_{as} AsO_3), the depolarized peaks at about 375 cm^{-1} to AsO_3 bending modes (δAsO_3) and the depolarized peaks at 270 cm^{-1} to AsOAs bending modes (δ AsOAs).

II. $As_mO_{2m+1}^{-m-2}$ arsenite chains of AsO_3 pyramids are present together with $As_nO_{3n+1}^{-n-2}$ arsenate chains of AsO_4 tetrahedra. Contrary to interpretation I, this interpretation assumes the presence of As^{3+} in arsenite chains as are found in crystalline and vitreous $KAsO_2$ ([21]). The peaks at 880 cm^{-1} can then be ascribed to νAsO^- of short chain-type arsenate ions as are found in $K_4As_2O_7$ or $K_3As_5O_{10}$([20, 22]), the strong, polarized peaks at 816-836 cm^{-1} to νAsO^- of arsenite chains, the depolarized peak at 377 cm^{-1} to δAsO_3 of arsenates and the depolarized peak at about 270 cm^{-1} to δAsOAs of arsenate or arsenite chains([20, 21]).

Arsenite chains of AsO_3 pyramids with m very large occur in crystalline and vitreous $KAsO_2$ where strong Raman peaks due to NBO stretching vibrations (νAsO^-) are found at 838 and 854 cm^{-1} respectively. The 854 cm^{-1} peak in the Raman spectra of vitreous $KAsO_2$ is relatively narrow and strongly polarized. The compound K_3AsO_3 contains isolated AsO_3^{3-} pyramids and has a strong νAsO^- peak at 782 cm^{-1}. Chains of AsO_3 pyramids having a chain length between m = ∞($KAsO_2$) and m = 1 (K_3AsO_3) may accordingly give rise to νAsO^- peaks between 780 and 850 cm^{-1}.

In the difference spectra the polarized peak, assigned here to νAsO^- of arsenites, is found at 816 cm^{-1} for x= 35, corresponding to short chains, and increases to 836 cm^{-1} for x = 10, corresponding to long chains. Contrary to the long chains the short arsenite chains need a relatively large number of charge-compensating alkali ions.

The polarizability of As^{3+} is much larger than that of As^{5+}, which gives rise to more intense Raman peaks for As^{3+} containing structures. This may explain the fact that, even though there is probably much more As^{5+} in the glass, the arsenite Raman peaks are still stronger.

The objections that can be made against interpretation I are:

- The peaks at 880 cm^{-1} should be completely depolarized if caused by ν_{as} AsO_3.
- The position of the strong polarized peaks at 816-836 cm^{-1} does not agree very well with the position of νAsO_3 peaks found for crystalline and vitreous $K_4As_2O_7$ which are present around 860 cm^{-1}.
- The position of the $\nu_s AsO_3$ peak should not vary with the glass composition.
- The separation in the position of the peaks, which are assigned in interpretation I to $\nu_s AsO_3$ and $\nu_{as} AsO_3$ is much larger than the separation found for vitreous and crystalline chain type arsenates([20]).
- Chemical analysis of silicate glasses generally shows qualitatively the presence of As^{3+} for $x < 35$.

The main objection against interpretation II is that the depolarized part of the 880 cm^{-1} peaks, ascribed to νAsO^- of $As_2O_7^{4-}$ or $As_3O_{10}^{5-}$ ions, is relatively large compared with the corresponding data for vitreous arsenates. Interpretation II is preferable as it gives the best agreement with the Raman data of vitreous and crystalline arsenites and arsenates.

No νAs-O-As peaks are found in the difference spectra; this may be explained by the fact that As-O-As stretching modes are relatively weak and broad for vitreous arsenates and arsenites([20, 21]) and by the overlap with the strong Si-O-Si stretching modes which are found at about the same position. At present no conclusions can be drawn, concerning the incorporation of arsenate and arsenite structures in the silicate network.

III.3 Temperature and composition effects on the As^{3+}/As^{5+} ratio

The Raman difference spectra were used to study relative shifts in As^{3+}/As^{5+} ratios by measuring the intensity ratios of the peaks at 816-836 cm^{-1} and the peaks at 880 cm^{-1} as a function of alkali composition x and temperature.
These peak intensity ratios are given for x=20 and x=30 in Table I. The ratios could not be determined for x=35, and x=10 because of the strong peak overlap.
From the data of table I an evident effect of the alkali composition on the As^{3+}/As^{5+} ratio can be concluded but no significant temperature effect was found.

Table I

X	Melting temp.	Intensity ratio $\nu(824,830)/\nu(880)$
20	1400	11 (± 2)
30	1300	5.8 (± .2)
30	1400	6.1 (± .2)
30	1500	5.5 (± .2)
30	1600	5.9 (± .2)

An O_2 development, caused by an increase of As^{3+}/As^{5+} on temperature increase, is often taken in the literature as the main mechanism of As_2O_3 fining. In a previous study (1) it was proposed however, that irreversible composition changes in the liquid phase during melting cause an important increase in As^{3+}/As^{5+} ratio. The present data support this mechanism and extend its validity to temperatures up to 1600°C.

IV Conclusions

From the Raman difference spectra of glasses with batch composition xK_2CO_3-(1-x)SiO_2 with and without 0.5 As_2O_3 added to the batch it is concluded that the following arsenate and arsenite structures occur:

- In the composition region $50 > x > 35$ mainly isolated AsO_4^{3-} groups are present; no Raman peaks which point to the presence of arsenite structures are found.
- In the composition region $35 > x > 10$ the AsO_4^{3-} groups which need a relatively large number of charge-compensating alkali ions, are not stable anymore. Trivalent arsenic is found in $As_mO_{2m+1}^{-m-2}$ chains of AsO_3 pyramids and pentavalent arsenic in $As_nO_{3n+1}^{-n-2}$ chains with n=2 or 3. The chain length m of the arsenite chains increases with decreasing x.

From the Raman peak intensity ratios shifts in the As^{3+}/As^{5+} ratio were examined. No significant effect of the melting temperature on the As^{3+}/As^{5+} ratio was found. However, the As^{3+}/As^{5+} ratio increases significantly as a function of glass composition, going from x=50 to x=10. The present results, together with those of ref. 1 lead to the following three stage mechanism of As_2O_3 fining in potassium silicate glass batches.

1. Attack of the SiO_2 grains in the batch by K_2CO_3 with the formation of crystalline $K_2Si_2O_5$ and a potassium-rich liquid phase containing metasilicate chains and large amounts of CO_3^{2-} ions. As_2O_3 reacts to K_3AsO_4 which dissolves in the liquid phase as AsO_4^{3-} ions.
2. When all the originally present K_2CO_3 has disappeared the potassium ions in the liquid phase diffuse into the SiO_2 grains via the crystalline $K_2O.2SiO_2$ layer to form more crystalline $K_2Si_2O_5$. With the decrease of the potassium concentration in the liquid phase the AsO_4^{3-} ions are not stable anymore and decompose into more condensed arsenates and arsenites; this is accompanied by the formation of O_2 gas. At the same time the solubility of the CO_3^{2-} ions in the liquid phase decreases drastically with the lowering of the potassium concentration. The resulting evolution of CO_2 from the liquid phase occurs prior to the O_2 development from the decomposition of arsenates; finally in the ideal case only O_2 gas remains in the bubbles and pores of the reacting glass batch.
3. At higher temperatures a raw silicate melt is formed in which the remaining SiO_2 dissolves. This dissolution of SiO_2 may be accompanied by a further increase of the As^{3+}/As^{5+} ratio in the liquid phase, which causes in its turn a further development of O_2 gas. This further O_2 development may contribute to the fining process by bubble growth. In the ideal case the silicate melt at the final melting temperature contains only O_2 bubbles; these bubbles may easily dissolve by diffusion of O_2 through the melt.([18,19]).

Acknowledgement

The author is indebted to J.G. van Lierop for sample preparation and to A.J. Hendriks for assistance with building of the computer system.

References

[1] H. Verweij, "Raman Study of the Reactions in a Glass-Forming Mixture with Molar Composition: $30K_2CO_3$-$70SiO_2$-$1AsO_3$", J. Am. Ceram. Soc., **62** [9-10] 450-455 (1979).

[2] W.L. Konijnendijk and J.H.J.M. Buster, "Raman Scattering Measurements of Arsenic-Containing Oxide Glasses", J. Non-Cryst. Solids, **17** [2] 293-97 (1975).

[3] W.L. Konijnendijk and J.H.J.M. Buster, "Raman Scattering Measurements of Silicate Glasses Containing AsO_4^{3-} Ions", J. Non-Cryst. **22** [2] 379-389 (1976).

[4] S. Bajo, "Volatalization of Arsenic (III, V), Antimony (III, V), and Selenium (IV, VI) from Mixtures of Hydrogen Fluoride and Perchloric Acid Solution: "Application to Silicate Analysis", Anal. Chem. **50** 649-51 (1978).

[5] J.A. Topp and W.J. Schmid, "Compensation of Source Fluctuations in Raman Spectroscopy by Quick Analog Dividing", Rev. Sci. Instr. **42** [11] 1683-86 (1971).

[6] T.C. Damen, S.P.S. Porto and B. Tell, "Raman Effect of Zinc Oxide", Phys. Rev., **142** [2] 570-74 (1966).

[7] S.A. Brawer and W.B. White, "Raman Spectroscopic Investigation of the Structure of Silicate Glasses: I", J. Chem. Phys. **63** [6] 2421-32 (1975).

[8] H. Verweij, H. van den Boom and R.E. Breemer, "Raman Scattering of Carbonate Ions Dissolved in Potassium Silicate Glasses", J. Am. Ceram. Soc. **60** [11-12] 529-34 (1976).

[9] H. Verweij, "Raman Study of the Structure of Alkali Germanosilicate Glasses: I" J. Non-Cryst. Sol. **33** [1] 41-54 (1979).

[10] H. Verweij, "Raman Study of the Structure of Alkali Germanosilicate Glasses: II", J. Non-Cryst. Sol. **33** [1] 55-69 (1979).

[11] H. Verweij and W.L. Konijnendijk, "Structural Units in K_2O-PbO-SiO_2 Glasses by Raman Spectroscopy", J. Am. Ceram. Soc. **59** [11-12] 517-21 (1976).

[12] H. Schweinsberg and F. Liebau, "Crystal Structure of $K_4(Si_8O_{18})$. New Layer-Type Silicate", Acta. Cryst. Sect. B, [30] Pt. 9 2206-17 (1974).

[13] M. Hass, "Raman Spectra of Vitreous Silica, Germania and Sodium Silicate Glasses", J. Phys. Chem. Solids, **31** 415-422 (1970).

[14] R.J. Bell, Methods in Computation Physics, Acad. Press. New York, p. 215, (1976).

[15] H. Verweij, "Raman Study of Glasses and Crystalline Compounds in the System K_3AsO_4-$KAsO_3$", Appl. Spectr. **33** [5] 509-15 (1979).

[16] H. Verweij and J.G. van Lierop, "Raman Spectra of Crystalline Compounds and Glasses in the System K_2O-As_2O_3", to be published.

[17] J.H. Hornstra and H. Verweij, "Crystal Structure of $K_5As_3O_{10}$", Acta. Cryst. **36**, sect. B, in press.

[18] C.H. Greene and H.A. Lee Jr., "Effect of As_2O_3 and $NaNO_3$ on the Solution of O_2 in Soda-Lime Glass", J. Am. Ceram. Soc., **48** [10] 528-33 (1965).

[19] C.H. Greene and D.R. Platts, "Behaviour of Bubbles of Oxygen and Sulfur Dioxide in Soda-Lime Glass", J. Am. Ceram. Soc. **52** [2] 106-109 (1969).

Manufacturers

A. Heraus, Hanau, W. Germany.

B. E. Merck, Darmstadt, W. Germany.

C. Degussa, Frankfurt, W. Germany.

D. Coherent Radiation, Palo Alto, California.

E. Jobin Yvon, Longjumeau, France.

F. ITT, Rochester, New York.

G. PAR, Princeton, New Jersey.

H. Digital, Maynard, Massachusetts.

I. Canberra, Meriden, Connecticut.

J. Philips, Eindhoven, The Netherlands.

K. Spectra Physics, Mountain View, California.

Summary

This thesis contains a collection of papers and manuscripts concerning the mechanisms of melting and fining reactions in silicate glass-forming mixtures containing As_2O_3. Fining is the process of disappearance of gas bubbles from glass melts. As_2O_3 is a so called fining agent. Fining agents are added to silicate glass batches to reduce the time needed for the glass melt to become bubble free. The aim of the investigations presented in this thesis, was to clarify the complete reaction mechanism of As_2O_3 fining.

Laser Raman spectroscopy was used as an analytical technique to study glass-forming reactions in a model system. Vitreous and crystalline phases were identified in glass-forming mixtures which had reacted for various times on different temperatures.

From the Raman spectroscopic results a mechanism for the reactions of As_2O_3 during the glass melting process could be derived. With this mechanism the effectiveness of As_2O_3 as a fining agent can be explained.

Samenvatting

Dit proefschrift bevat een verzameling artikelen en manuscripten rond de mechanismen van smelt- en louterprocessen in silicaatglasvormende mengsels die As_2O_3 bevatten.
Louteren is het proces van verdwijnen van gasbellen uit een glassmelt. As_2O_3 is een zogenaamd "loutermiddel".
Loutermiddelen worden toegevoegd aan silicaatglas gemengen om de tijd te bekorten die nodig is voor de glassmelt om bellenvrij te worden. Het doel van de onderzoekingen die in dit proefschrift zijn gepresenteerd was om het volledige reactiemechanisme van As_2O_3 loutering op te helderen.

Laser Raman spectroscopie werd gebruikt als een analytische techniek om glasvormingsreacties in een modelsysteem te bestuderen. Glasachtige en kristallijne reactieproducten werden geidentificeerd in glasvormende mengsels die gedurende verschillende tijden op diverse temperaturen gereageerd hadden.

Uit de Raman spectroscopische resultaten kon een mechanisme worden afgeleid voor de reacties van As_2O_3 tijdens het glassmelt proces. Met dit mechanisme kan de effectiviteit van As_2O_3 als loutermiddel worden verklaard.

STELLINGEN

bij het proefschrift van

H. Verweij

21 oktober 1980

I

Het loutergedrag van silicaatglasvormende mengsels wordt voor het grootste deel bepaald door chemische reacties tijdens het smelten.

Dit proefschrift.

II

Het ontmenggedrag van silicaatglazen bij hoge temperaturen kan grote gevolgen hebben voor het glaslouterproces.

III

De kwaliteit van de tegenwoordige televisieprogramma's behoeft voor fabrikanten van beeldschermen geen aanleiding te zijn om zich druk te maken over een paar gasbelletjes in het glas.

IV

De mogelijkheid van vorming van copolymeren uit organische en oxidisch anorganische monomeren dient nader te worden onderzocht.

V

Het recente inzicht dat water in glas niet is ingebouwd als Si-O-H groepen maar als gecomplexeerd H_2O, is van groot belang voor de controle van de optische absorptie van glas.

VI

Vanwege onvoorspelbare opladingsverschijnselen is het zeer de vraag of de geleiders koolstof en goud wel betrouwbaar voor energiecalibratie kunnen worden toegepast bij ESCA en Augermetingen aan niet-geleiders.

D. A. Stephenson, N.J. Binkowski,
J. Non-Cryst. Sol. **22** 399-421 (1976)

VII

Indien dieetadvisering in de verstrekkingenpakketten van ziekenfondsen en particuliere ziektekostenverzekeringen in Nederland wordt opgenomen, zal blijken dat het kostenbesparende effect hiervan ten onrechte is gebagatelliseerd.

VIII

De toenemende secularisatie in de westerse wereld heeft grote gevolgen voor de muzikale vorming van de jongere generaties.

IX

Wat betreft de toepassing van computers blijkt de Nederlandse tuinder zich minder conservatief op te stellen dan de gemiddelde wetenschappelijke onderzoeker.

X

Met de invoering van lasers in discotheken heeft men de bezoekers, naast een mogelijke gehoorsbeschadiging, nu ook de kans op geheel of gedeeltelijk verlies van het gezichtsvermogen te bieden.

XI

Het feit dat tegenwoordig, vooral in de Verenigde Staten, veel wetenschappelijke contacten worden gelegd tijdens trimoefeningen, zal op den duur van invloed moeten zijn bij de selectie van wetenschappelijke onderzoekers.

Eindhoven, 21 oktober 1980